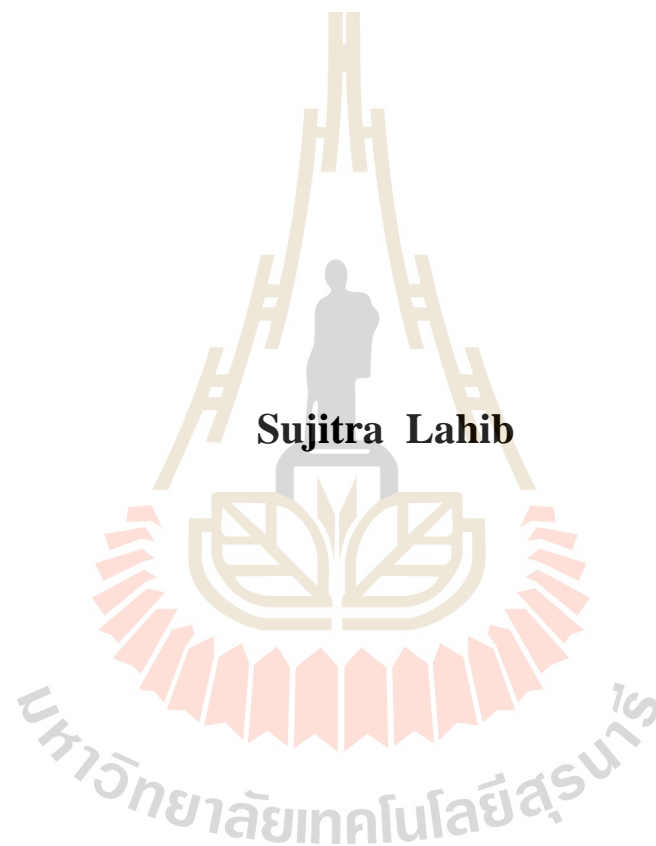


**EFFECT OF SURFACE SUBSIDENCE ON MECHANICAL
STABILITY OF CEMENT SEAL IN EXPLORATION
BOREHOLE**



**A Thesis Submitted in Partial Fulfillment of the Requirements for the
Degree of Master of Engineering in Civil, Transportation and
Geo-resources Engineering
Suranaree University of Technology**

Academic Year 2018

ผลกระทบจากการทรุดตัวของผิวดินต่อเสถียรภาพเชิงกลศาสตร์ของซีเมนต์อัด
ในหลุมเจาะสำรวจ



นางสาวสุจิตรา หล้าหีบ

วิทยานิพนธ์นี้เป็นส่วนหนึ่งของการศึกษาตามหลักสูตรปริญญาวิศวกรรมศาสตรมหาบัณฑิต
สาขาวิศวกรรมโยธา ขนส่ง และทรัพยากรธรณี
มหาวิทยาลัยเทคโนโลยีสุรนารี
ปีการศึกษา 2561

**EFFECT OF SURFACE SUBSIDENCE ON MECHANICAL
STABILITY OF CEMENT SEAL IN EXPLORATION BOREHOLE**

Suranaree University of Technology has approved this thesis submitted in partial fulfillment of the requirements for a Master's Degree.

Thesis Examining Committee



(Asst. Prof. Dr. Akkhapun Wannakomol)

Chairperson



(Asst. Prof. Dr. Decho Phueakphum)

Member (Thesis Advisor)



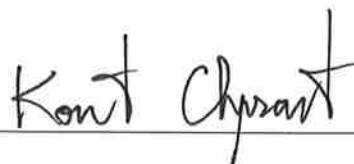
(Asst. Prof. Dr. Pornkasem Jongpradist)

Member



(Prof. Dr. Santi Meansiri)

Vice Rector for Academic Affairs
and Internationalization



(Assoc. Prof. Ft. Lt. Dr. Kontorn Chamniprasart)

Dean of Institute of Engineering

สุจิตรา หล้าหีบ : ผลกระทบจากการทรุดตัวของผิวดินต่อเสถียรภาพเชิงกลศาสตร์ของซีเมนต์อุดในหลุมเจาะสำรวจ (EFFECT OF SURFACE SUBSIDENCE ON MECHANICAL STABILITY OF CEMENT SEAL IN EXPLORATION BOREHOLE)
อาจารย์ที่ปรึกษา : ผู้ช่วยศาสตราจารย์ ดร. เค โช เพ็ถกภูมิ, 71 หน้า.

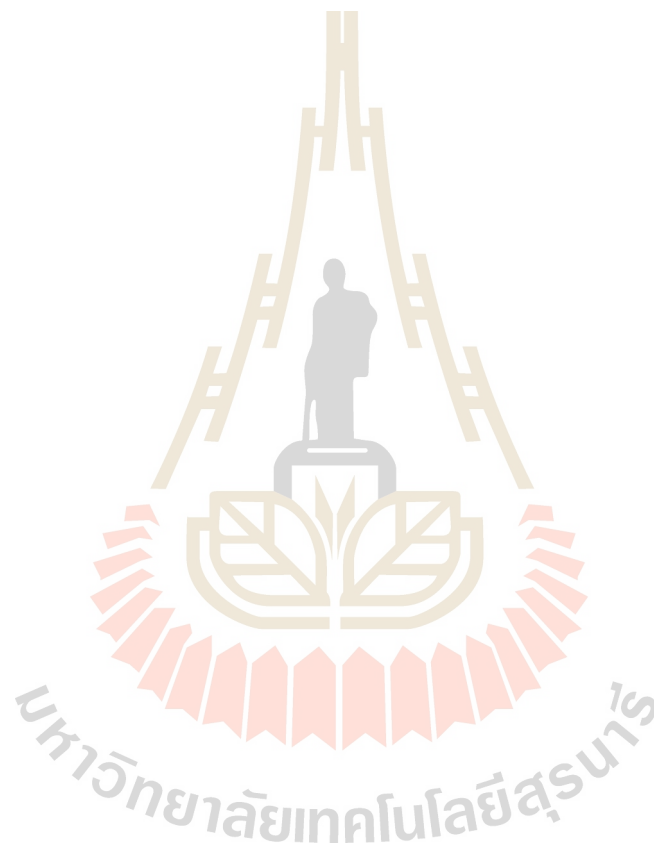
วัตถุประสงค์ของงานวิจัยนี้ เพื่อประเมินศักยภาพเชิงกลศาสตร์ของปูนซีเมนต์สำหรับใช้เป็นวัสดุอุดหลุมเจาะสำรวจในชั้นเกลือหิน ปูนซีเมนต์อุดหลุมเจาะ 3 ชนิด ถูกนำมาใช้ในการศึกษา ซึ่งประกอบด้วย ปูนซีเมนต์ล้วน ปูนซีเมนต์ผสมทราย และปูนซีเมนต์ผสมดินตะกอนประปา โดยที่ปูนซีเมนต์ปอร์ตแลนด์ประเภทที่ 5 ถูกนำมาใช้ ทั้งนี้เนื่องจากมีสมบัติความต้านทานต่อซัลเฟตสูง ส่วนผสม 2 อัตราส่วน (1:1 และ 1:0.5) ระหว่างปูนซีเมนต์และทราย และปูนซีเมนต์และดินตะกอนประปาได้ถูกจัดเตรียม จากนั้นนำส่วนผสมที่ใช้เป็นวัสดุอุดหลุมเจาะผสมกับสารละลายโซเดียมคลอไรด์อิ่มตัวในอัตราส่วนของน้ำเกลืออิ่มตัวต่อปูนซีเมนต์ผันแปรจาก 0.6:1 0.8:1 และ 1:1 โดยน้ำหนัก ตัวอย่างทั้งหมดถูกบ่มภายใต้สารละลายโซเดียมคลอไรด์อิ่มตัวเป็นเวลา 28 วัน ก่อนที่จะนำมาทดสอบ โดยคุณสมบัติทางกลศาสตร์ของตัวอย่างประกอบด้วย การทดสอบแรงดึงแบบกดสี่จุด การทดสอบแรงกดในแกนเดียวและการทดสอบแรงกดในสามแกน ผลการทดสอบระบุว่าความเค้นกดและสัมประสิทธิ์ความยืดหยุ่นมีค่าลดลงและอัตราส่วนบิวชองมีค่าสูงขึ้นเมื่อสัดส่วนของสารละลายโซเดียมคลอไรด์อิ่มตัวต่อปูนซีเมนต์มีค่าเพิ่มขึ้น การเพิ่มขึ้นของสัดส่วนระหว่างสารละลายโซเดียมคลอไรด์อิ่มตัวต่อปูนซีเมนต์ส่งผลให้ความเค้นยึดติดและมุมของความเสียดทานภายในลดลงเพียงเล็กน้อย โดยค่ากำลังกดในแกนเดียวและสัมประสิทธิ์ความยืดหยุ่นที่สูงที่สุดจากการทดสอบมีค่าเท่ากับ 24.25 เมกะปาสกาล และ 19.01 จิกะปาสกาล ซึ่งได้จากส่วนผสมของปูนซีเมนต์และทรายที่ใช้อัตราส่วนผสมระหว่างน้ำเกลืออิ่มตัวต่อปูนซีเมนต์เท่ากับ 0.6:1 ค่าความเค้นดึงจากการทดสอบการบิดคดมีค่าผันแปรจาก 2.36 ถึง 3.61 เมกะปาสกาล ซึ่งมีแนวโน้มลดลงเมื่ออัตราส่วนระหว่างสารละลายโซเดียมคลอไรด์อิ่มตัวต่อซีเมนต์เพิ่มขึ้น ส่วนผสมระหว่างปูนซีเมนต์และทรายให้ค่าความเค้นดึงจากการทดสอบการบิดคดที่สูงกว่าส่วนผสมระหว่างปูนซีเมนต์ล้วนและส่วนผสมซีเมนต์และดินตะกอนประปาเกณฑ์กำลังเฉือนของคูลอมบีและพลังงานความเครียดถูกนำมาประยุกต์ใช้เพื่อหาค่าปัจจัยความปลอดภัยของวัสดุอุดในหลุมเจาะเมื่อมีการทรุดตัวของผิวดินในรูปแบบของการใช้ค่าความเค้นเฉือนและค่าความเค้นดึงสูงสุดที่เกิดขึ้น ผลการคำนวณระบุว่าค่าปัจจัยความปลอดภัยมีค่าเพิ่มขึ้นเมื่อความลึกของหลุมเจาะเพิ่มขึ้นและมีค่าการทรุดตัวของผิวดินลดลง ผลที่ได้

SUJITRA LAHIB : EFFECT OF SURFACE SUBSIDENCE ON
MECHANICAL STABILITY OF CEMENT SEAL IN EXPLORATION
BOREHOLE. THESIS ADVISOR : ASST. PROF. DECHO PHUEKPHUM,
Ph.D., 71 PP.

SLUDGE/SAND/CEMENT/STRAIN ENERGY

The objective of this study is to determine the mechanical performance of cement seal in exploration borehole of rock salt formation. Three cement seal mixtures have been used in this study including pure cement, cement-sand, and cement-sludge. The commercial grade Portland cement type V is selected due to its sulfate resistance. Two mixing ratios (1:1 and 1:0.5) of cement-to-sand and cement-to-sludge are prepared. The cement seal mixtures have been mixed with NaCl saturated brine using brine-to-cement ratios of 0.6:1, 0.8:1 and 1:1 by weight. All specimens are cured under saturated brine for 28 days. The mechanical properties of the samples have been examined by performing the four-point bending, uniaxial and triaxial tests. The results indicate that the compressive strength and elastic modulus decrease and Poisson's ratio increases with increasing brine-to-cement ratio. The increasing of brine-to-cement ratio slightly decreases the cohesion and internal friction angle. The highest compressive strength and elastic modulus are 24.25 MPa and 19.01 GPa obtained from the cement-sand mixture with brine-to-cement ratio of 0.6:1. The bending tensile strengths ranging from 2.36 to 3.61 MPa. They tend to decrease with increasing brine-to-cement ratio for all cement seal mixtures. Cement-sand mixture gives higher tensile strengths than those of pure cement and cement-sludge mixture. The Coulomb and strain energy criteria are applied to determine the factors of safety of the materials in

borehole during subsidence in terms of shear strength and bending tensile strength. The factors of safety increase when depth increases and surface subsidence decreases. The findings can be used to assess the stability of the cement seals in borehole drilled in the subsidence area.



School of Geotechnology

Academic Year 2018

Student's Signature สุจิตรา หล้าสีป

Advisor's Signature PN

ACKNOWLEDGMENTS

I wish to acknowledge the funding support from Suranaree University of Technology (SUT).

I would like to express my sincere thanks to Asst. Prof. Dr. Decho Phueakphum for his valuable guidance and efficient supervision. I appreciate his strong support, encouragement, suggestions and comments during the research period. I also would like to Prof. Dr. Kittitep Fuenkajorn express my gratitude to and Asst. Prof. Dr. Prachya Tepnarong for their constructive advice, valuable suggestions and comments on my research works. Grateful thanks are given to all staffs of Geomechanics Research Unit, Institute of Engineering who supported my work.

Finally, I would like to thank beloved parents for their love, support and encouragement.

Sujitra Lahib

มหาวิทยาลัยเทคโนโลยีสุรนารี

TABLE OF CONTENTS

	Page
ABSTRACT (THAI)	I
ABSTRACT (ENGLISH).....	III
ACKNOWLEDGEMENTS.....	V
TABLE OF CONTENTS.....	VI
LIST OF TABLES	X
LIST OF FIGURES	XIII
SYMBOLS AND ABBREVIATIONS.....	XVIII
CHAPTER	
I INTRODUCTION.....	1
1.1 Background and rationale	1
1.2 Research objectives.....	2
1.3 Research methodology.....	2
1.3.1 Literature review	3
1.3.2 Sample collection and preparation.....	4
1.3.3 Laboratory test	4
1.3.3.1 Uniaxial compressive strength test.....	4
1.3.3.2 Triaxial compressive strength tests	5
1.3.3.3 Four point bending test.....	5
1.3.4 Potential Application	5

TABLE OF CONTENTS (Continued)

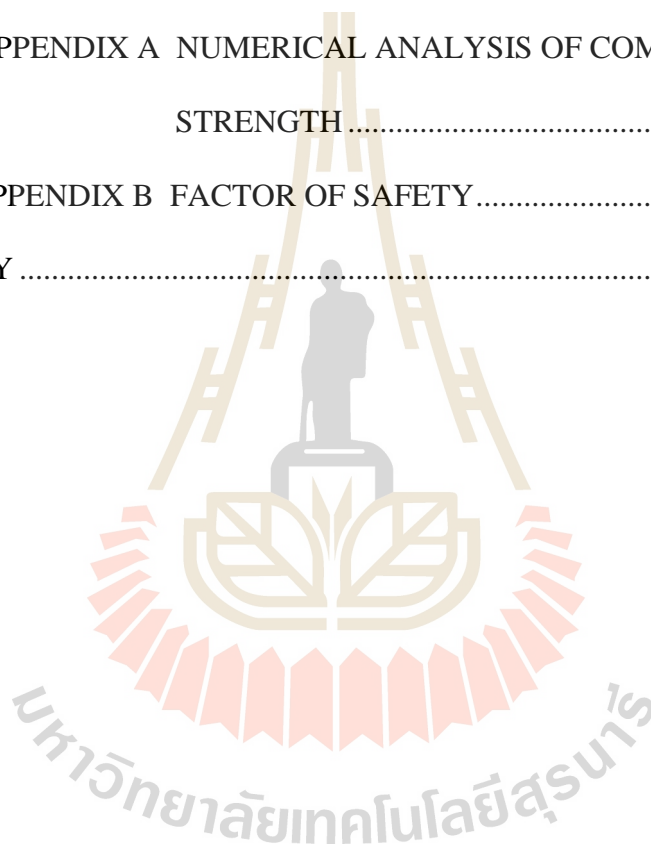
	Page
1.3.5 Discussions and conclusion	5
1.3.6 Thesis writing	5
1.4 Scope and limitations	5
1.5 Thesis contents	6
II LITERATURE REVIEW	7
2.1 Introduction.....	7
2.2 Rock salt in northeast region of Thailand	7
2.3 Subsidence influence on underground borehole	10
2.4 Borehole sealing.....	12
2.5 Mechanical properties sealing materials	13
2.5.1 Pure cement	14
2.5.2 Cement mixed with sand	16
2.5.3 Cement mixed with sludge	18
III SAMPLE PREPARATION	22
3.1 Introduction.....	22
3.2 Material preparation.....	22
3.2.1 Portland cement type V	22
3.2.2 Sand	23
3.2.3 Sludge	23
3.2.4 Saturated brine	26

TABLE OF CONTENTS (Continued)

	Page
3.3 Cement slurry preparation.....	26
3.4 Sample preparation	28
IV LABORATORY TESTING.....	35
4.1 Introduction.....	35
4.2 Test methods.....	35
4.2.1 Compression Test	35
4.2.2 Four Point Bending Test.....	37
4.3 Test results	38
4.3.1 Compression test results	38
4.3.2 Four point bending test results.....	52
4.4 Discussions and Conclusions.....	59
V POTENTIAL APPLICATION.....	60
5.1 Introduction.....	60
5.2 Strain Energy Density	60
5.3 Strain Energy Applications	62
5.4 Factor of Safety.....	64
5.5 Discussions and Conclusions.....	67
VI DISCUSSIONS AND CONCLUSIONS.....	68
6.1 Discussions	68
6.2 Conclusions.....	69

TABLE OF CONTENTS (Continued)

	Page
6.3 Recommendations for future studies	71
REFERENCES	72
APPENDICES	
APPENDIX A NUMERICAL ANALYSIS OF COMPRESSIVE STRENGTH	83
APPENDIX B FACTOR OF SAFETY	85
BIOGRAPHY	98



LIST OF TABLES

Table		Page
2.1	Slope surface subsidence.....	11
2.2	Compressive and tensile strengths of cement seals.....	17
3.1	Typical chemical compositions of ordinary Portland cement type V (ASTM C150).....	23
3.2	Results of oxide concentrations in the sludge samples.....	25
3.3	Atterberg's limits and specific gravity of sludge.....	26
3.4	Specimen dimensions after preparation.....	30
4.1	Results of the uniaxial compression test.....	39
4.2	Cohesions and friction angles of cement mixtures.....	51
4.3	Four-point bending test results of cement mixtures.....	53
5.1	Summary of Tensile stresses and strains.....	61
B.1	Tensile strain energy ($W_{T,i}$) of the pure cement in borehole as brine to cement ratio = 0.6.....	86
B.2	Tensile strain energy ($W_{T,i}$) of the cement mixed with sand in borehole as brine to cement ratio = 0.6.....	86
B.3	Tensile strain energy ($W_{T,i}$) of the cement mixed with sludge in borehole as brine to cement ratio = 0.6.....	87
B.4	Tensile strain energy ($W_{T,i}$) of the pure cement in borehole as brine to cement ratio = 0.8.....	88

LIST OF TABLES (continued)

Table	Page
B.5 Tensile strain energy ($W_{T,i}$) of the cement mixed with sand in borehole as brine to cement ratio = 0.8.....	88
B.6 Tensile strain energy ($W_{T,i}$) of the cement mixed with sludge in borehole as brine to cement ratio = 0.8.....	89
B.7 Tensile strain energy ($W_{T,i}$) of the pure cement in borehole as brine to cement ratio = 1.0.....	90
B.8 Tensile strain energy ($W_{T,i}$) of the cement mixed with sand in borehole as brine to cement ratio = 1.0.....	90
B.9 Tensile strain energy ($W_{T,i}$) of the cement mixed with sludge in borehole as brine to cement ratio = 1.0.....	91
B.10 Maximum shear stress (τ_i) of the pure cement in borehole as brine to cement ratio = 0.6.....	92
B.11 Maximum shear stress (τ_i) of the cement mixed with sand in borehole as brine to cement ratio = 0.6.....	92
B.12 Maximum shear stress (τ_i) of the cement mixed with sludge in borehole as brine to cement ratio = 0.6.....	93
B.13 Maximum shear stress (τ_i) of the pure cement in borehole as brine to cement ratio = 0.8.....	94
B.14 Maximum shear stress (τ_i) of the cement mixed with sand in borehole as brine to cement ratio = 0.8.....	94

LIST OF TABLES (continued)

Table		Page
B.15	Maximum shear stress (τ_i) of the cement mixed with sludge in borehole as brine to cement ratio = 0.8.....	95
B.16	Maximum shear stress (τ_i) of the pure cement in borehole as brine to cement ratio = 1.0.....	96
B.17	Maximum shear stress (τ_i) of the cement mixed with sand in borehole as brine to cement ratio = 1.0.....	96
B.18	Maximum shear stress (τ_i) of the cement mixed with sludge in borehole as brine to cement ratio = 1.0.....	97

LIST OF FIGURES

Figure		Page
1.1	Research methodology.....	3
2.1	Sakon Nakhon and Khorat Basins containing rock salt ⁶ in the northeast of Thailand.....	8
2.2	Compressive strength according to the sludge content with different curing times (a) and Flexural strength according to the sludge content with different curing times (b).....	20
2.3	Uniaxial compressive strengths for B:C and S:C mixtures with W:C 10:10, 8:10, 12.5:10, 40:10 at 3 days of curing.....	21
2.4	Normal stress and peak shear stress of grouting material in sandstone fracture.....	21
3.1	Portland-pozzolan used in this study.....	22
3.2	Particle size distribution of sand.....	24
3.3	Particle size distribution of sludge.....	24
3.4	The mixing container used to prepare cement slurry.....	27
3.5	PVC molds with curing cement mixture.....	28
3.6	Some specimens prepared for uniaxial compression test (UCS) (a), triaxial compression test (TRI) (b) and four point bending test (FPB) (c).....	29
4.1	Uniaxial compression test apparatus.....	36
4.2	Triaxial compression test apparatus.....	36

LIST OF FIGURES (Continued)

Figure	Page
4.3 Four point bending test apparatus.....	37
4.4 Examples of post-test specimens from uniaxial compression strength test.....	38
4.5 Uniaxial compressive strength (σ_c) as a function of brine-to-cement ratio.....	39
4.6 Elastic modulus (E) as a function of brine-to-cement ratio.....	40
4.7 Poisson's ratio (ν) as a function of brine-to-cement ratio.....	40
4.8 Examples of post-test specimens from triaxial compressive strength tests.....	41
4.9 Stress-strain curves for cement: brine = 1:1.....	42
4.10 Stress-strain curves for cement: brine = 1:0.8.....	42
4.11 Stress-strain curves for cement: brine = 1:0.6.....	43
4.12 Stress-strain curves for cement: sand: brine = 1:1:1.....	43
4.13 Stress-strain curves for cement: sand: brine = 1:1:0.8.....	44
4.14 Stress-strain curves for cement: sand: brine = 1:1:0.6.....	44
4.15 Stress-strain curves for cement: sludge: brine = 1:1:1.....	45
4.16 Stress-strain curves for cement: sludge: brine = 1:1:0.8.....	45
4.17 Stress-strain curves for cement: sludge: brine = 1:1:0.6).....	46
4.18 Triaxial compressive strength tests results for cement: brine = 1:1 in form of Mohr's circles and Coulomb criterion.....	46
4.19 Triaxial compressive strength tests results for cement: brine = 1:0.8 in form of Mohr's circles and Coulomb criterion.....	47

LIST OF FIGURES (Continued)

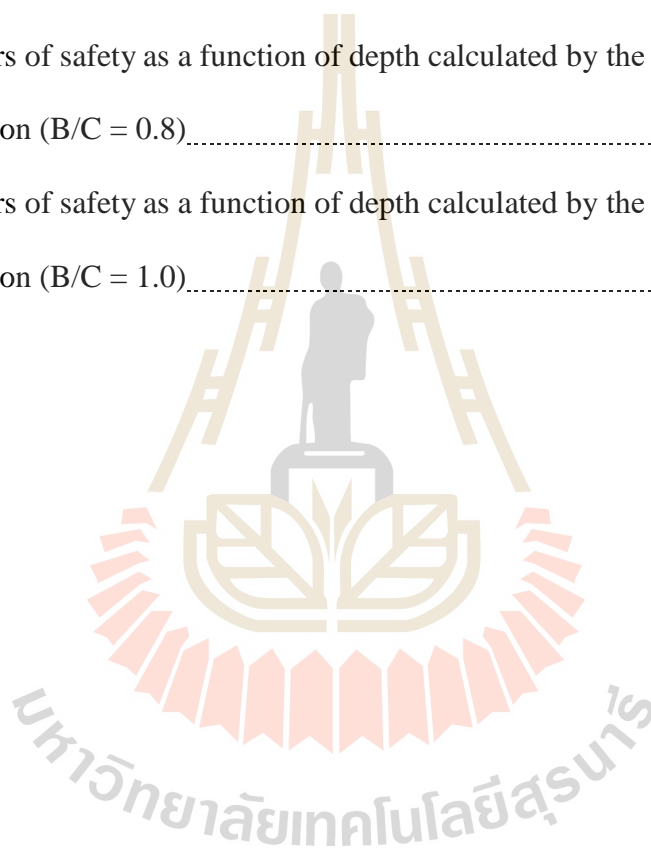
Figure	Page
4.20 Triaxial compressive strength tests results for cement: brine = 1:0.6 in form of Mohr's circles and Coulomb criterion.....	47
4.21 Triaxial compressive strength tests results for cement: sand: brine = 1:1:1 in form of Mohr's circles and Coulomb criterion.....	48
4.22 Triaxial compressive strength tests results for cement: sand: brine = 1:1:0.8 in form of Mohr's circles and Coulomb criterion.....	48
4.23 Triaxial compressive strength tests results for cement: sand: brine = 1:1:0.6 in form of Mohr's circles and Coulomb criterion.....	49
4.24 Triaxial compressive strength tests results for cement: sludge: brine = 1:0.5:1 in form of Mohr's circles and Coulomb criterion.....	49
4.25 Triaxial compressive strength tests results for cement: sludge: brine = 1:0.5:0.8 in form of Mohr's circles and Coulomb criterion.....	50
4.26 Triaxial compressive strength tests results for cement: sludge: brine = 1:0.5:0.6 in form of Mohr's circles and Coulomb criterion.....	50
4.27 Cohesion (MPa) as function of brine-to-cement ratio.....	51
4.28 Friction angles (degrees) as function of brine-to-cement ratio.....	52
4.29 Examples of pre-test and post-test specimens from four-point bending test...	53
4.30 Tensile stress-strain curves of cement mixture.....	54
4.31 Tensile stress-strain curves of cement-to-sand mixture.....	54
4.32 Tensile stress-strain curves of cement-to-sludge mixture.....	55

LIST OF FIGURES (Continued)

Figure	Page
4.33 Compressive stress-strain curves of cement mixture.....	55
4.34 Compressive stress-strain curves of cement-to-sand mixture.....	56
4.35 Compressive stress-strain curves of cement-to-sludge mixture.....	56
4.36 Tensile strength (σ_T) as a function of brine-to-cement ratio.....	57
4.37 Tensile strain (ε_T) as a function of brine-to-cement ratio.....	57
4.38 Compressive modulus (E_C) as a function of brine-to-cement ratio.....	58
4.39 Tensile modulus (E_T) as a function of brine-to-cement ratio.....	58
5.1 Total strain energy densities (W_T) as a function of brine to cement ratios (B/C).....	62
5.2 Cement seal in borehole under bending with maximum slope of 3×10^{-3}	65
5.3 Factors of safety as a function of depth calculated by tensile strain energy (a) and the Coulomb's criterion (b).....	66
A.1 Uniaxial compressive strength as a function of compressive strength at the end of four-point bending test.....	84
B.1 Factors of safety as a function of depth calculated by tensile strain energy (B/C = 0.6).....	87
B.2 Factors of safety as a function of depth calculated by tensile strain energy (B/C = 0.8).....	89
B.3 Factors of safety as a function of depth calculated by tensile strain energy (B/C = 1.0).....	91

LIST OF FIGURES (Continued)

Figure	Page
B.4 Factors of safety as a function of depth calculated by the Coulomb's criterion (B/C = 0.6).....	93
B.5 Factors of safety as a function of depth calculated by the Coulomb's criterion (B/C = 0.8).....	95
B.6 Factors of safety as a function of depth calculated by the Coulomb's criterion (B/C = 1.0).....	97



SYMBOLS AND ABBREVIATIONS

α	=	Multiplier parameters
β	=	Empirical parameters
ϕ	=	Internal friction angle [degree]
σ	=	Normal stress [MPa]
σ_1, σ_3	=	Principle stress [MPa]
σ_c	=	Compressive strength [MPa]
σ_T	=	Tensile strength [MPa]
$\sigma_{T,i}$	=	Maximum induced tensile stresses
τ	=	Shear stress [MPa]
τ_i	=	Induced shear stress [MPa]
θ	=	Slope angles occurs at free end of borehole [degree]
ε	=	Strain [mill-strain]
ε_c	=	Compressive strain [mill-strain]
ε_T	=	Tensile strain [mill-strain]
$\varepsilon_{T,i}$	=	Induced tensile strains
ν	=	Poisson's ratio
ω	=	Uniform distributed load [N/m]
A	=	Cross section area of borehole [m ²]
c	=	Cohesion [MPa]
C	=	Horizontal distance away from axis [m]
d	=	Diameter [mm]

SYMBOLS AND ABBREVIATIONS (Continued)

E	=	Elastic modulus [Pa]
E_c	=	Compressive modulus [Pa]
E_T	=	Tensile modulus [Pa]
I	=	Moment of inertia [m ⁴]
l	=	Borehole depth [m]
L	=	Support span [mm]
M	=	Bending moment [N·m]
P	=	Load [N]
r	=	Radius [m]
V	=	Shear force [N]
W	=	Strain energy density [kPa]
$W_{T,i}$	=	Induced tensile strain energy

CHAPTER I

INTRODUCTION

1.1 Background and rationale

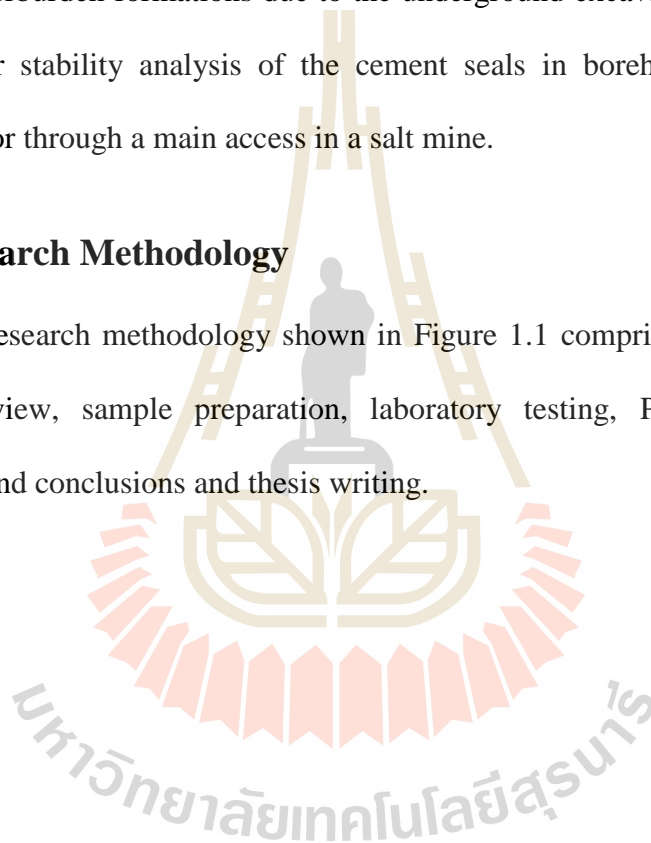
The penetrations of geological formations for the purpose of salt and potash exploration in the Maha Sarakham formation can have a detrimental impact on the environment. Boreholes that penetrate aquitards may allow migration and mixing of groundwater of different qualities, and may contaminate aquifers. Open boreholes may allow premature and unnecessary depressurization of formations, and may result in wasting of natural resources. The sealing method can be used to prevent or minimize the detrimental effects that may result from leaving geological penetrations open. Sealing abandoned exploratory drill hole is a partial important. The seals will ensure that the water protection layer (Middle Salt member) will remain impervious, and that the portions of the drill hole penetration the Lower Salt member will not become flow path of water or brine from the Lower Clastic Member into the mine openings. More important the borehole seal must be specifically designed to suite the site-specific for conditions where formation subsidence, may occur due to the underground excavations. The seals should be able to sustain the deformation and movement of the subsiding overburden formations due to the underground excavation.

1.2 Research Objective

The objective of this study is to assess the mechanical performance of the commercial grade cement mixtures seal in borehole. Their results are compared in terms of compressive and tensile strengths, elastic modulus and Poisson's ratio. The sealing materials should be able to sustain the deformation and movement of the subsiding overburden formations due to the underground excavations. The results are necessary for stability analysis of the cement seals in borehole to prevent water inflows into or through a main access in a salt mine.

1.3 Research Methodology

The research methodology shown in Figure 1.1 comprises 6 steps; including literature review, sample preparation, laboratory testing, Potential Application, discussions and conclusions and thesis writing.



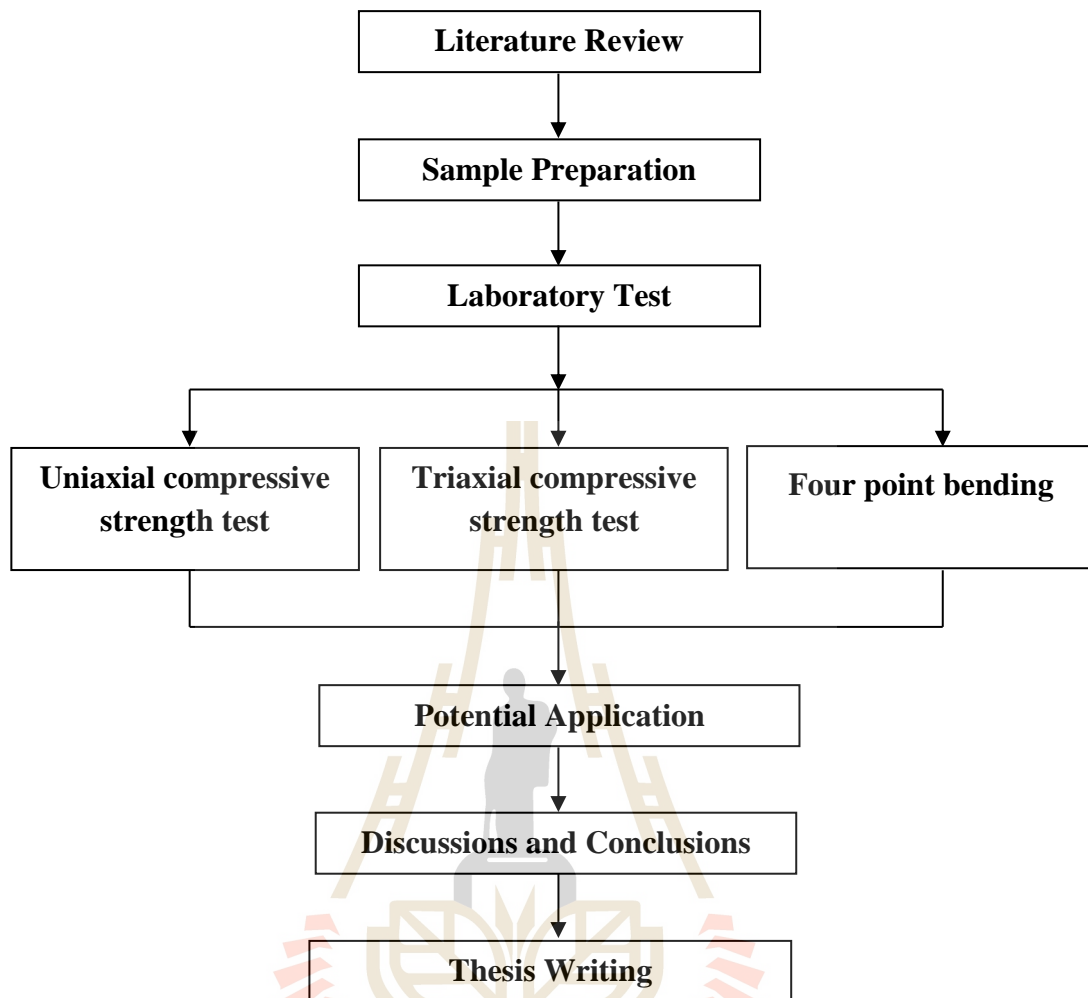


Figure 1.1 Research methodology.

1.3.1 Literature review

Literature review is carried out to study the previous researches and case studies to improve on understanding of sealing in salt and potash mines. The sources of information are from text books, journals, technical reports and conference papers. A summary of the literature review is given in the thesis.

1.3.2 Sample preparation

The grouting materials used in this research are

- 1) commercial grade Portland cement type V
- 2) sand with particle sizes less than 1 mm
- 3) water treatment sludge with particle sizes less than 75 μm

The mixing ratios of the cement-to-sand (C:S) of 1:1 and cement-to-sludge (C:SL) of 1:0.5 by weight. The ratios of brine to cement (B/C) vary from 1, 0.8 and 0.6. The brine is prepared from pure halite mixed with distilled water in plastic tank and stirred continuously. The grout preparation follows the API American Petroleum Institute No.10 (American Petroleum Institute, 1986). The cement slurry mixtures are poured and cured in 54 mm diameter PVC pipes for use in the mechanical testing. The specimens are cured in PVC pipe under saturated brine at room temperature before testing. A total of 135 specimens are prepared for the basic mechanical properties.

1.3.3 Laboratory tests

Characterization testing provides the compressive strength (σ_c), Elastic Modulus (E), Poisson's ratio (ν) and Tensile strength (σ_t) of cement grout.

1.3.3.1 Uniaxial compressive strength test

The procedures follow, as much as practical, the ASTM standards (D7012). During test, the axial and lateral deformations are monitored. The failure load is recorded

1.3.3.2 Triaxial compressive strength tests

The tests are performed in accordance with the ASTM standard (D7012). The load is applied along specimen axis with confining pressures of 0.35, 0.70, 1.05, 1.40, and 1.75 MPa until failure occurred.

1.3.3.3 Four point bending test

The tensile strength test is performed in accordance with ASTM standard (D6272) in the bending configurations.

1.3.4 Potential Application

The results can be compared with the Coulomb and the tensile strain energy can be used to assume the borehole stability.

1.3.5 Discussions and conclusion

Discussions are made on the reliability and adequacies of the approaches used here. Future research needs are identified. All research activities, methods, and results are documented and compiled in the thesis. The research or findings are published in the conference proceedings or journals.

1.3.6 Thesis writing

All study activities, methods, and results are documented and compiled in the thesis.

1.4 Scope and limitations

The scope and limitations of the research include as follows

1. The cement grout is prepared from the commercial grade Portland cement type V following ASTM (C150) standard practice, the NaCl saturated brine is used as mixing fluid.

2. Three cement mixtures are tested including:

- 1) Cement:Brine
- 2) Cement:Sand:Brine
- 3) Cement:Sludge:Brine

3. Uniaxial compression testing specimen length and diameter ratio (L/D) of

2.5. Up to 45 samples have been tested.

4. Triaxial compression test following specimen length and diameter ratio (L/D) of 2.0 with confining pressures of 0.35, 0.70, 1.05, 1.40, and 1.75 MPa. Up to 45 samples have been tested.

5. Four point bending test with specimen length and diameter ratio (L/D) of 4 are performed with applied loading rate of 4×10^{-4} MPa/s. A tested of 45 samples have been tested.

6. All specimens are cured for 28 days before testing.

7. All tests are conducted under ambient temperature.

8. The cement slurry mixtures follow API standard practice.

1.5 Thesis contents

Chapter I describes the background and rationale, the objectives, the methodology and scope and limitations of the research. Chapter II summarizes results of the literature review. Chapter III describes the sample preparation. Chapter IV describes the laboratory testing and test results. Chapter V describes the application of this research. Chapter VI summarizes the research results, and provides recommendations for future research studies.

CHAPTER II

LITERATURE REVIEW

2.1 Introduction

This chapter gives the results of literature review carried out to improve an understanding of cement seal in boreholes in salt and potash mines. Study the experimental researches on the rock salt in northeast region of Thailand, subsidence influence on underground borehole, borehole sealing and mechanical properties sealing materials. Information is from books, journals, technical reports and conference papers.

2.2 Rock salt in northeast region of Thailand

Rock salt formation in Thailand is located in the Khorat plateau as shown in Figure 2.1. The Khorat plateau covers 150,000 square kilometers, from 14° to 19° northern latitude and 101° to 106° eastern longitude. The northern and eastern edges of the plateau lie close to Laos and the southern one close to Cambodia (Utharoon, 1993).

Rock salt is separated into 2 basins: Sakon Nakhon Basin and Khorat Basin. The Sakon Nakhon Basin in the north has an area about 17,000 square kilometers. It covers the area of Nong Khai, Udon Thani, Sakon Nakhon, Nakhon Phanom, and Mukdahan provinces and extends to some part of Laos. The Khorat Basin is in the south, which has about 33,000 square kilometers. The basin covers the area of Nakhon Ratchasima, Chaiyaphum, Khon Kaen, Maha Sarakham, Roi Et, Kalasin,

Yasothon, Ubon Ratchathani provinces and the north of Buriram, Surin, and Sisaket provinces (Suwanich, 1986).

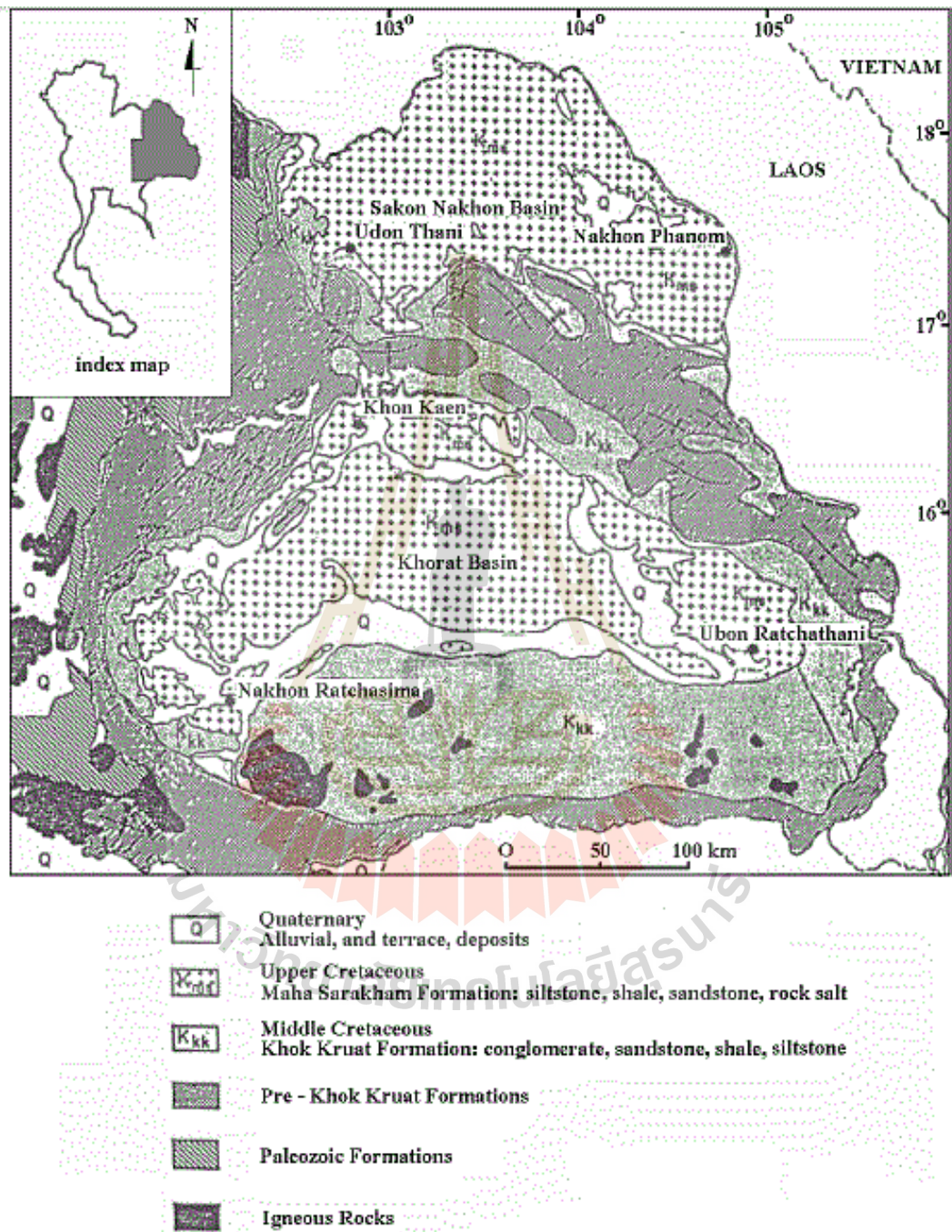


Figure 2.1 Sakon Nakhon and Khorat Basins containing rock salt in the northeast of Thailand (modified from Rattanajarurak, 1990 and Utha-aaron, 1993 adapted from Geological Map of Thailand, scale 1:2,500,000).

The Department of Mineral Resources has drill 194 drilled holes between 1976 and 1977 for the exploration of potash (Japakasetr, 1985; Japakasetr and Workman, 1981; Sattayarak, 1983, 1985; Japakasetr, 1992; Japakasetr and Suwanich, 1982). Some holes are drilled through rock salt layers to the Khok Kruat Formation (Yumuang et al., 1986; Supajanya et al., 1992; Utha-aroon, 1993; Warren, 1999). The sequences of rock layers from the bottom of this formation up to the top of the Maha Sarakham Formation are as follows.

1) Red bed sandstone or dense greenish gray siltstone sometime intercalate with reddish-brown shale.

2) Basal anhydrite with white to gray color, dense, lies beneath the lower rock salt and lies on the underlying Khok Kruat Formation.

3) Lower rock salt, the thickest and cleanest rock salt layer, except in the lower part which contains organic substance. The thickness exceeds 400 meters in some areas and form salt domes with the thickness up to 1,000 meters, with the average thickness of 134 meters.

4) Potash, 3 types were found; carnallite ($\text{KCl}\cdot\text{MgCl}_2\cdot 6\text{H}_2\text{O}$) with orange, red and pink color, sylvinite (KCl) rarely found, white and pale orange color, an alteration of carnallite around salt domes, and techydrite ($\text{CaCl}_2\cdot 2\text{MgCl}_2\cdot 12\text{H}_2\text{O}$) often found and mixed with carnallite, orange to yellow color caused by magnesium, the dissolved mineral occurred in place.

5) Rock salt, thin layers with average thickness of 3 meters, red, orange, brown, gray and clear white colors.

6) Lower clastic, clay and shale, relatively pale reddish-brown color and mixed with salt ore and carnallite ore.

7) Middle salt, argillaceous salt, pale brown to smoky color, thicker than the upper salt layer with average thickness of 70 meters, carnallite and sylvite may be found at the bottom part.

8) Middle clastic, clay and shale, relatively pale reddish brown color and intercalated with white gypsum.

9) Upper salt, dirty, mixed with carbon sediment, pale brown to smoky color or orange color when mixed with clay and 3 to 65 meters thick.

10) Upper anhydrite, thin layer and white to gray color.

11) Clay and claystone, reddish brown color, occurrence of siltstone and sandstone in some places.

12) Upper sediment, brownish gray clay and soil in the upper part, and sandy soil and clay mixed with brown, pink and orange sandy soil in the lower part.

2.3 Subsidence influence on underground borehole

The subsidence is an inevitable consequence of underground mining. Whenever a cavity is created underground, due to the mining of minerals or for any other reason, the stress field in the surrounding strata is disturbed (Bozeman, 2002; Bell et al., 2000; Johnson, 2005; Chrzanowski et al., 1997; Mancini et al., 2009). These stress changes produce deformations and displacements of the strata, the extent of which depends on the magnitude of the stresses and the cavity dimensions (Sahu and Lokhande, 2015). With time, supporting structures deteriorate and the cavity enlarges, resulting in instability. This induces the superjacent strata to move into the void. Gradually, these movements work up to the surface, manifesting them as a depression. This is commonly referred to as subsidence. Thus mine subsidence may

be defined as ground movements that occur due to the collapse of overlying strata into mine voids. Surface subsidence generally entails both vertical and lateral movements (Hartman, 1992).

Singh (1992) states that the subsidence consists of five major components, which influence damage to surface structure and renewable resources are vertical displacement, horizontal displacement, slope, vertical strain and vertical curvature. The maximum surface slope of 3×10^{-3} to ensure that the subsidence slope will not impact the engineering structures and natural resources on the surface within mine area (Table 2.1).

Table 2.1 Slope surface subsidence.

Type of Damage	Slope Limit ($\times 10^{-3}$)	References
Functional (undulations and water accumulation)	5	Kratzsch (1983)
Large scale cracking affecting base/subgrade; severe	10	Sowers(1962)
local gradient; potholes	10-20	Kratzsch (1983)
Risk of derailment and rider discomfort	12.5	Kratzsch (1983)
	10	Saxena and Singh (1980)
Moderately reduced productively	2-3	Inferred
Severely reduced productively	6	Pierce et al., (1983)
	6-8	Fehrenbacher et al., (1978)
	5-8	Annon (1951)
Railroad	10	Singh (1992)
Road	5	
Farmland	2-3	

2.4 Borehole sealing

The sealing of mine openings and boreholes divided into permanent, temporary, and semi-permanent sealing (Gray and Gray, 1992) as well as the sealing of groundwater wells into three categories: temporary sealing, sealing actively used boreholes, and sealing for permanent decommissioning (Smith, 1994).

Fuenkajorn and Daemen (1996) classify borehole sealing into two main categories:

- 1) Sealing actively used boreholes
- 2) Sealing unused boreholes

Sealing actively used boreholes involves sealing of the annular zone between casing or pipe and the host rock and sealing of open boreholes that will be used in the future. The reasons for sealing of actively used boreholes are to protect the casing from corrosion, to prevent blowouts by quickly forming a seal, to protect the casing from shock loads in drilling deeper, and to seal off zones of circulation or thief zones (Economides et al., 1998). Sealing unused boreholes represent permanent sealing, which mainly involves sealing of any abandoned boreholes or wells. The primary function of seals for unused boreholes is to isolate zones of gas or liquid, which mainly emphasizes on environmental protection (Fuenkajorn and Daemen, 1996). The reasons for sealing of unused boreholes are to prevent groundwater contamination, to prevent poor aquifer groundwater from moving between water-bearing zones, to conserve aquifer yield and artesian pressure, and to remove any physical hazard (Smith, 1993). Sealing of borehole in rock has been developed approximately 20 years ago. The intensive research and development of this technology have been done by Prof. Jaak J.K. Daemen (Fuenkajorn and Daemen,

1996). Most of the research has been emphasized on the mechanical, hydrological and chemical properties of sealing materials. Parts of research have involved with design of borehole sealing in rock.

Fuenkajorn (2007) designs methodology and process for sealing of boreholes in rock mass have been derived. The design criteria present from relevant experimental researches are used to select the sealing materials for each rock unit, and to develop the seal specifications. The results of selecting appropriate sealing materials, which include mixtures of cement, bentonite, and granular materials. The seal system performance (seal, host rock and their interface) is evaluated in terms of the mechanical stability, containment integrity and chemical compatibility, while considering the economic constraints and the local resources.

The length of cementitious seals should be sufficient such that they can maintain their mechanical stability. Based on the results from laboratory testing and numerical analyses on the shearing strength of borehole seal in rock, Akgun and Daemen (1991c) conclude that permanent abandonment borehole seals should be designed with a length-to-diameter ratio of four or greater.

2.5 Mechanical properties sealing materials

Sealing materials should be selected for specific seal locations considering the borehole conditions and in situ stresses and their subsequent changes, as well as the geomechanical and chemical properties of the surrounding rock mass. For permanent sealing, the physical and chemical compatibility among seals, backfill and surrounding rock should be taken into account so that the originally intended seal

functions are maintained. Sealing materials will ensure flow path of water or brine into the mine openings where formation subsidence.

2.5.1 Pure cement

Akgun (1997) conducts series of the bond strength between cement grout and host rock. Two types of expandable cement grout formulation are Self-Stress I grout slurry is prepared by mixing 659 g of Self-Stress I cement formulation with 493 g of NaCl-saturated brine and Saltbond II grout slurry is prepared by mixing 1000 g of Class H cement, 450 g of NaCl-saturated brine, 64 g of D604 (a liquid additive) and 4.4 g of M45 (an anti-foam agent). The results of push-out tests on cement grout plugs in salt average interface shear strengths ranged from 2 to 12 MPa. Hence, bonding between rock salt and Saltbond II cement grout plugs is better than for Self-Stress I cement grout.

Akgun and Daemen (2002) study the degrees of saturation of the cement plugged cylinder that affected strength of the expansive cement by conducting push-out test. The study factor includes the relationship between the degree of saturation versus the strength of cement, as well as the radius of sealing sample versus the strength of cement. Rock specimen is a cylinder shaped tuff with hollowed out at the center. Radiuses of the hollows are 6.35, 12.70, 25.40 and 50.80 mm. The outer radius ranges between 38.10 and 93.66 mm. Degree of saturation of the test samples are divided into three levels 1) completely dry, 2) low saturated degree, and 3) medium saturated degree. The tests reveal that the axial strength (friction between cement and rock) and the shear strength are high in the sample with higher degree of saturation, and are lower in the smaller specimen diameter. The results from the test

indicate that in order to obtain low permeability and high strength seals, the location of cement sealing should be submerged in groundwater.

Akgun and Daemen (2004) study an expansive cementitious borehole plug emplaced in an underground opening in the vicinity which generate radial stresses on the walls of the opening due to an axial stress apply to the borehole plug due to plug swelling. As these radial stresses might lead to the tensile fracturing of the rock, minimizing or preferably eliminating tensile stresses in rock was particularly important to preserve waste containment. Presents the theoretical radial (normal) stress distribution and tensile strength in a borehole plug-rock system due to combine axial, thermal and lateral loading, along with analysis indicate that the mean tensile strength of rock exceed the tensile strength of in-situ borehole plugs, and suggest that the rock hosting in-situ borehole plugs is fairly stable against tensile fracturing. The tensile strengths of rock measured in this study represent low bounds due to the absence of confining pressure.

Samaiklang and Fuenkajorn (2013) study the mechanical and hydraulic performance of commercial grade cement grouts in rock fracture. The results are compared in terms of compressive strength, tensile strength, bond strength and push-out strength for against rock fracture. All grouts are prepared by mixing at the water-cement ratio of 0.60. The compressive strength after 28 day curing times is 25.77 ± 2.54 MPa and the average tensile strength is 2.80 ± 0.27 MPa. The bond strength test and push-out test results indicate that the bond strength between the cured grout and Phu Kradung sandstone fractures is varying from 1.03 to 2.53 MPa, and the push-out strength varying from 4.06 to 5.55 MPa.

Pattani and Tepnarong (2015) study the cement seals in the rock salt to minimize brine circulation and potential leakage along a main access of salt mine. Weight composition of grouting cement slurry is commercial grade Portland cement with chloride resistant agent 1000 g mix saturated brine (NaCl) 670 g, anti-form agent 10 g and a liquid additive including expansion 10 g. After 28 day curing times the uniaxial compressive and Brazilian tensile strengths are 20.06 ± 3.82 MPa and 2.89 ± 0.19 MPa, respectively. The direct shear tests results indicate the frictional resistance at cement-salt interface with a friction angle of 44 degrees and a cohesion of 2.12 MPa. The normal stiffness is 7.67 GPa/m. The shear stiffness is 6.60 GPa/m. The push-out test results show significantly the higher frictional resistance at the interface than does the direct shear testing. The axial shear strength of the borehole cement seal is 5.05 MPa.

2.5.2 Cement mixed with sand

Sand is a major component of concrete and without the sand, concrete will not function as intended. The properties of a specific concrete mix will be determined by the proportion and type of sand used to formulate the concrete. In general, aggregate used for concrete must be well-graded to produce a dense mass with minimum voids. Aggregate that is not well-graded may reduce the strength of finished concrete and increase the cost of the mix because of the additional paste required to fill voids. The cement mixed with sand shows higher compressive strength, tensile strength, elastic modulus modulus (Yang et al., 1997; Donza et al., 2002; Güneyisi et al., 2004; Olugbenga, 2007; Moghadam and Khoshbin, 2012; Rahmani et al., 2012; Bumanisa and Bajarea, 2017). This section summarizes

compressive and tensile strength of cementitious seals obtained by various researchers (Table 2.2).

Table 2.2 Compressive and tensile strengths of cement seals.

Mix proportion cement:fine:coarse	Brine/ cement ratio	Compressive strength (MPa)	Tensile strength (MPa)	References
1: 3: 0	0.39	41.60	-	Kaushik and Islam (1995)
1: 1.37: 1.86	0.40	49.50	-	
1: 1.48: 2.22	0.48	39.50	-	
1: 1.51: 4.01	0.47	33.47	8.08	Mbadike and Elinwab (2011)
1: 1.66: 4.24	0.50	32.22	3.39	
1: 1.61: 4.03	0.55	31.38	8.18	
1: 1.5: 3	0.40	29.27	-	Kaushik and Islam (1995)
	0.45	26.80	-	
1: 2: 4	0.40	22.91	-	
	0.45	19.98	-	
1: 1.66: 2.49	0.40	65.63	4.83	Anwar and Roushdi (2013)
1: 1.74: 2.61		78.77	4.88	
1: 1.83: 2.75		80.34	4.96	
1: 2: 4	0.60	21.93	-	Olutoge et al., (2014)
1: 1.41: 2.69	0.41	42.14	6.56	Raju et al., (2014)
1: 1.5: 2.83	0.43	40.98	6.00	
1: 1.8: 3.31	0.45	41.34	-	Tiwari et al., (2014)
1: 1.78: 2.83	0.47	31.10-33.18	-	Maniyal and Patil (2015)
1: 1.43: 2.47	0.41	35.67-37.63	-	
1: 1.5: 4	0.47	33.50	8.10	Elinwa et al., (2016)
1: 1.5: 3	0.55	22.91	5.39	Premchand et al., (2016)
1: 1.22: 2.54	0.42	36.00	8.50	Karthikeyan and Nagarajan (2016)
1: 1.5: 3	0.30	23.51	3.82	Agrawal and Chandak (2017)
1: 4: 0		10.83	0.42	
1: 2.96: 0	0.50	34.00	5.20	Caronge et al., (2017)
1: 2.09: 4.04	0.45	37.04	5.83	Gawande et al., (2017)
1: 2: 4	0.50	46.46	-	Guo et al., (2018)

Hashemi et al. (2015) study the behavior of these materials, thick wall hollow cylinder (TWHC) and solid cylindrical synthetic specimens are designed and prepared by adding Portland cement and water to sand grains. The effect of borehole size on TWHC specimens reveals that with the increasing borehole size, the ductility of the specimen decreases, however, the axial and lateral stiffness of the TWHC specimen remain unchanged. Under different confining pressures the lateral strain at the initiation point of borehole breakout is considerably lower in a larger size borehole (20 mm) compared to that in a smaller one (10 mm). Also, it is observed that the level of peak strength increment in TWHC specimens decreases with increasing confining pressure.

2.5.3 Cement mixed with sludge

Kuo et al. (2007) study the feasibility of sludge as a substitute for a portion of fine aggregates in cement mortars. The compressive strengths of cement mortars with various percentages of organo-modified reservoir sludge (OMRS) particles were measured and then compared to those of plain cement mortars. The experimental results indicate that it could be possible to replace up to 30% by weight of fine aggregates by OMRS particles in a cement mortar for normal practice.

Deethouw and Tepnarong (2014) assess the performance of sludge-mixed cement grouts for sealing boreholes in rock salt. The results indicate that the viscosity of grout slurry tends to increase as the sludge-mixed cement (S:C) ratio increases. The compressive strength after 28 day curing times is 9.58 ± 0.52 MPa. The highest compressive strength is from S:C = 5:10. The average tensile strength is 1.99 ± 0.14 MPa. The highest ability of cement grouts decreases. Similarities and

discrepancies of the grouting performance in terms of mechanical and hydraulic properties are compared.

Chatveera et al. (2006) determine the mechanical and durability of mortar to replace cement with dry sludge ash. This research studies the chemical compositions and physical properties of the dry sludge ash, including the compressive strength and modulus of elasticity. The durability aspects, such as drying shrinkage and weight loss due to acid attack, were investigated. Binder materials containing various proportions between the sludge ash and Portland cement 0% to 100% by weight are prepared with the water to the binder material ratios of 0.5, 0.6, and 0.7. The results indicate when increasing the percentage of sludge water in mixing water, the drying shrinkage and weight loss due to acid attacks increased, and the slump and strength decreased.

Mun (2007) studies the physical properties and compared to those of a commercial sintered lightweight aggregate for nonstructural concrete. Portland cement (OPC) is mixed four types of lightweight coarse aggregate with the ratios of clay: sewage sludge ratio of 1:1, 1:3, and 1:5. In cases of the aggregate with higher mixing ratios of sewage sludge, the compressive strength is over 15 MPa and the flexural strength is over 3 MPa. The density ranges from 1,400 to 1,500 kg/m³ at a curing time of 14 days.

Valls et al. (2004) study the concrete consisting of Portland cement with dry sludge, four percentages of sludge in the cement mix: reference concrete or 0, 2.5, 5 and 10%. The results indicate that compressive and flexural strength increase with increasing of curing time and they decrease with increasing sludge content (Figure 2.2).

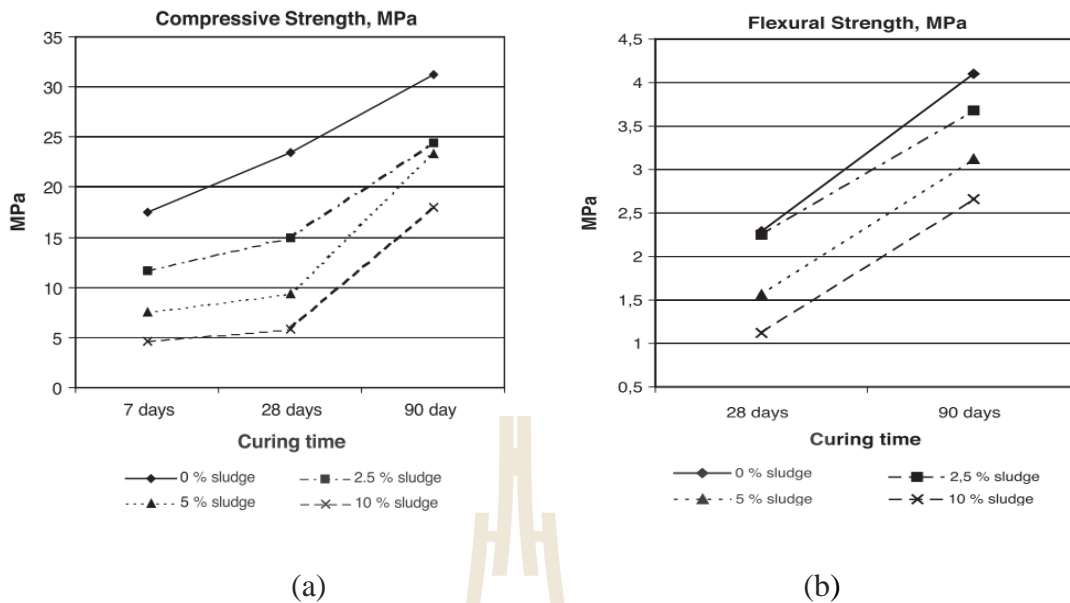


Figure 2.2 Compressive strength according to the sludge content with different curing times (a) and Flexural strength according to the sludge content with different curing times (b) (Valls et al., 2004).

Wetchasat (2013) assesses the performance of sludge mixed with the commercial grade Portland cement type I for reducing permeability of fractures in sandstone. The results indicate that the suitable mixing ratios for sludge:cement (S:C) are 1:10, 3:10, 5:10 with water-cement ratio of 1:1 by weight. For S:C = 3:10, the highest compressive strength are 1.22 MPa (Figure 2.3). The shear strength of grouted fractures varies from 0.22 to 0.90 MPa under normal stresses ranging from 0.25 to 1.25 MPa (Figure 2.4).

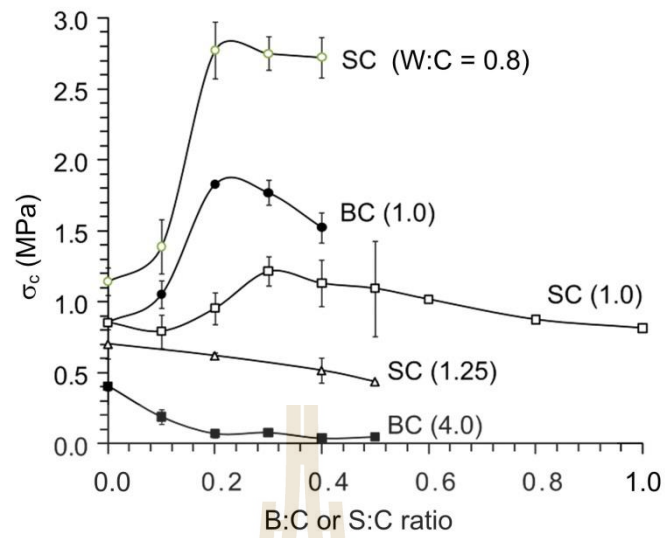


Figure 2.3 Uniaxial compressive strengths for B:C and S:C mixtures with W:C 10:10, 8:10, 12.5:10, 40:10 at 3 days of curing (Wetchasat, 2013).

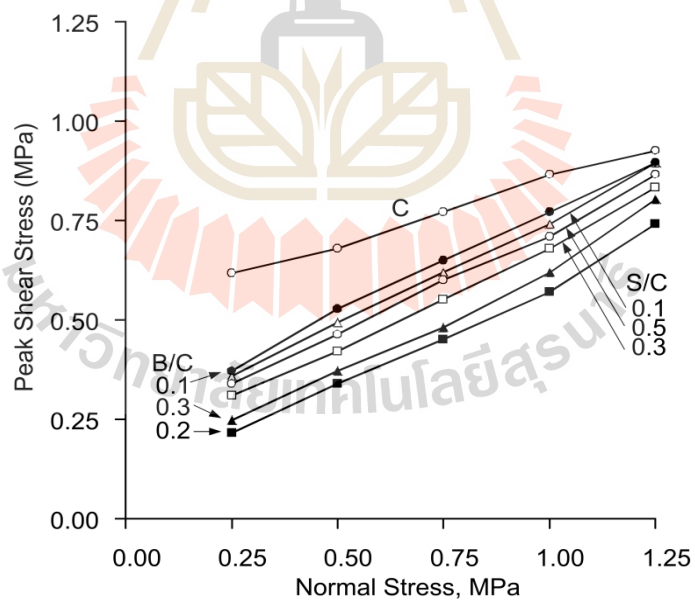


Figure 2.4 Normal stress and peak shear stress of grouting material in sandstone fracture (Wetchasat, 2013).

CHAPTER III

SEAL MATERIAL PREPARATION

3.1 Introduction

This chapter describes basic characteristics of materials test. Materials uses in this experiment are Portland cement, sand, sludge and saturated brine. Nine mixing proportions of sealing materials are made for basic mechanical property tests. Preparation of these samples follows, as much as practicable, the ASTM standard practice (ASTM D7012).

3.2 Material preparation

3.2.1 Portland cement type V

Portland-pozzolan cement is selected due to its low brine demand, sulfate resistance and widely used in construction industry (Figure 3.1). The chemical compositions of these materials are given in Table 3.1.



Figure 3.1 Portland-pozzolan used in this study.

Table 3.1 Typical chemical compositions of ordinary Portland cement type V

(ASTM C150).

Compositions	(% weight)
Tricalcium Silicate (C ₃ S)	38.0
Dicalcium Silicate (C ₂ S)	43.0
Tricalcium aluminate (C ₃ A)	4.6
Tetracalcium alumino ferrite (C ₄ AF)	9.0
Magnesium oxide (MgO)	1.9
Sulfur trioxide (SO ₃)	1.8
Ignition loss	0.9
Calcium oxide (CaO)	0.8

3.2.2 Sand

Sand is an important building material. It abundantly occurs in nature and is formed by the decomposition of rocks. The most important factor concerning sand used in concrete is that it must be clean. Figure 3.2 shows particle size distribution of the sand. The particle sizes less than 1 mm is used in this study.

3.2.3 Sludge

Sludge is collected from the dewatering plant of Bang Khen Water Treatment Plant located in Bangkok Metropolis. The grain size distribution curve is shown in Figure 3.3. The dried sludge is sieved through a mesh no. 200 with particle sizes less than 75 μm used in this research. Tables 3.2 and 3.3 show chemical compositions and the Atterberg's limits are index properties of the sludge. The chemical compositions are determined by X-Ray Fluorescence (XRF).

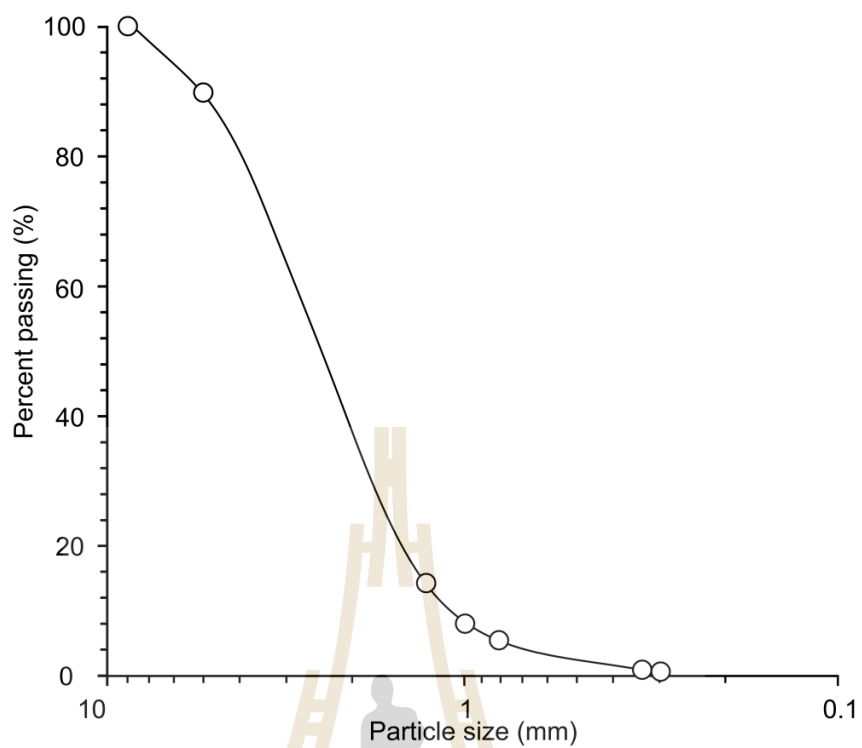


Figure 3.2 Particle size distribution of sand.

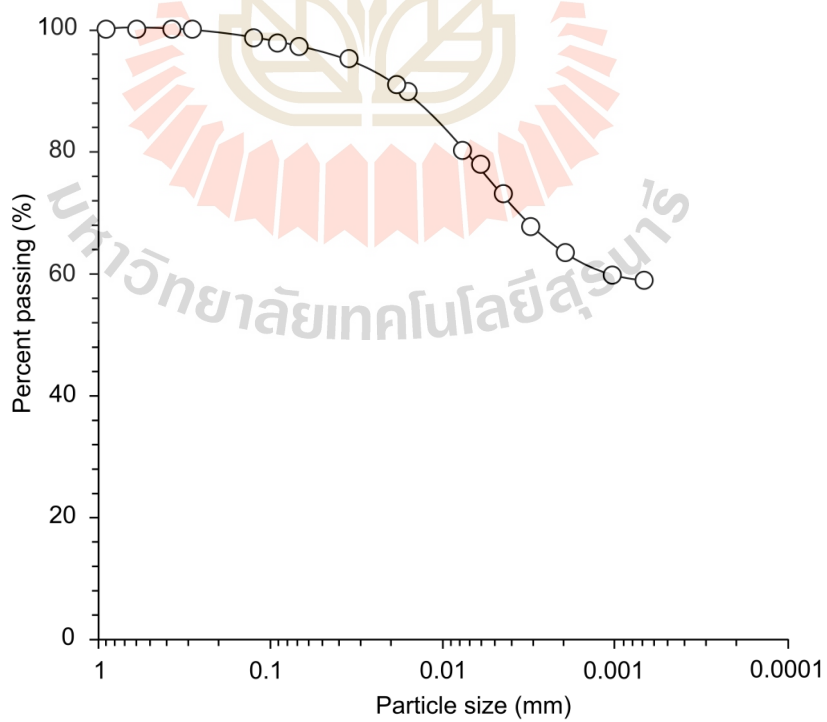


Figure 3.3 Particle size distribution of sludge.

Table 3.2 Results of oxide concentrations in the sludge samples.

Oxide	Concentration (% weight)	
	SUT	TU ²
Na ₂ O	0.22	0.37
MgO	0.96	1.43
Al ₂ O ₃	23.47	25.76
SiO ₂	52.37	59.44
P ₂ O ₅	0.34	0.30
SO ₃	0.55	0.37
Cl	0.07	-
K ₂ O	1.55	2.39
CaO	0.79	0.91
TiO ₂	0.79	0.83
V ₂ O ₅	0.02	-
Cr ₂ O ₃	0.02	-
MnO	0.22	-
Fe ₂ O ₃	6.33	7.84
CuO	0.01	-
Rb ₂ O	0.01	-
SrO	0.01	-
Y ₂ O ₃	<0.01	-
ZrO ₂	0.03	-
Nb ₂ O ₅	<0.01	-
BaO	0.01	-
CeO ₂	N/D	-
LOI. at 1,025 °C	12.20	3.06
Total	100	-

Note: ¹SUT = Suranaree University of Technology Laboratory (Wetchasat, 2013)

²TU = Tummasart University Laboratory (after Hadsanan et al., 2006)

³N/D = Not detectable

Table 3.3 Atterberg's limits and specific gravity of sludge.

Atterberg Limits	Sludge (%weight)	
	SUT ¹	KU ²
Liquid limit	55	69
Plastic limit	22	42
Plasticity index	23	28
Specific gravity	2.56	-

Note: ¹SUT = Suranaree University of Technology Laboratory (Wetchasat, 2013)

²KU = Kasetsart University Laboratory after (Kanchanamai, 2003)

3.2.4 Saturated brine

Saturated brine is prepared by mixing pure salt (NaCl) with distilled water in plastic tank. It is stirred continuously for 30 minutes. The proportion of salt to water is about 39.1% by weight. The SG of the saturated brine in this study is 1.211 at 21 °C. The specific gravity of saturated brine can be calculated by:

$$SG_{\text{Brine}} = \rho_{\text{Brine}} / \rho_{\text{water}} \quad (3.1)$$

Where SG_{Brine} is specific gravity of saturated brine

ρ_{Brine} is density of saturated brine (measured with a hydrometer (kg/m³))

ρ_{water} is density of water equal 1,000 kg/m³

3.3 Cement slurry preparation

The components of cement slurry are commercial grade Portland cement mixed with sludge, sand and saturated brine. The mixing weight ratio of cement-to-sand (C:S) and cement-to-sludge (C:SL) are 1:1 and 1:0.5 respectively. The ratios of

brine-to-cement (B/C) vary from 1, 0.8 to 0.6. The cement slurry is performed according to American Petroleum Institute (1986) and Akgun and Daemen (1997). The saturated brine is poured into the mixing container (Figure 3.4) at a low mixture speed, and all components are added to the materials within 15 seconds. After all the cement is added, the slurry is mixed at high speed for additional 35 seconds. The cement slurry mixtures are poured and cured in 54 mm diameter PVC pipes for use in the mechanical testing. Figure 3.5 shows the specimens are cured in PVC pipe under saturated brine at room temperature (ASTM C192) for 28 days before testing.



Figure 3.4 The mixing container used to prepare cement slurry.

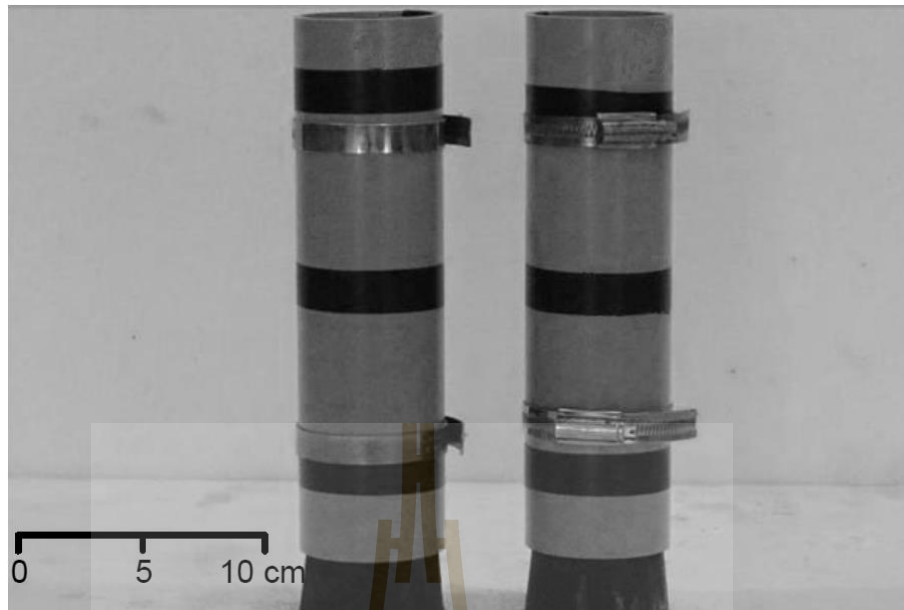


Figure 3.5 PVC molds with curing cement mixture.

3.4 Sample preparation

The specimens preparation used for compression test follow the applicable ASTM standard practice (D7012) and the ISRM suggested methods, as much as practical. The cylindrical specimens with a diameter of 54 mm. The L/D ratios of specimens are 2.5 for the uniaxial compression test and 2.0 for the triaxial compression test. The ratio of specimen for the four point bending test length to specimen diameter (L/D) is 4.0. A strain gage (TML, PFL-20-11-1L, 20 mm) is installed to measure tensile strains at the center of the specimen in horizontal. The main axis of the specimen is parallel. Gage length is 20 mm. and gage factor is $2.13 \pm 1\%$. A total of 135 specimens are prepared for basic mechanical properties testing. Some specimens are shown in Figure 3.6. Table 3.4 summarizes the specimen number, dimensions, and density

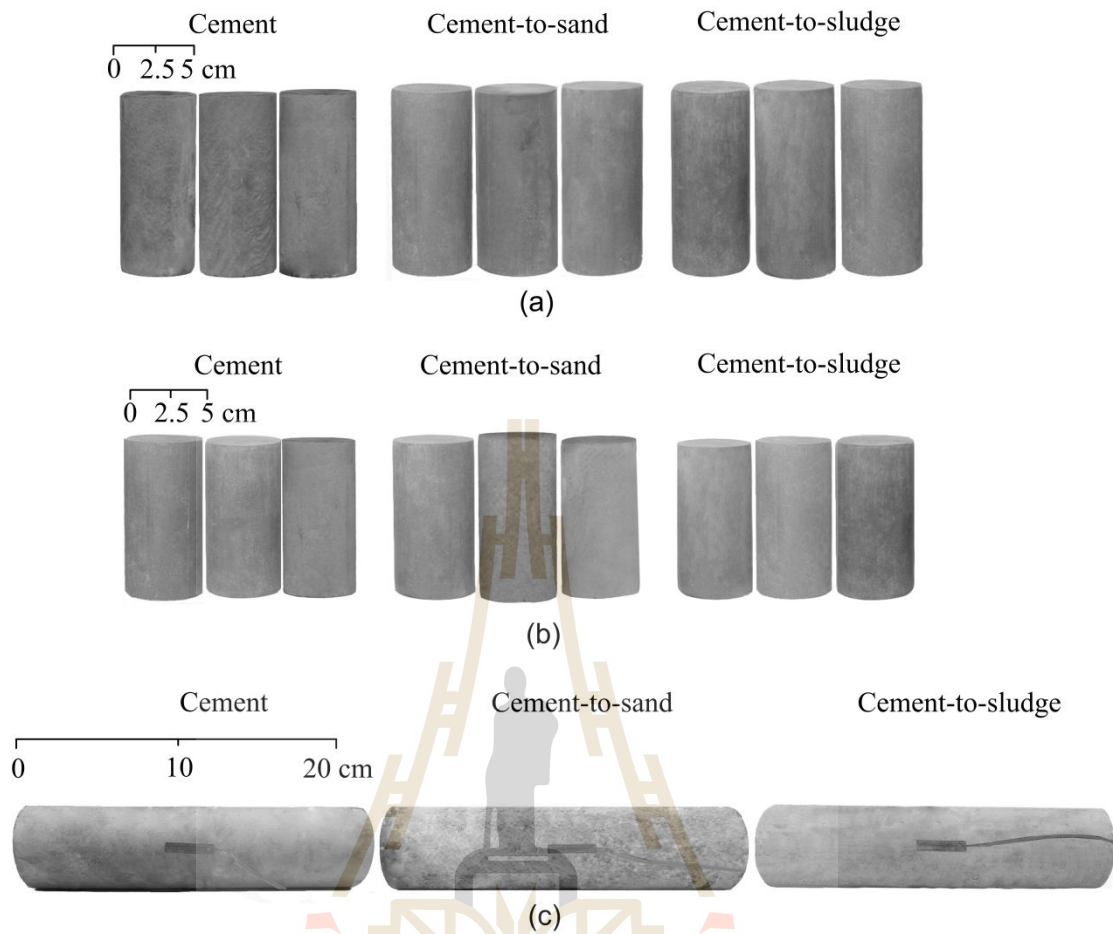


Figure 3.6 Some specimens prepared for uniaxial compression test (UCS) (a), triaxial compression test (TRI) (b) and four point bending test (FPB) (c).

Table 3.4 Specimen dimensions after preparation.

Specimen No.	Diameter (mm)	Height (mm)	Density (g/cc)
C-UCS-1.0-1	54.80	136.96	1.70
C-UCS-1.0-2	54.34	136.12	1.68
C-UCS-1.0-3	54.56	135.98	1.73
C-UCS-1.0-4	55.02	136.84	1.71
C-UCS-1.0-5	54.46	137.00	1.78
C-UCS-0.8-1	54.90	136.80	1.80
C-UCS-0.8-2	54.80	137.10	1.81
C-UCS-0.8-3	55.00	137.18	1.80
C-UCS-0.8-4	54.98	137.37	1.82
C-UCS-0.8-5	54.16	137.46	1.83
C-UCS-0.6-1	55.12	138.00	1.85
C-UCS-0.6-2	54.74	137.88	1.84
C-UCS-0.6-3	55.08	138.48	1.88
C-UCS-0.6-4	54.20	136.10	1.90
C-UCS-0.6-5	54.66	136.24	1.86
CS-UCS-1.0-1	55.10	137.68	1.85
CS-UCS-1.0-2	55.14	138.00	1.88
CS-UCS-1.0-3	54.98	137.90	1.89
CS-UCS-1.0-4	54.88	138.14	1.87
CS-UCS-1.0-5	55.12	138.66	1.86
CS-UCS-0.8-1	54.78	137.40	1.98
CS-UCS-0.8-2	55.04	138.22	1.97
CS-UCS-0.8-3	54.86	137.92	1.99
CS-UCS-0.8-4	54.98	137.64	1.95
CS-UCS-0.8-5	55.02	138.28	2.00
CS-UCS-0.6-1	54.84	137.40	2.13
CS-UCS-0.6-2	55.40	138.24	2.15
CS-UCS-0.6-3	55.14	138.46	2.20
CS-UCS-0.6-4	54.40	136.26	2.17
CS-UCS-0.6-5	55.68	138.88	2.18

Table 3.4 Specimen dimensions after preparation (continue).

Specimen No.	Diameter (mm)	Height (mm)	Density (g/cc)
CSL-UCS-1.0-1	54.32	136.00	1.68
CSL-UCS-1.0-2	54.66	136.50	1.66
CSL-UCS-1.0-3	54.80	137.12	1.70
CSL-UCS-1.0-4	54.74	137.24	1.64
CSL-UCS-1.0-5	55.02	138.28	1.62
CSL-UCS-0.8-1	54.98	137.88	1.74
CSL-UCS-0.8-2	55.12	138.90	1.72
CSL-UCS-0.8-3	54.70	137.16	1.75
CSL-UCS-0.8-4	54.56	137.40	1.74
CSL-UCS-0.8-5	55.14	138.58	1.71
CSL-UCS-0.6-1	55.20	138.14	1.83
CSL-UCS-0.6-2	54.90	137.64	1.80
CSL-UCS-0.6-3	55.12	138.66	1.77
CSL-UCS-0.6-4	55.04	138.20	1.76
CSL-UCS-0.6-5	55.18	138.72	1.79
C-TRI-1.0-1	53.82	107.28	1.71
C-TRI-1.0-2	53.54	107.40	1.70
C-TRI-1.0-3	54.00	107.18	1.73
C-TRI-1.0-4	53.46	107.20	1.71
C-TRI-1.0-5	53.32	107.06	1.72
C-TRI-0.8-1	53.54	107.00	1.79
C-TRI-0.8-2	53.80	106.48	1.80
C-TRI-0.8-3	53.10	107.24	1.80
C-TRI-0.8-4	53.34	106.96	1.81
C-TRI-0.8-5	53.52	106.90	1.84
C-TRI-0.6-1	53.08	106.78	1.88
C-TRI-0.6-2	53.38	107.00	1.86
C-TRI-0.6-3	53.82	107.42	1.88
C-TRI-0.6-4	54.00	107.46	1.90
C-TRI-0.6-5	53.54	107.50	1.89

Table 3.4 Specimen dimensions after preparation (continue).

Specimen No.	Diameter (mm)	Height (mm)	Density (g/cc)
CS-TRI-1.0-1	53.52	108.00	1.86
CS-TRI-1.0-2	53.28	107.90	1.87
CS-TRI-1.0-3	53.74	107.94	1.88
CS-TRI-1.0-4	53.16	107.88	1.87
CS-TRI-1.0-5	53.60	107.86	1.88
CS-TRI-0.8-1	53.28	107.54	1.96
CS-TRI-0.8-2	53.14	107.56	1.95
CS-TRI-0.8-3	54.02	108.14	1.99
CS-TRI-0.8-4	53.72	107.90	1.97
CS-TRI-0.8-5	53.66	107.76	2.10
CS-TRI-0.6-1	53.48	107.40	2.14
CS-TRI-0.6-2	53.80	107.74	2.18
CS-TRI-0.6-3	53.12	107.00	2.20
CS-TRI-0.6-4	53.20	107.14	2.19
CS-TRI-0.6-5	53.54	107.22	2.21
CSL-TRI-1.0-1	53.86	108.10	1.67
CSL-TRI-1.0-2	54.02	108.56	1.68
CSL-TRI-1.0-3	53.44	108.04	1.70
CSL-TRI-1.0-4	53.50	107.90	1.66
CSL-TRI-1.0-5	53.72	107.94	1.64
CSL-TRI-0.8-1	53.66	107.82	1.75
CSL-TRI-0.8-2	53.36	107.74	1.76
CSL-TRI-0.8-3	53.40	107.66	1.75
CSL-TRI-0.8-4	53.86	107.84	1.74
CSL-TRI-0.8-5	53.92	107.56	1.77
CSL-TRI-0.6-1	53.24	107.40	1.83
CSL-TRI-0.6-2	53.84	107.44	1.80
CSL-TRI-0.6-3	54.04	108.04	1.84
CSL-TRI-0.6-4	53.28	107.76	1.86
CSL-TRI-0.6-5	53.48	107.42	1.81

Table 3.4 Specimen dimensions after preparation (continue).

Specimen No.	Diameter (mm)	Height (mm)	Density (g/cc)
C-FPB-1.0-1	54.12	221.68	1.70
C-FPB-1.0-2	54.00	221.74	1.70
C-FPB-1.0-3	54.06	220.98	1.72
C-FPB-1.0-4	54.10	220.90	1.71
C-FPB-1.0-5	54.96	221.00	1.71
C-FPB-0.8-1	54.80	220.88	1.80
C-FPB-0.8-2	53.90	220.70	1.80
C-FPB-0.8-3	55.00	221.18	1.81
C-FPB-0.8-4	54.02	220.86	1.82
C-FPB-0.8-5	54.54	220.90	1.85
C-FPB-0.6-1	55.12	221.48	1.90
C-FPB-0.6-2	54.26	220.84	1.89
C-FPB-0.6-3	54.08	220.58	1.88
C-FPB-0.6-4	54.20	220.64	1.90
C-FPB-0.6-5	55.16	221.28	2.00
CS-FPB-1.0-1	55.00	221.76	1.87
CS-FPB-1.0-2	54.92	221.92	1.87
CS-FPB-1.0-3	54.70	221.56	1.88
CS-FPB-1.0-4	54.88	222.02	1.87
CS-FPB-1.0-5	55.20	222.28	1.90
CS-FPB-0.8-1	54.45	221.78	1.94
CS-FPB-0.8-2	54.62	221.84	1.96
CS-FPB-0.8-3	54.10	221.64	2.00
CS-FPB-0.8-4	54.72	221.44	1.99
CS-FPB-0.8-5	54.68	221.80	2.11
CS-FPB-0.6-1	54.70	221.92	2.18
CS-FPB-0.6-2	54.86	221.48	2.20
CS-FPB-0.6-3	54.82	221.36	2.22
CS-FPB-0.6-4	54.90	221.30	2.21
CS-FPB-0.6-5	55.04	221.98	2.25

Table 3.4 Specimen dimensions after preparation (continue).

Specimen No.	Diameter (mm)	Height (mm)	Density (g/cc)
CSL-FPB-1.0-1	54.92	222.14	1.70
CSL-FPB-1.0-2	54.66	221.20	1.68
CSL-FPB-1.0-3	54.78	221.18	1.71
CSL-FPB-1.0-4	54.64	221.70	1.69
CSL-FPB-1.0-5	54.28	221.46	1.64
CSL-FPB-0.8-1	54.40	221.52	1.75
CSL-FPB-0.8-2	54.96	221.66	1.77
CSL-FPB-0.8-3	54.42	221.26	1.78
CSL-FPB-0.8-4	54.68	221.90	1.79
CSL-FPB-0.8-5	54.52	222.00	1.80
CSL-FPB-0.6-1	54.84	221.74	1.85
CSL-FPB-0.6-2	54.28	221.00	1.88
CSL-FPB-0.6-3	54.44	221.60	1.89
CSL-FPB-0.6-4	54.56	221.48	1.82
CSL-FPB-0.6-5	54.92	222.74	1.85



CHAPTER IV

LABORATORY TESTING

4.1 Introduction

This chapter describes the methods and results of laboratory tests. The tests are divided into three groups; i.e. uniaxial compression test, triaxial compression test and four-point bending test.

4.2 Test methods

4.2.1 Compression test

The sample preparation and test procedure for the compression testing follow the applicable ASTM standard practice (D7012) and the ISRM suggested methods, as much as practical. The compressive strengths of the mixtures after curing for 28 days are measured from cylindrical specimens with no mind diameters of 54 mm. The L/D ratio of the specimens is 2.5 for the uniaxial compression test. The axial and lateral deformations are monitored during the test (Figure 4.1). The L/D ratio for the triaxial compression test is 2.0. The test apparatus of triaxial compression test is shown in Figure 4.2. The hydraulic pump is used as for the application of confining pressure. The confining pressures are from 0.34, 0.68, 1.02, 1.36 to 1.70 MPa. The axial stress is applied at a constant rate of 0.1-0.5 MPa/second until failure. The failure occurs within 5-15 minutes of loading under each confining pressure. The post-failure characteristics are observed. Based on the Coulomb's criterion the shear strength is represented by Jaeger et al., (2007);

$$\tau = c + \sigma_n \tan \phi \quad (4.1)$$

where τ is shear strength (MPa), c is cohesion (MPa), σ_n is normal stress (MPa) and ϕ is internal friction angle (degrees).

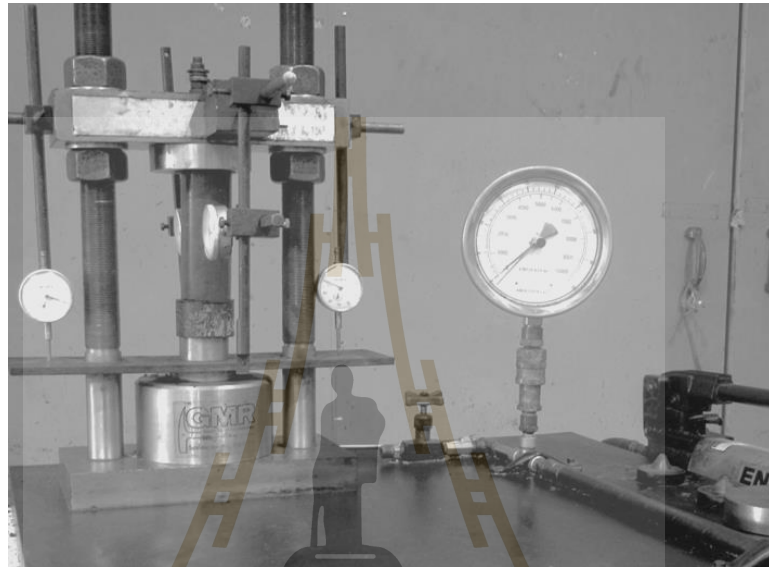


Figure 4.1 Uniaxial compression test apparatus.



Figure 4.2 Triaxial compression test apparatus.

4.2.2 Four point bending test

The test method and calculation for the four point bending test follow the ASTM standard practice (D6272). A data logger (TC-32K) connected a switching box (Type B-2760) is used to monitor the induced tensile strains while loading. The tensile stress at the crack initiation point can be calculated by ASTM D6272-10:

$$\sigma_T = 16PL/3\pi d^3 \quad (4.2)$$

where σ_T is tensile stress (MPa), P is applied load (N), L is support span (220 mm), and d is specimen diameter (54 mm). The load is applied under constant rate which is equivalent to the induced stress rate of 4×10^{-4} MPa/s at the center of the specimens. The specimen deformations are monitored and used to calculate the principal strains during loading. The readings are recorded every 50 N of load increment until failure (Figure 4.3).

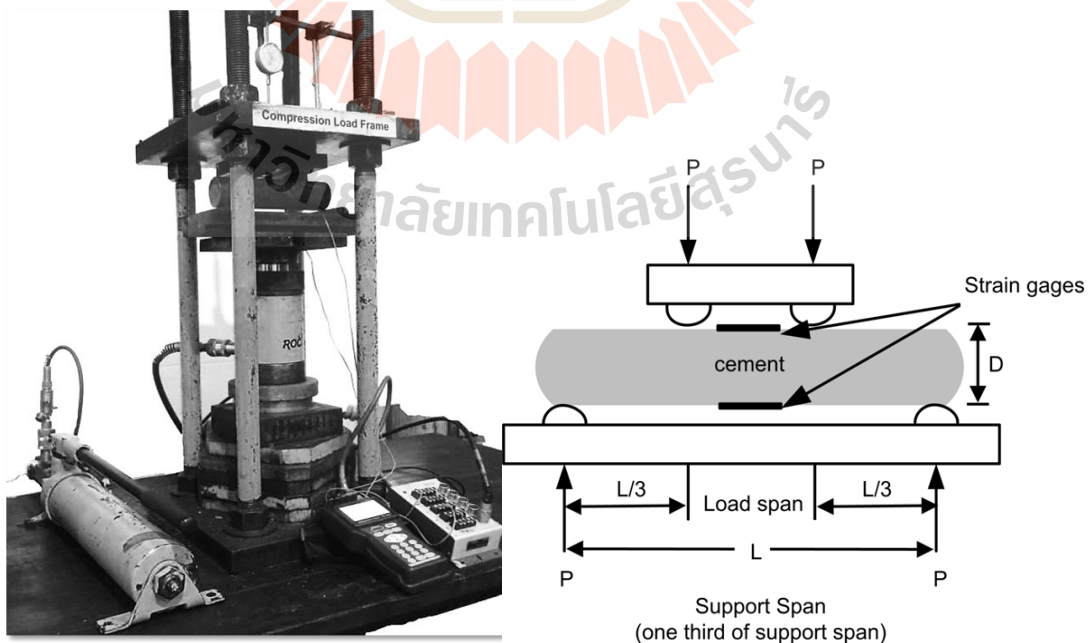


Figure 4.3 Four point bending test apparatus.

4.3 Test results

4.3.1 Compression test results

Some post-test specimens obtained from the uniaxial compression test are shown in Figure 4.4. Extensile like splitting parallel to the core axis is observed. Pores and micro-cracks in the specimen have been attributed as the cause of axial splitting. The results of uniaxial compressive strength test are shown in Table 4.1. Figure 4.5 plots the uniaxial compressive strength as a function of brine-to-cement ratio. The compressive strength increases as B/C ratio decreases. Under the same B/C ratio, the cement-sand mixtures show higher strengths than those of the pure cement and cement-sludge mixtures. The elastic moduli decrease and Poisson's ratios increase with increasing B/C ratio, as shown in Figures 4.6 and 4.7, respectively. The specimens mixed with sand tend to show higher elastic modulus and lower Poisson's ratio than those mixed with sludge.

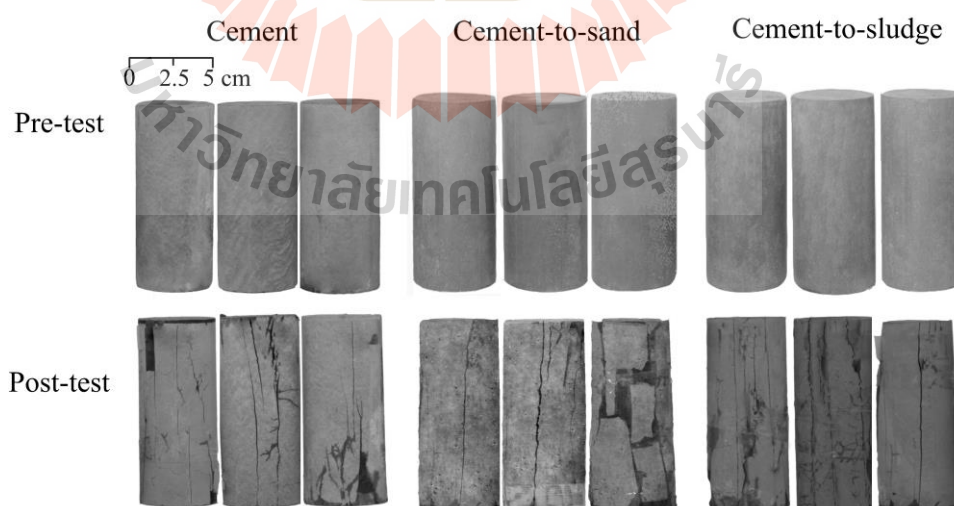
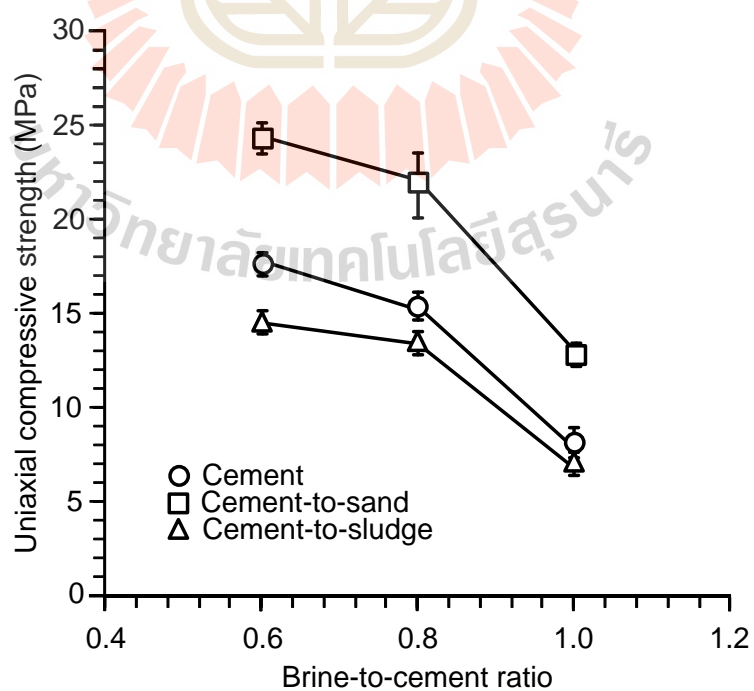


Figure 4.4 Examples of post-test specimens from uniaxial compression strength test.

Table 4.1 Results of the uniaxial compression test.

Mixtures	Brine-to-cement ratios	Uniaxial compressive strength (MPa)	Elastic modulus (GPa)	Poisson's ratio
Cement	1.0	7.80	12.13	0.16
	0.8	15.23	13.77	0.13
	0.6	16.50	16.33	0.12
Cement-to-sand	1.0	12.39	14.17	0.15
	0.8	21.85	15.50	0.11
	0.6	24.25	19.01	0.10
Cement-to-sludge	1.0	7.14	10.31	0.18
	0.8	13.42	12.19	0.14
	0.6	15.39	14.98	0.13

**Figure 4.5** Uniaxial compressive strength (σ_c) as a function of brine-to-cement ratio.

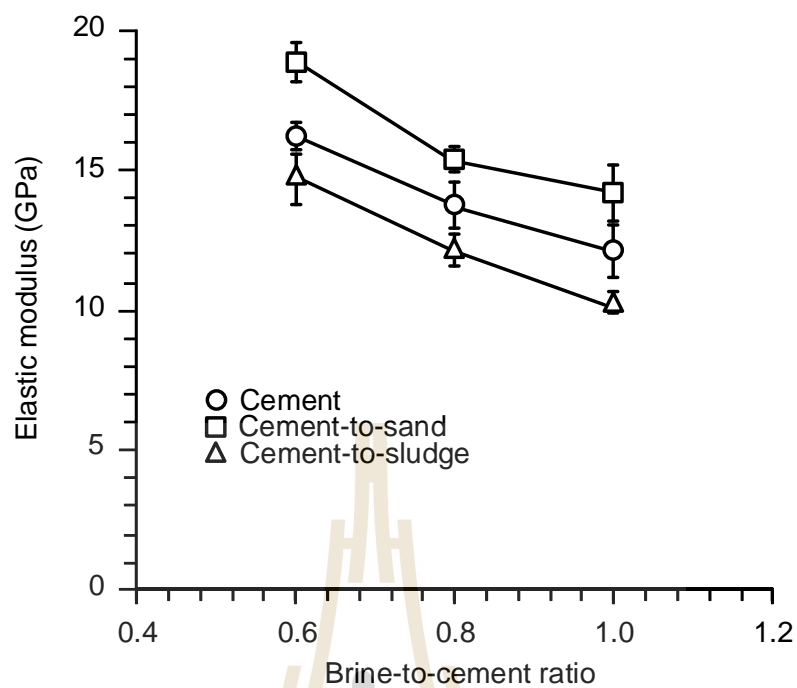


Figure 4.6 Elastic modulus (E) as a function of brine-to-cement ratio.

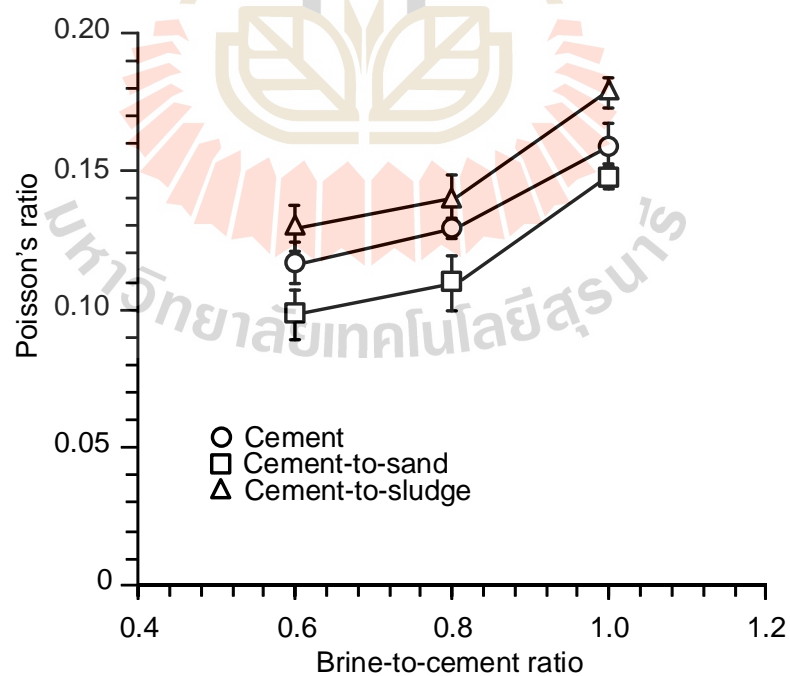


Figure 4.7 Poisson's ratio (ν) as a function of brine-to-cement ratio.

Figure 4.8 shows some post-test specimens obtained from the triaxial compression test under various confining pressures (σ_3). Shearing failure is observed under high confining pressure while extension failure is found in low confining pressure specimens. Figures 4.9 to 4.17 show the stress-strain curves under different confining pressures and B/C ratios. The diagrams show that higher confining pressures result in higher stresses and strains at failure. The compressive strength increases as B/C ratio decreases. Under the same B/C ratio, the cement-sand mixture shows higher strengths than those of the cement pure and cement-sludge mixtures. The elastic modulus and Poisson's ratio are determined from the tangent of the stress-strain curves at about 50% of the failure stress. Figures 4.18 through 4.26 show the Mohr circles of the results with shear stress as ordinates and normal stress as abscissas. The cohesion and internal friction angle are summarized in Table 4.2. It suggests that increasing the B/C ratio slightly decreases the cohesions and friction angles of the mixtures are shown in Figure 4.27 and Figure 4.28 respectively. The average cohesion and friction angle of the mixtures range from 2.33 to 3.38 MPa and 44 to 55 degrees.

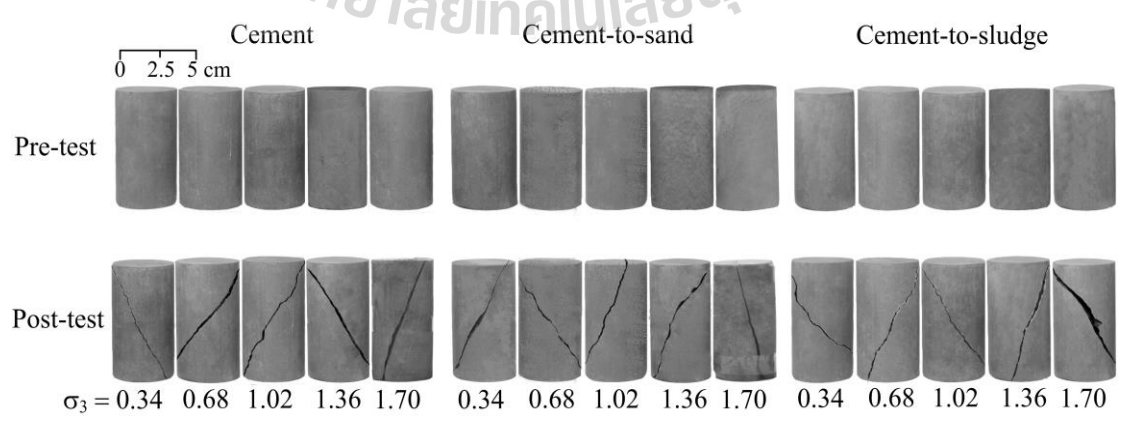


Figure 4.8 Examples of post-test specimens from triaxial compressive strength tests.

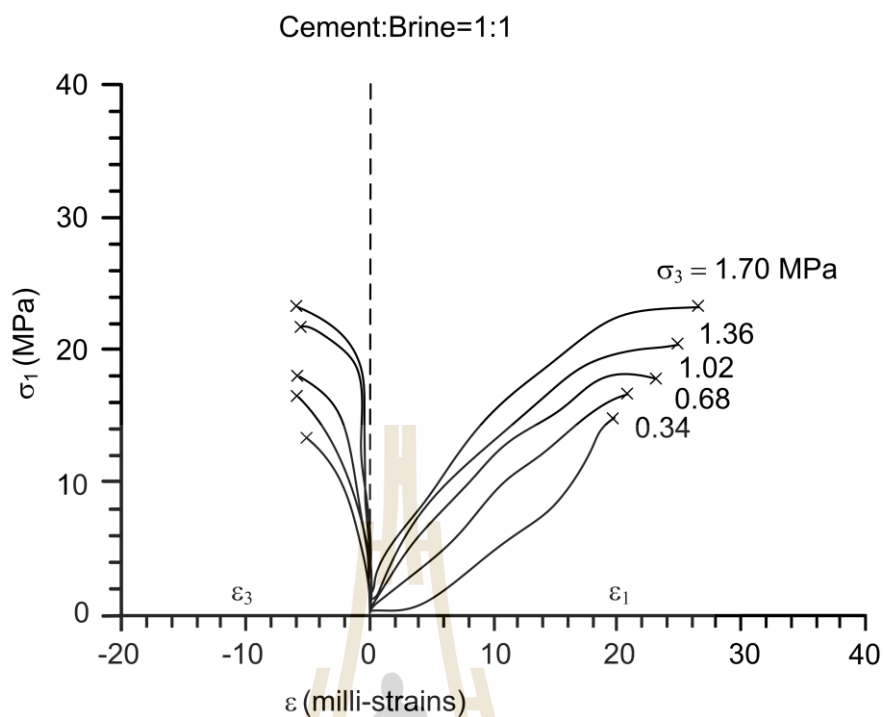


Figure 4.9 Stress-strain curves for cement: brine = 1:1.

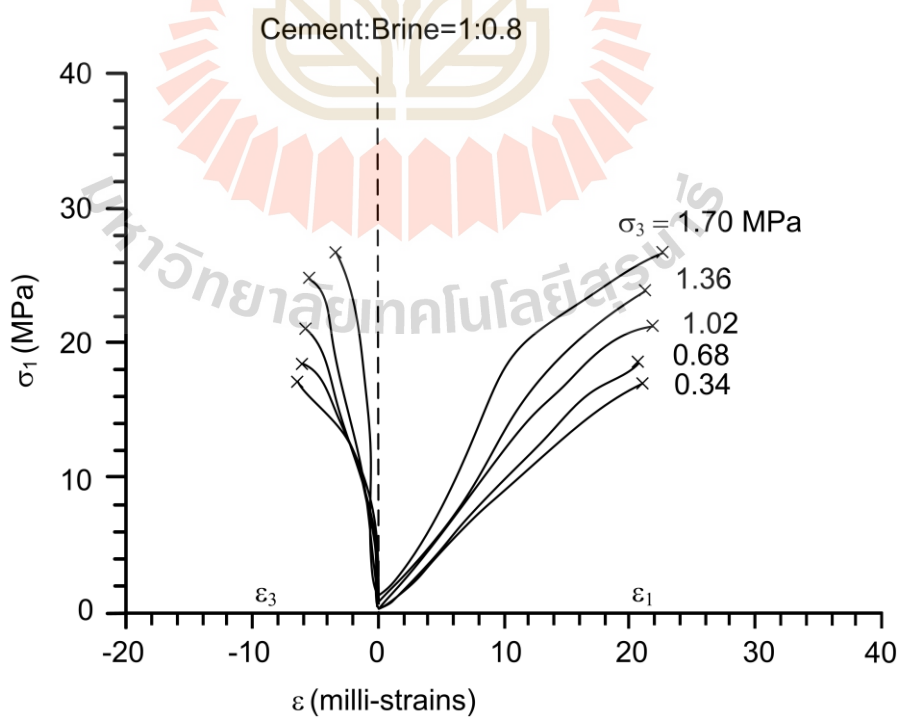


Figure 4.10 Stress-strain curves for cement: brine = 1:0.8.

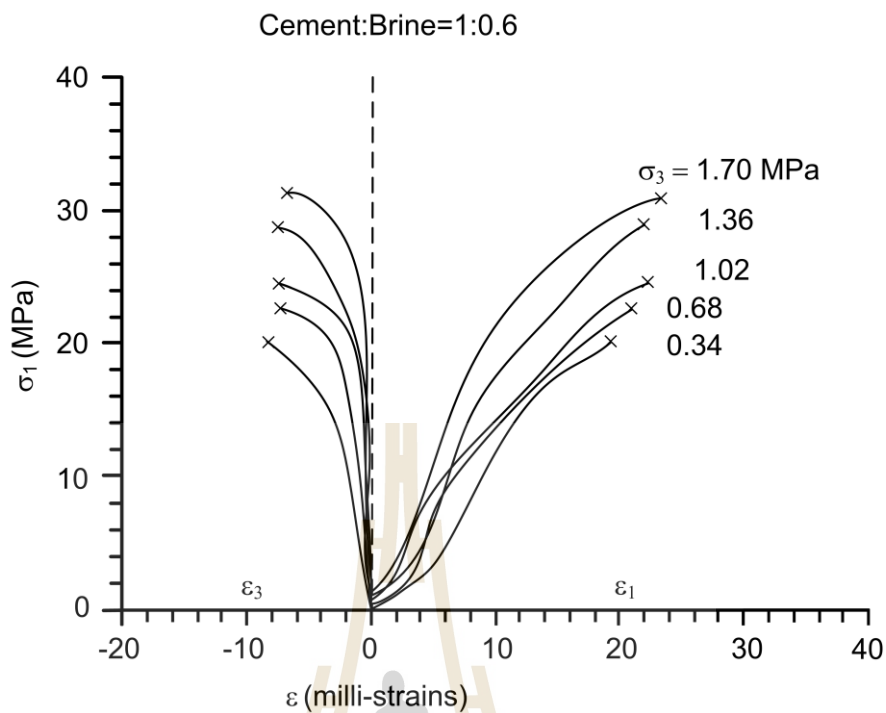


Figure 4.11 Stress-strain curves for cement: brine = 1:0.6.

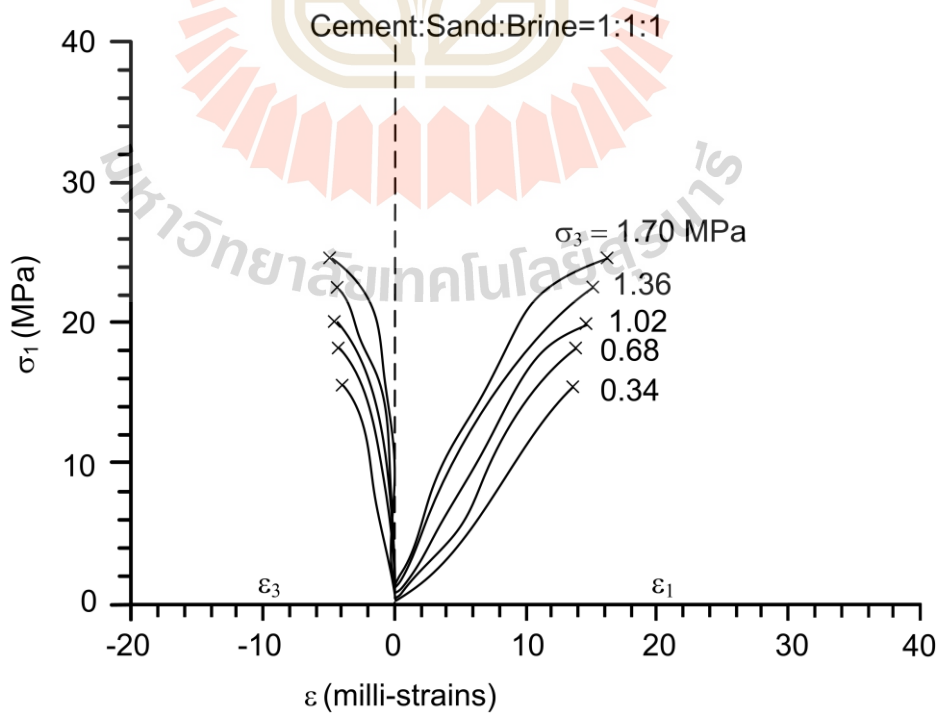


Figure 4.12 Stress-strain curves for cement: sand: brine = 1:1:1.

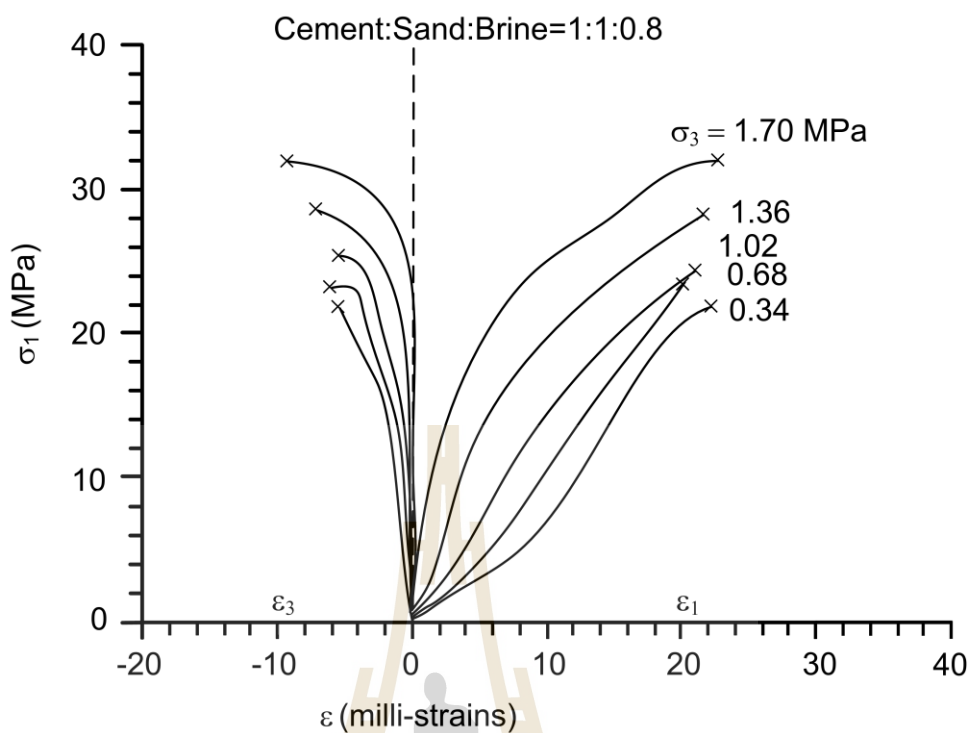


Figure 4.13 Stress-strain curves for cement: sand: brine = 1:1:0.8.

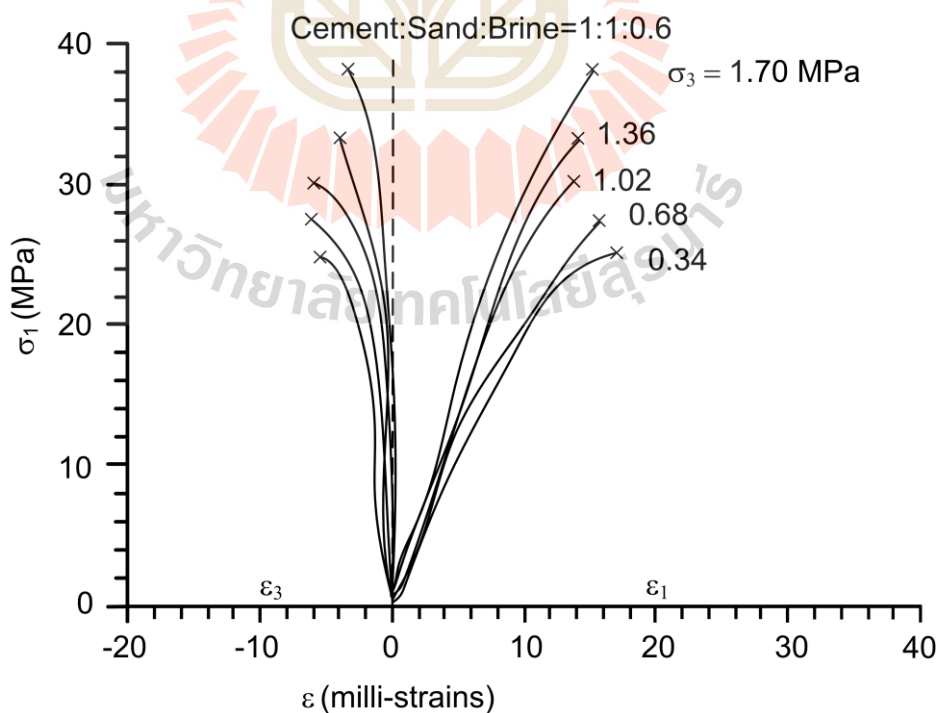


Figure 4.14 Stress-strain curves for cement: sand: brine = 1:1:0.6.

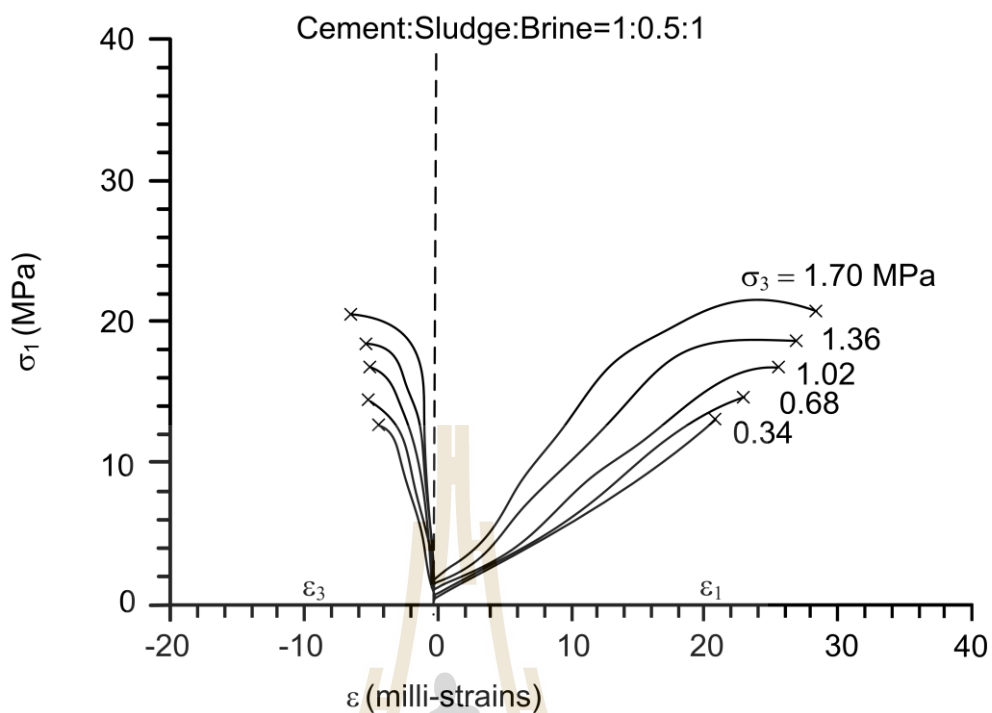


Figure 4.15 Stress-strain curves for cement: sludge: brine = 1:1:1.

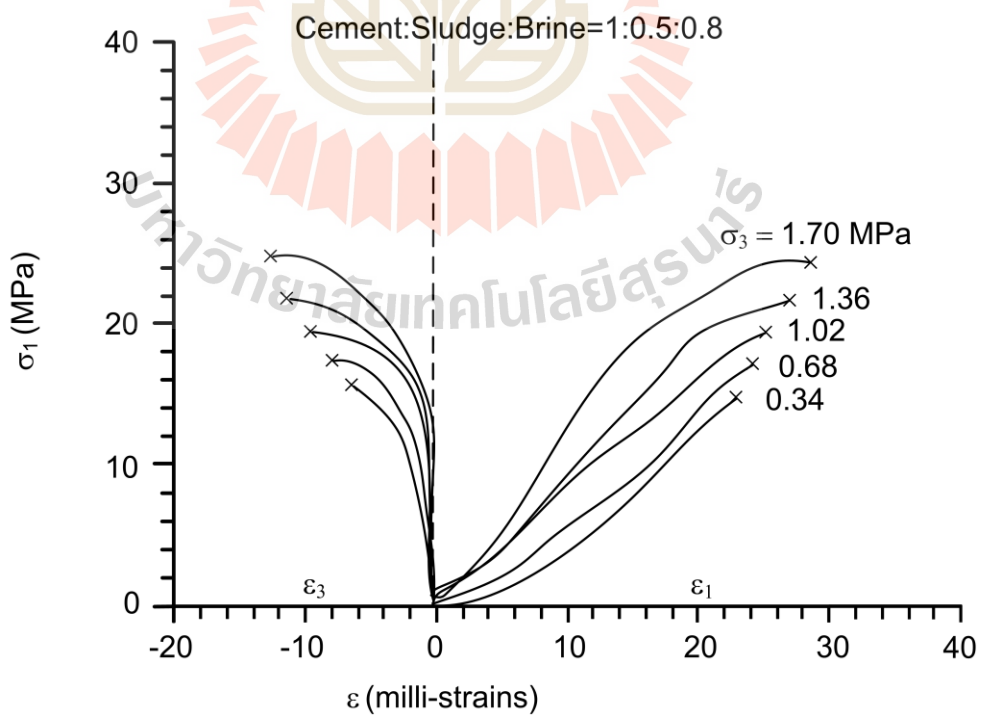


Figure 4.16 Stress-strain curves for cement: sludge: brine = 1:1:0.8.

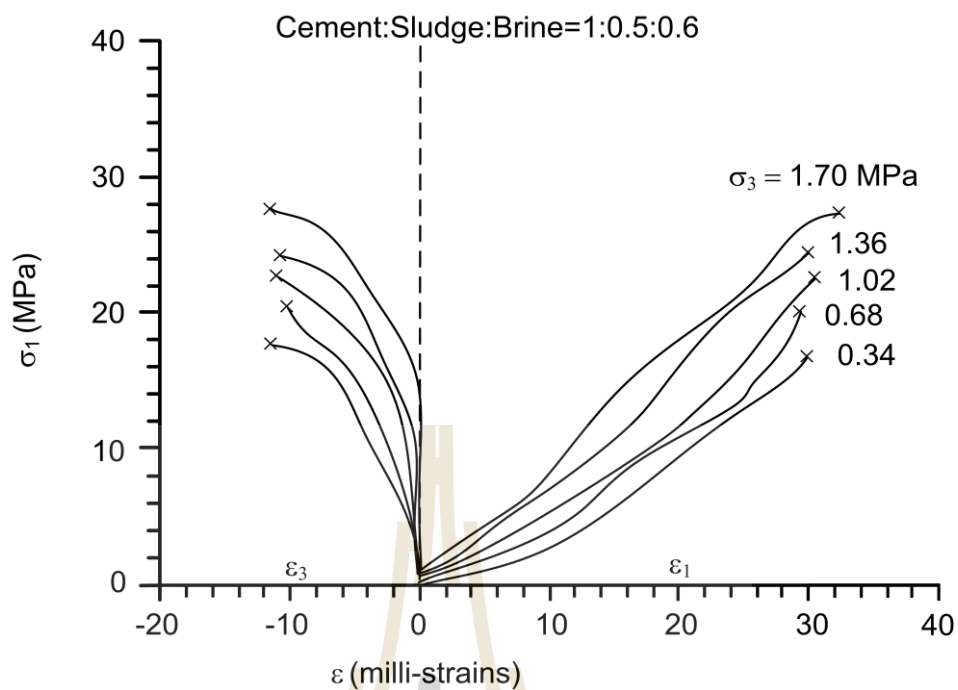


Figure 4.17 Stress-strain curves for cement: sludge: brine = 1:1:0.6.

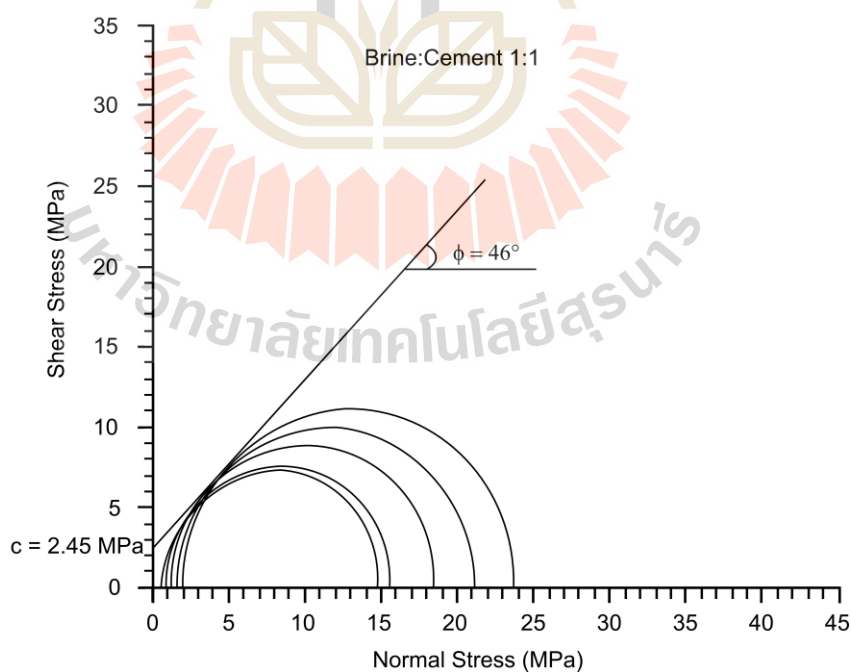


Figure 4.18 Triaxial compressive strength tests results for cement: brine = 1:1 in form of Mohr's circles and Coulomb criterion.

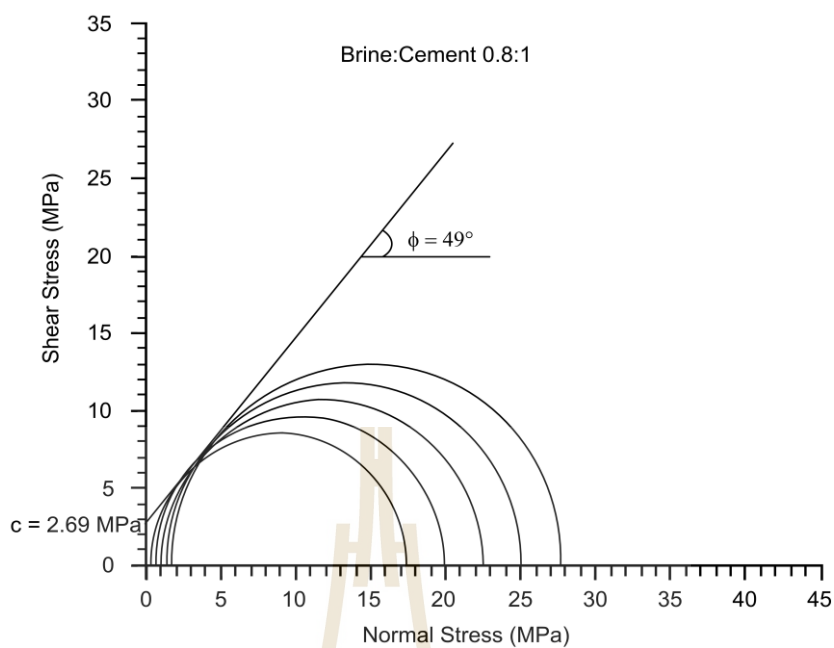


Figure 4.19 Triaxial compressive strength tests results for cement: brine = 1:0.8 in form of Mohr's circles and Coulomb criterion.

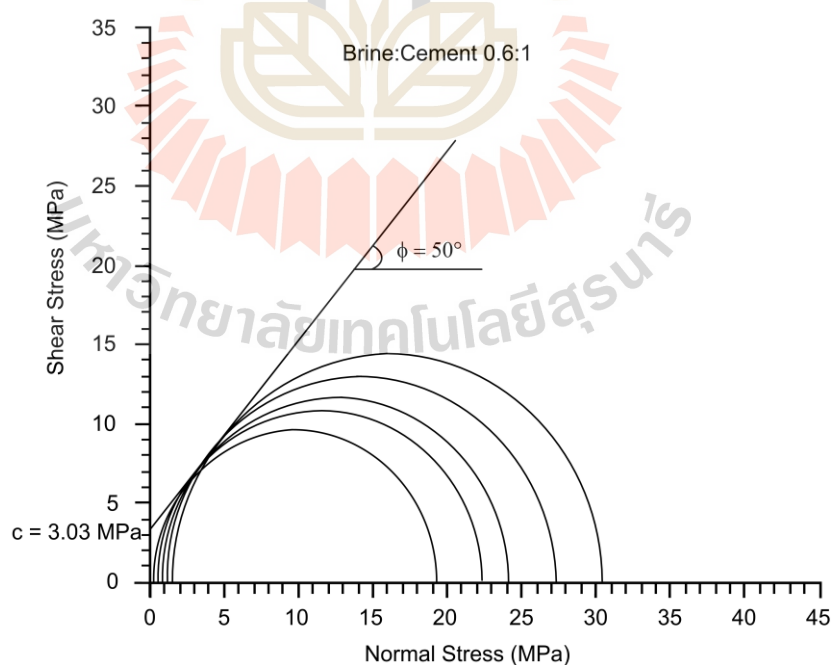


Figure 4.20 Triaxial compressive strength tests results for cement: brine = 1:0.6 in form of Mohr's circles and Coulomb criterion.

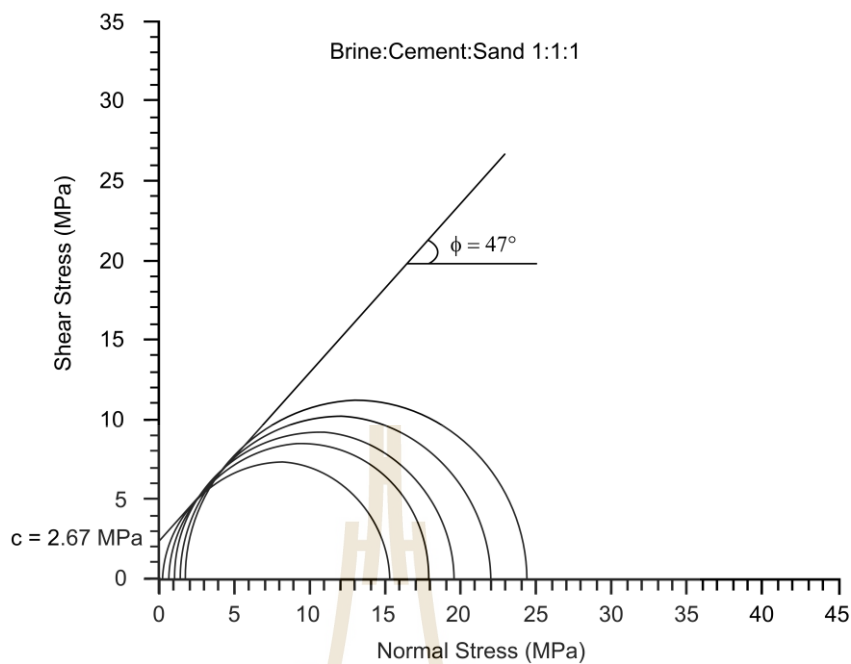


Figure 4.21 Triaxial compressive strength tests results for cement: sand: brine = 1:1:1 in form of Mohr's circles and Coulomb criterion.

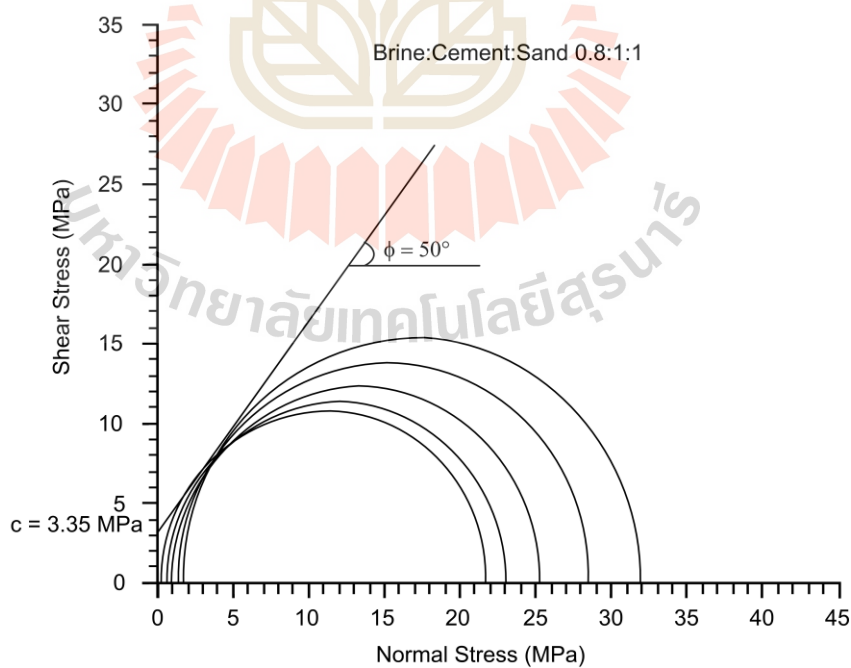


Figure 4.22 Triaxial compressive strength tests results for cement: sand: brine = 1:1:0.8 in form of Mohr's circles and Coulomb criterion.

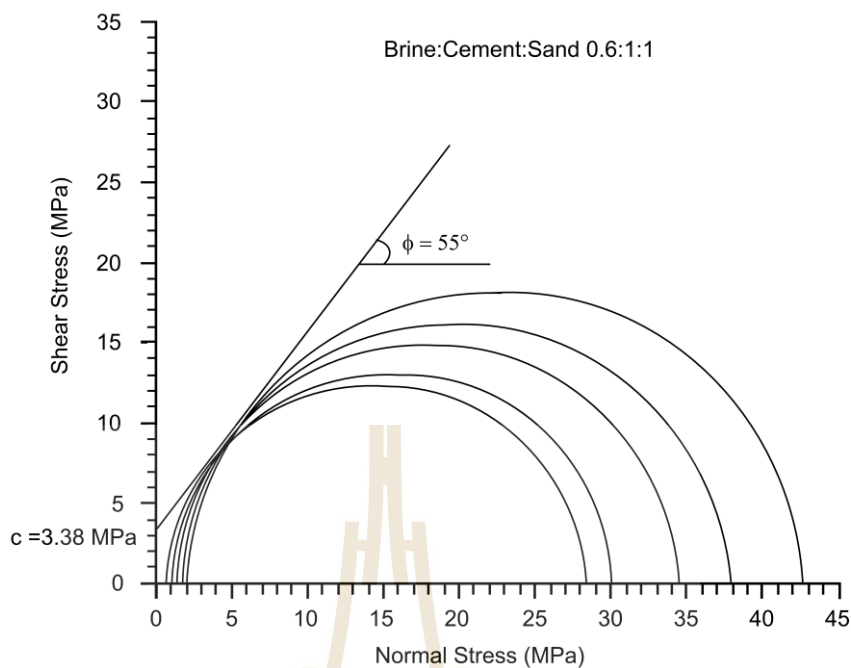


Figure 4.23 Triaxial compressive strength tests results for cement: sand: brine = 1:1:0.6 in form of Mohr's circles and Coulomb criterion.

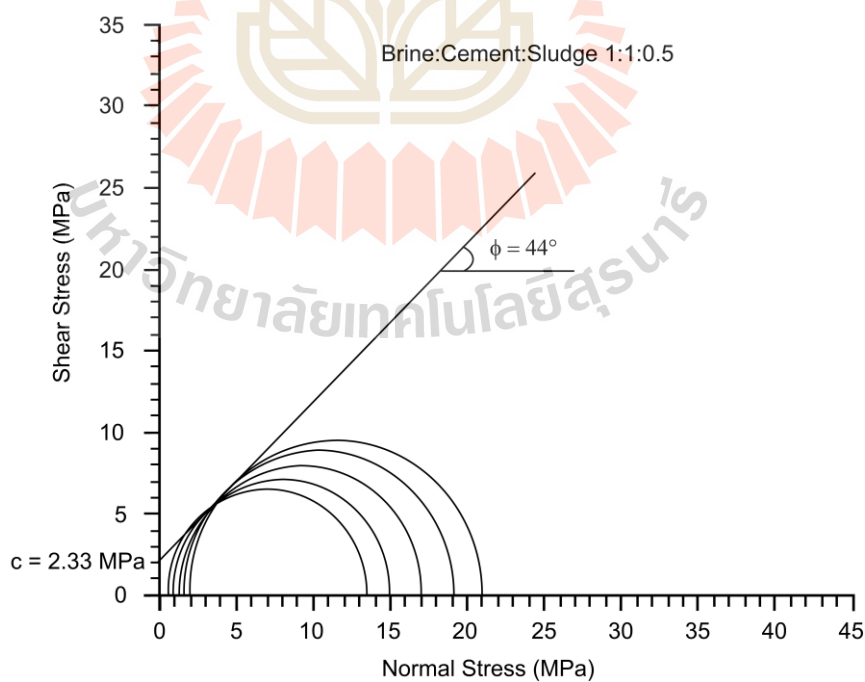


Figure 4.24 Triaxial compressive strength tests results for cement: sludge: brine = 1:0.5:1 in form of Mohr's circles and Coulomb criterion.

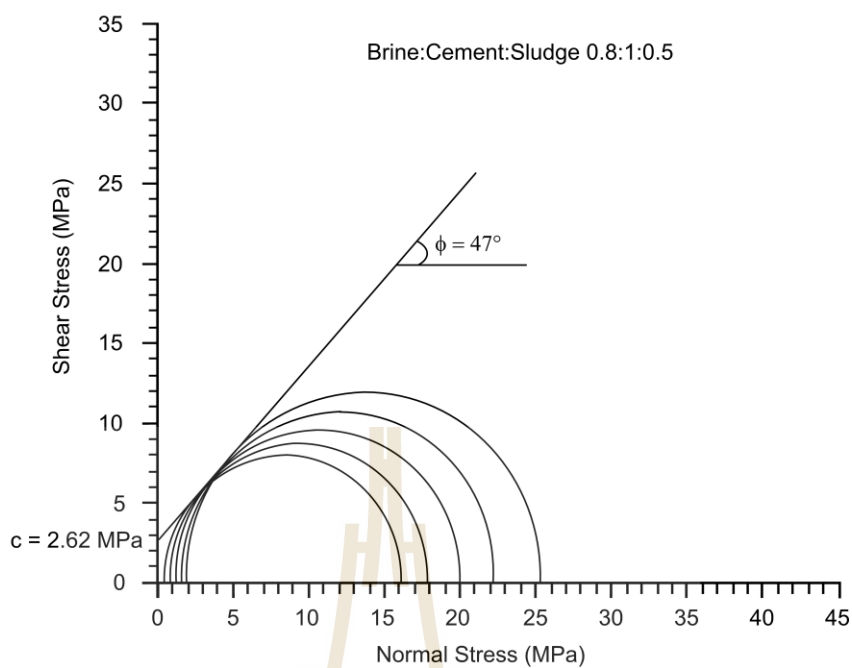


Figure 4.25 Triaxial compressive strength tests results for cement: sludge: brine = 1:0.5:0.8 in form of Mohr's circles and Coulomb criterion.

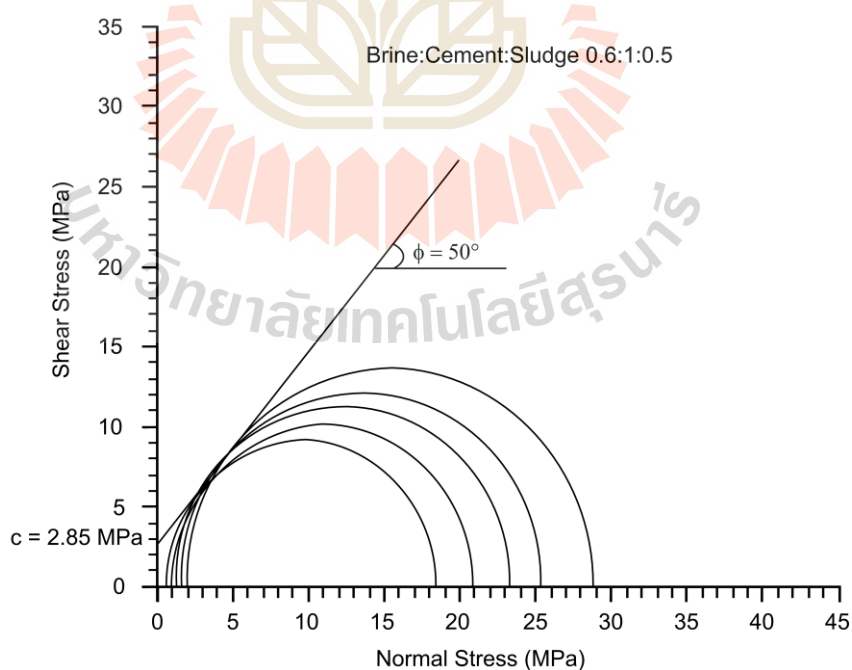
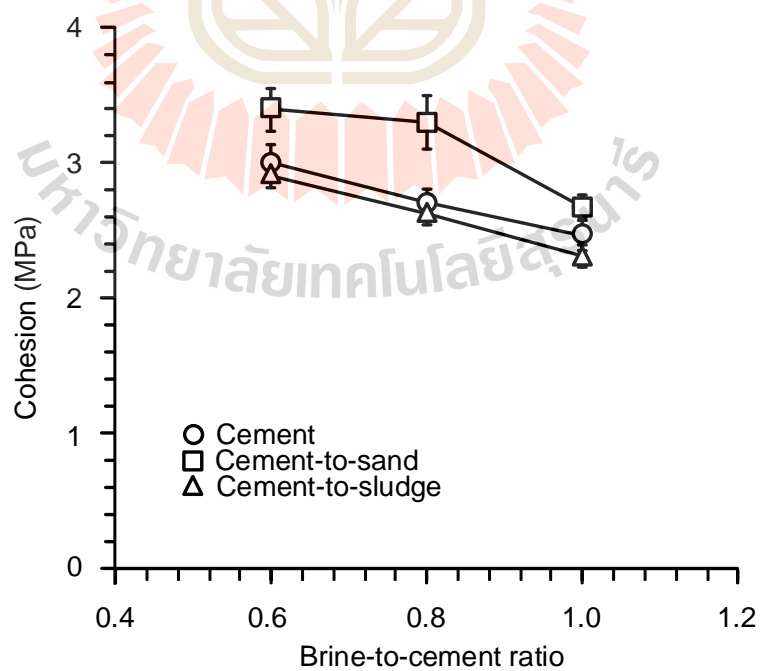


Figure 4.26 Triaxial compressive strength tests results for cement: sludge: brine = 1:0.5:0.6 in form of Mohr's circles and Coulomb criterion.

Table 4.2 Cohesions and friction angles of cement mixtures.

Mixtures	Brine-to-cement ratios	Friction angles (degrees)	Cohesions (MPa)
Cement	1	46	2.45
	0.8	49	2.69
	0.6	50	3.03
Cement-to-sand	1	47	2.67
	0.8	50	3.35
	0.6	55	3.38
Cement-to-sludge	1	44	2.33
	0.8	47	2.62
	0.6	50	2.85

**Figure 4.27** Cohesion (MPa) as function of brine-to-cement ratio.

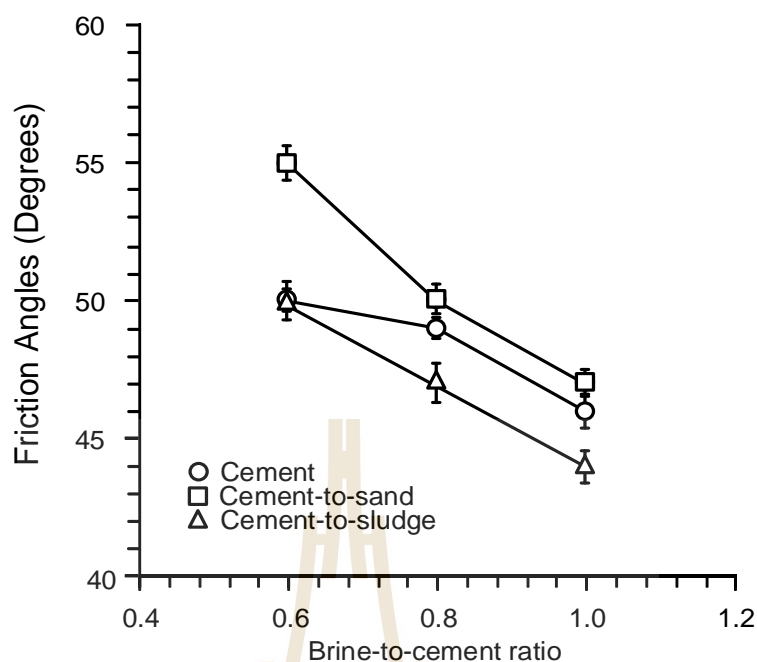


Figure 4.28 Friction angles (degrees) as function of brine-to-cement ratio.

4.3.2 Four point bending test results

Figure 4.29 shows some post-test specimens from the four point bending test under different cement mixtures. The fractures are induced at the center of specimen for all testing. The compressive and tensile moduli (E_C and E_T) can be calculated from the linear portion of the stress-strain curves. Table 4.3 summarizes the tensile stresses and strains at failure and the elastic moduli obtained from the four point bending test. It is found that the tensile strengths, compressive strengths, strains and deformation moduli decrease with ratios (Figures 4.30 to 4.32). This is probably due to that the increase of liquid can lower the bonding strength of the cement mixtures. The compressive modulus is slightly higher than tensile modulus. Numerical analysis is used the relationship between compressive strength at the end of four-point bending test and uniaxial compressive strength. The proposed criterion

fits well to the test data with polynomial equations are shown in Figure A.1 in Appendix A. The maximum compressive strength are cement mix with sand.

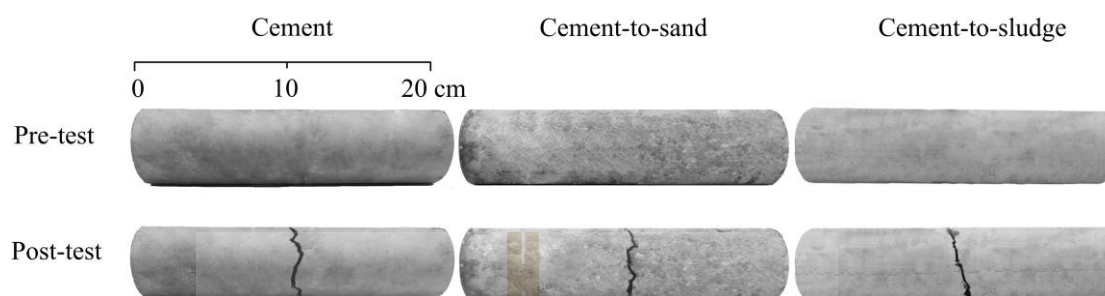


Figure 4.29 Examples of pre-test and post-test specimens from four-point bending test.

Table 4.3 Four-point bending test results of cement mixtures.

Mixtures	B/C	σ_T (MPa)	ϵ_T (milli-strains)	ϵ_C (milli-strains)	E_T (GPa)	E_C (GPa)
Cement	1	2.53	-0.234	0.174	8.80	11.00
	0.8	2.92	-0.269	0.165	10.10	11.90
	0.6	3.36	-0.348	0.154	12.53	14.19
Cement-to-sand	1	2.99	-0.312	0.220	9.96	13.65
	0.8	3.35	-0.336	0.183	11.68	14.66
	0.6	3.61	-0.382	0.136	14.18	17.30
Cement-to-sludge	1	2.36	-0.214	0.187	8.47	10.57
	0.8	2.73	-0.247	0.176	9.98	11.40
	0.6	3.14	-0.333	0.170	11.95	13.13

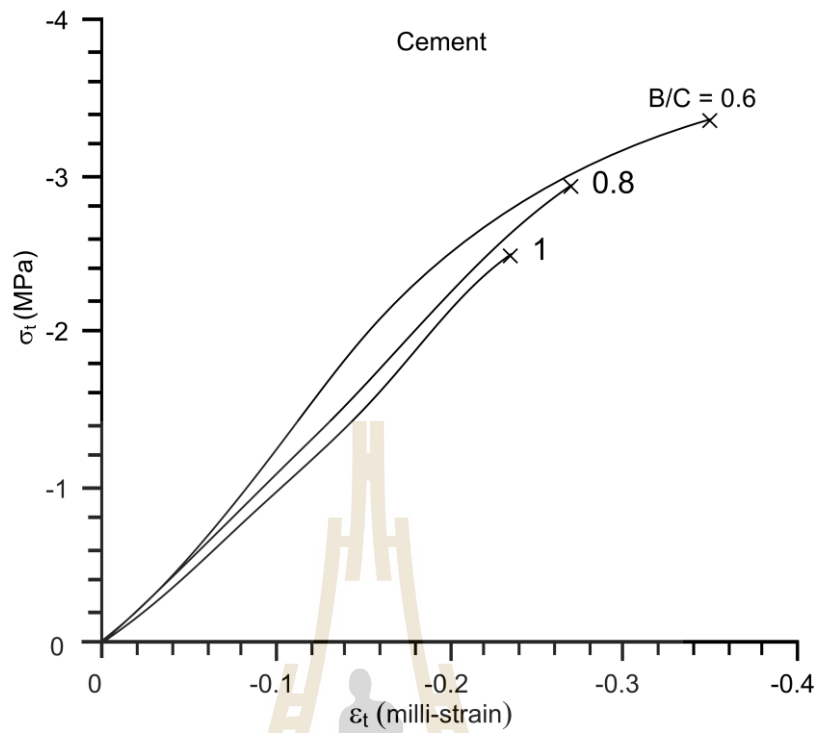


Figure 4.30 Tensile stress-strain curves of cement mixture.

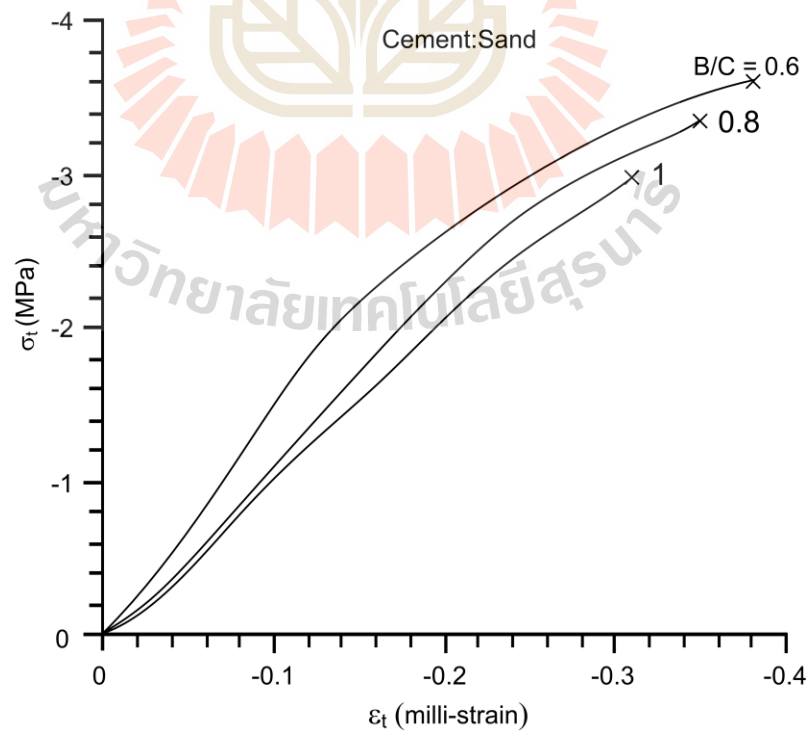


Figure 4.31 Tensile stress-strain curves of cement-to-sand mixture.

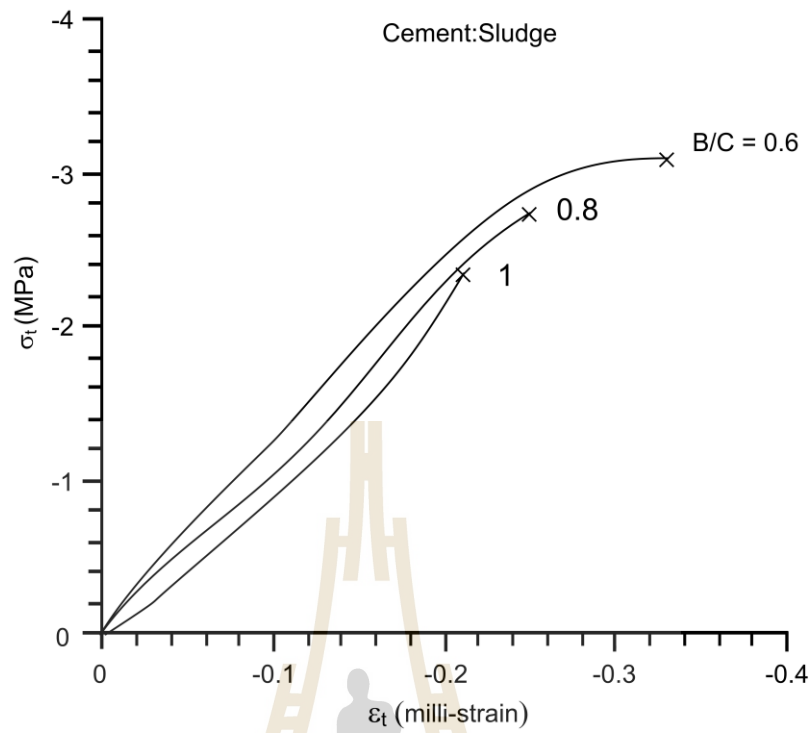


Figure 4.32 Tensile stress-strain curves of cement-to-sludge mixture.

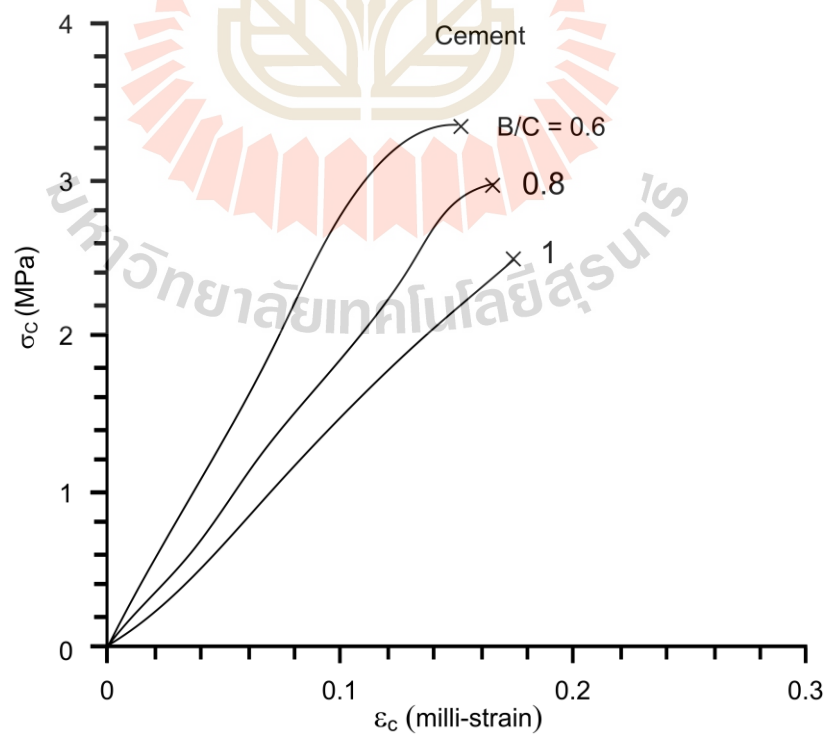


Figure 4.33 Compressive stress-strain curves of cement mixture.

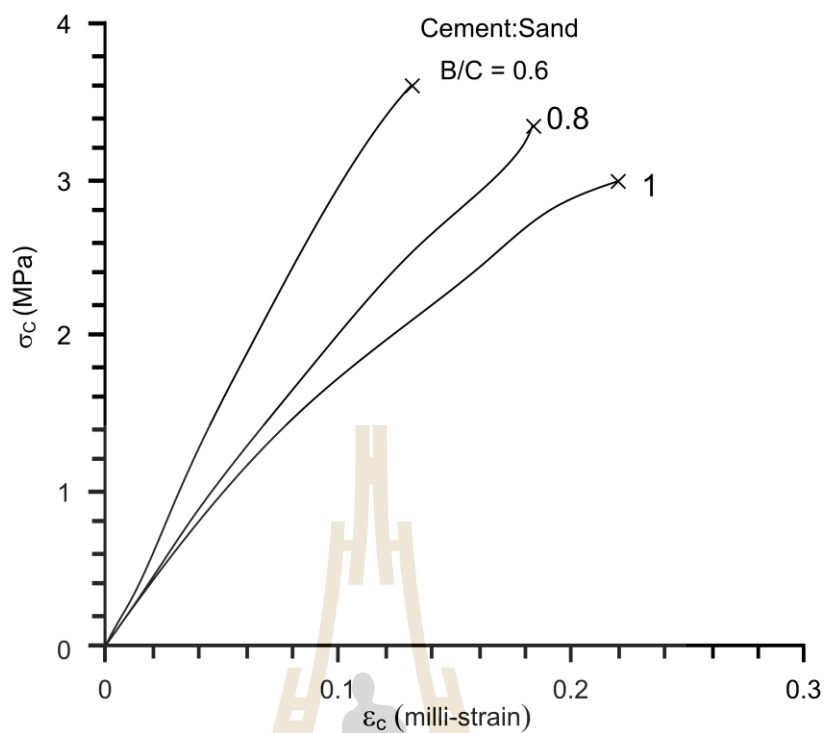


Figure 4.34 Compressive stress-strain curves of cement-to-sand mixture.

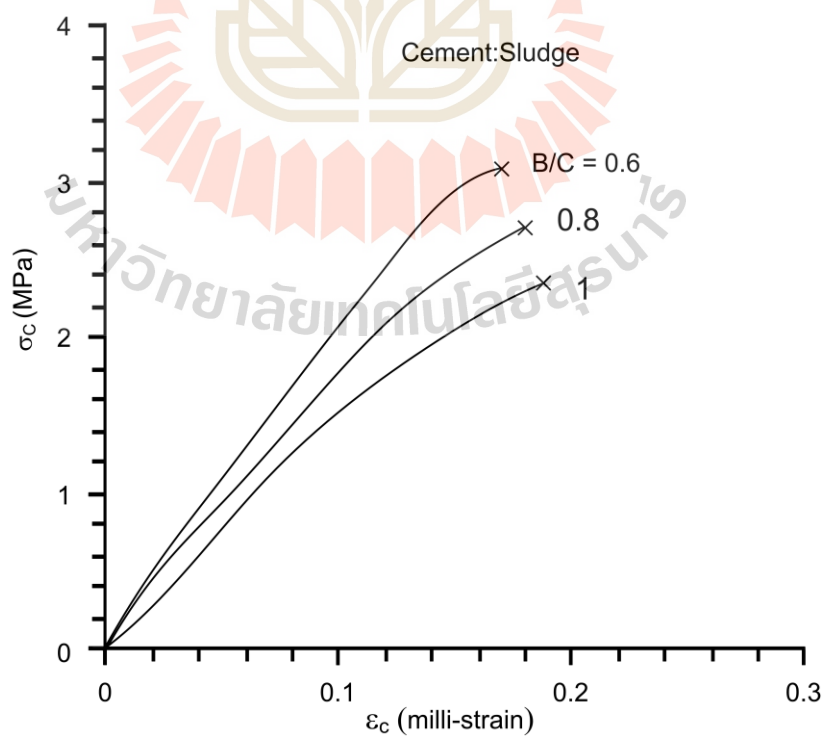


Figure 4.35 Compressive stress-strain curves of cement-to-sludge mixture.

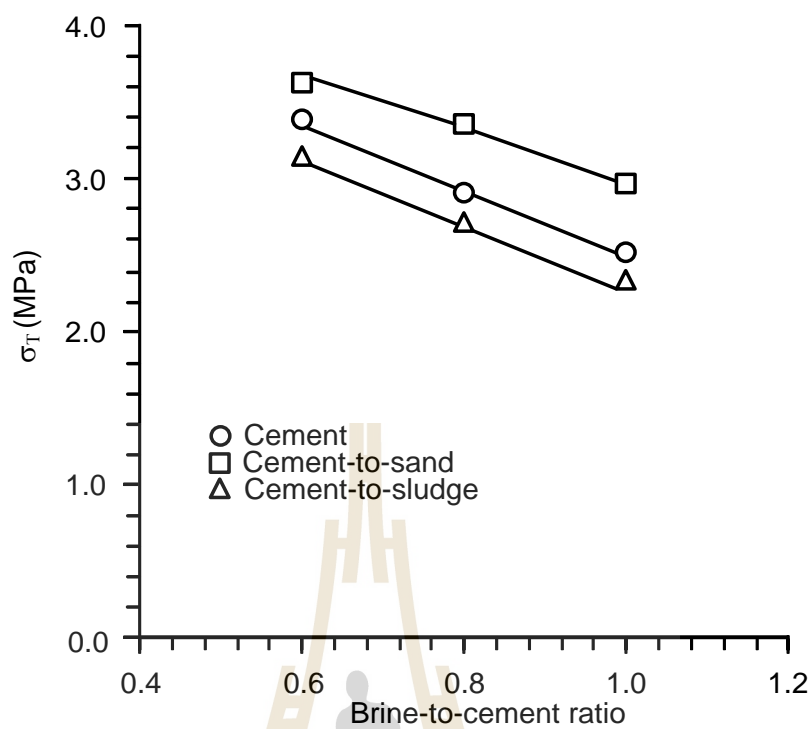


Figure 4.36 Tensile strength (σ_T) as a function of brine-to-cement ratio.

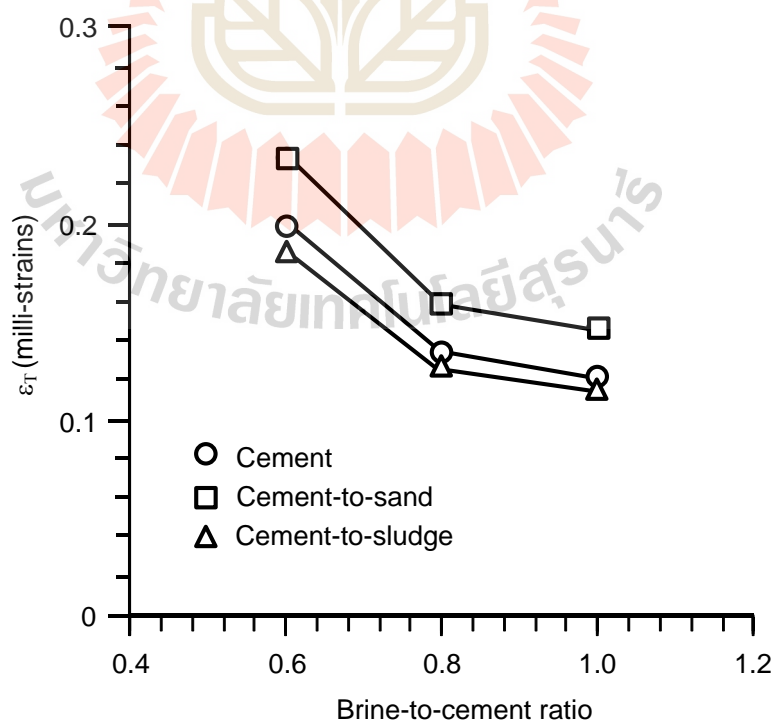


Figure 4.37 Tensile strain (ϵ_T) as a function of brine-to-cement ratio.

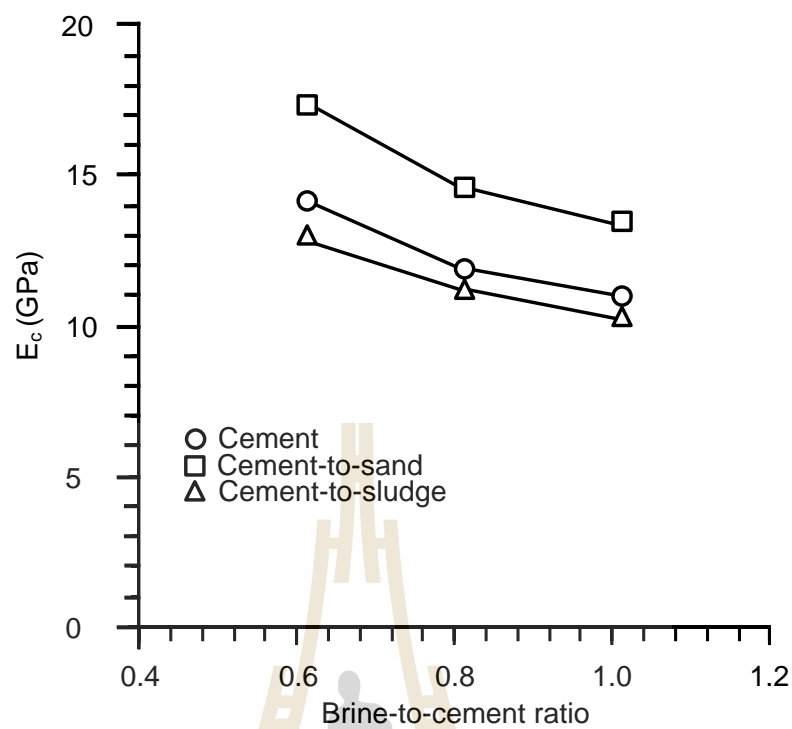


Figure 4.38 Compressive modulus (E_c) as a function of brine-to-cement ratio.

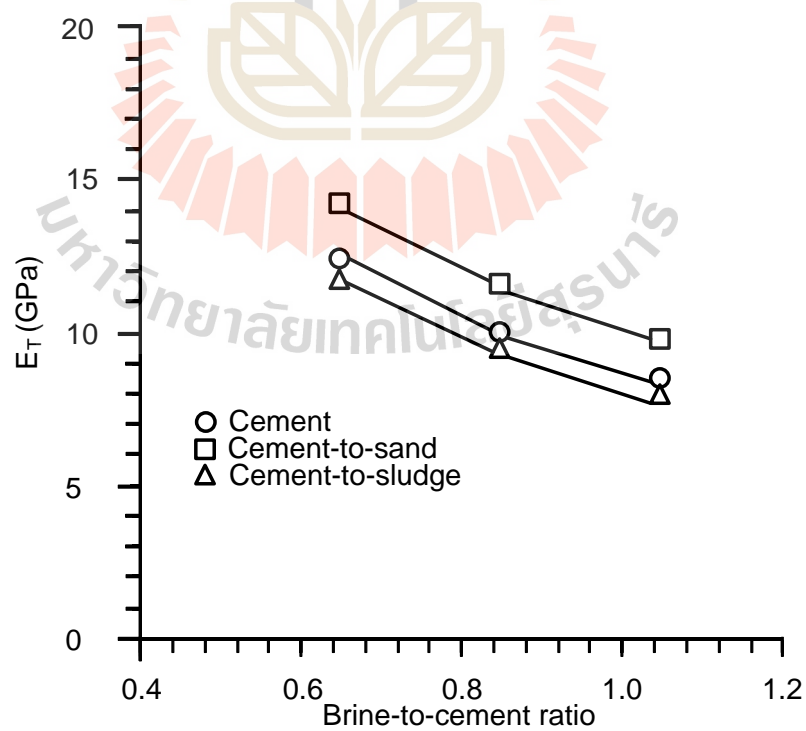
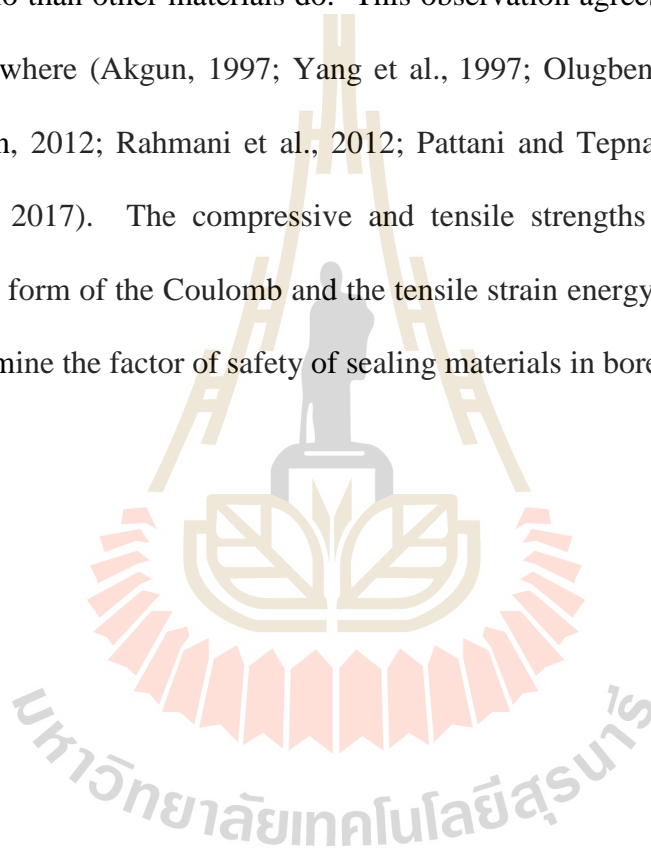


Figure 4.39 Tensile modulus (E_T) as a function of brine-to-cement ratio.

4.4 Discussions and Conclusions

The compression and four-point bending tests have been performed to obtain the mechanical properties of cement-aggregate mixtures for use as sealing materials in and nearby boreholes drilled in and nearby subsidence area. The results indicate that the cement mixed with sand shows higher strength and elastic modulus and lower Poisson's ratio than other materials do. This observation agrees well with the results obtained elsewhere (Akgun, 1997; Yang et al., 1997; Olugbenga, 2007; Moghadam and Khoshbin, 2012; Rahmani et al., 2012; Pattani and Tepnarong, 2015; Bumanis and Bajarea, 2017). The compressive and tensile strengths are used to develop criteria in the form of the Coulomb and the tensile strain energy. The two criteria are used to determine the factor of safety of sealing materials in boreholes.



CHAPTER V

POTENTIAL APPLICATION

5.1 Introduction

The purpose of this chapter is to determine the factor of safety (FS) for cement seal in borehole considers the strain energy under tension and the Coulomb's criterion under shear stress. The sealing materials should be able to sustain the deformation and movement of the subsiding overburden formations due to the underground excavations.

5.2 Strain Energy Density

The strain energy density principle is applied here to describe tensile strengths and deformability of the cement mixtures. Assuming that the crack initiation point is under uniaxial tensile stress condition, the total strain energy density (W_T) can be calculated from the tensile stress and strain at failure using the relation prepared by Jaeger (2007):

$$W_T = 1/2(\sigma_T \cdot \varepsilon_T) \quad (5.1)$$

where σ_T and ε_T are the tensile stress and strain at failure. Table 5.1 summarizes the tensile stress and strain results.

To develop a strength criterion based on the strain energy density principle, the total strain energy that the specimen can sustain before tensile failure occurs can

be presented as a function of brine-to-cement ratio (B/C). Figure 5.1 plots the W_T as a function of the ratio. A linear trend is obtained which can be described by:

$$W_T = \alpha(B/C) + \beta \quad (5.2)$$

where α and β are empirical parameters.

Table 5.1 Summary of the tensile stresses and strains.

Mixtures	brine to cement ratios	σ_T (MPa)	ϵ_T (milli-strains)
Cement	1.0	2.53	0.234
	0.8	2.92	0.269
	0.6	3.36	0.348
Cement-to-sand	1.0	2.99	0.312
	0.8	3.35	0.336
	0.6	3.61	0.382
Cement-to-sludge	1.0	2.36	0.214
	0.8	2.73	0.247
	0.6	3.14	0.333

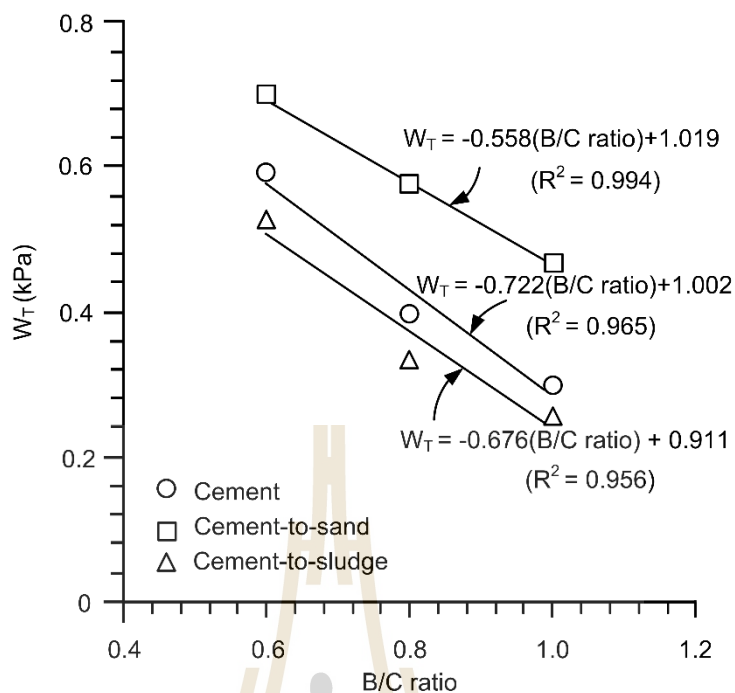


Figure 5.1 Total strain energy densities (W_T) as a function of brine to cement ratios (B/C).

Their numerical values are given in Figure 5.1. Regression analyses are performed to determine the parameters in Equations (5.2). The proposed criterion fits well to the test data with the correlation coefficients (R^2) greater than 0.9. The results show that the strain energy densities of the mixtures decrease with increasing ratio. The cement-sand mixture shows higher strain energy than those of the pure cement and cement-sludge mixtures. This depends on the tensile strength of the mixtures (represented by σ_T). Higher tensile strengths lead to higher total strain energy.

5.3 Strain Energy Applications

Borehole drilled in or nearby subsidence areas may be subjected to large strains under tension and shear forces. The stability of sealing material is necessary to

prevent water inflows into the salt and potash mine openings underneath. The strain-energy equation proposed above and the Coulomb's criterion can be applied to determine the factors of safety of the cement seal in the borehole. The tensile strain energy ($W_{T,i}$) of the mixtures in borehole can be induced by the formation movement above the mine horizon, which can be determined as Jaeger et al. (2007):

$$W_{T,i} = 1/2(\sigma_{T,i} \cdot \varepsilon_{T,i}) \quad (5.3)$$

where $\sigma_{T,i}$ is the maximum induced tensile stresses, and $\varepsilon_{T,i}$ is the induced tensile strains occurred in borehole which can be calculated from Pytel and Kiusalaas (2003) as follows:

$$\sigma_{T,i} = MC/I \quad (5.4)$$

$$\varepsilon_{T,i} = \sigma_{T,i}/E \quad (5.5)$$

where M is bending moment ($N \cdot m$), C is horizontal distance away from the borehole axis (m) and I is the moment of inertia: (m^4).

$$M = \omega l^2/2 \quad (5.6)$$

$$\omega = 6\theta EI/\lambda^3 \quad (5.7)$$

$$I = \pi/4 \cdot r^4 \quad (5.8)$$

where ω is uniform distributed load (N/m), l is borehole depth (m), θ is the slope angle induced at the top of borehole and r is borehole radius (m). The uniform distributed load is assumed here primarily to induce the bending of the cement

column to obtain the maximum inclination angle of 0.172 degrees. In this study θ is taken as 0.172 degrees which is equivalent to the surface slope of 3×10^{-3} (Figure 5.2). This maximum value is suggested by Singh (1992) to ensure that the subsidence slope will not impact the engineering structures and natural resources on the surface within mine area.

To determine the factor of safety based on the Coulomb's criterion, the maximum shear stress at fix end (bottom) of the borehole can be determined as:

$$\tau_i = 4V/3A \quad (5.9)$$

where V is shear force: $V = \omega \cdot l$ (N) and A is cross section area of borehole (m^2). (5.10)

5.4 Factor of Safety

The factor of safety (FS) for cement seal in borehole considers the strain energy under tension and the Coulomb's criterion under shear stress.

$$\text{Tensile strain energy criterion: } FS = W_T/W_{T,i} \quad (5.11)$$

$$\text{Coulomb's shear criterion: } FS = \tau/\tau_i \quad (5.12)$$

where $W_{T,i}$ and τ_i are the induced tensile strain energy and shear stress. Figure 5.3 (a) shows the factors of safety calculated from tensile energy as a function of depths for the surface slope of 3×10^{-3} . The factors of safety increase with depths. If the boreholes are over 250 m depth, their cement seal should be stable (no tensile failure occurs). For shallow boreholes (less than 250 m) it is possible that tensile failure may occur particularly for the subsidence slopes of 3×10^{-3} or greater. Figure 5.3 (b) shows

the factors of safety against the shear stress based on the Coulomb's criterion. They also increase with depth. All cement mixtures can sustain the shear stresses induced by the formation movement even at the point where the maximum surface slope is allowed (3×10^{-3}). Factor of safety of the tensile stresses and shear stresses in borehole are illustrated in Appendix B.

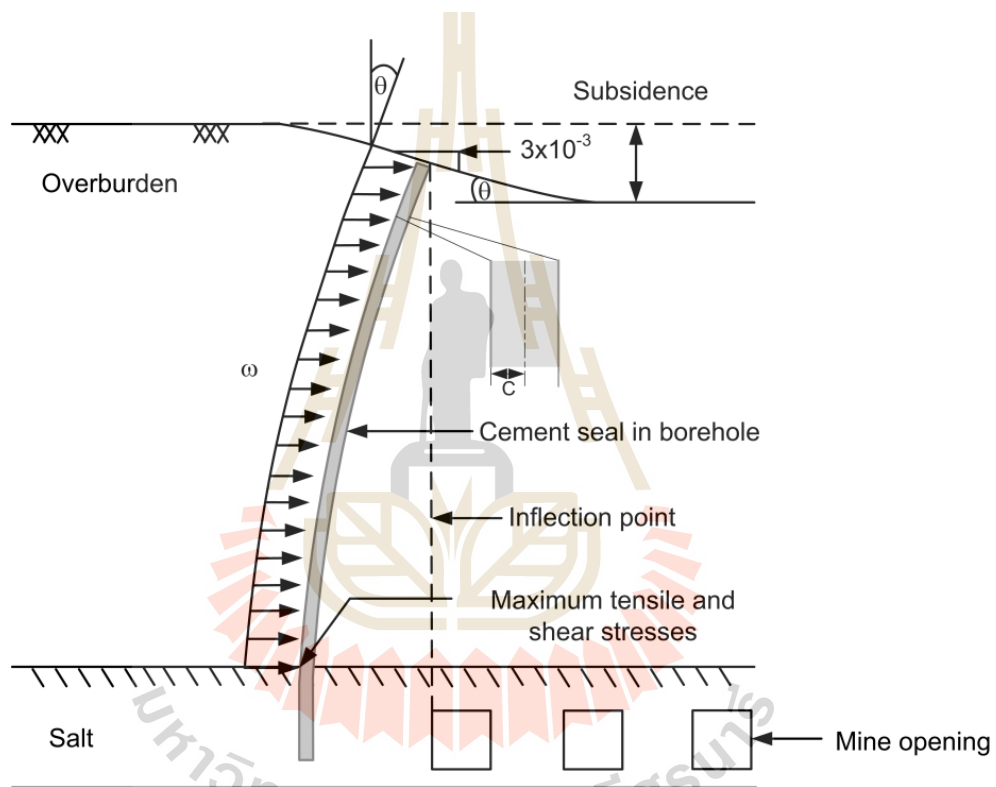


Figure 5.2 Cement seal in borehole under bending with maximum slope of 3×10^{-3} .

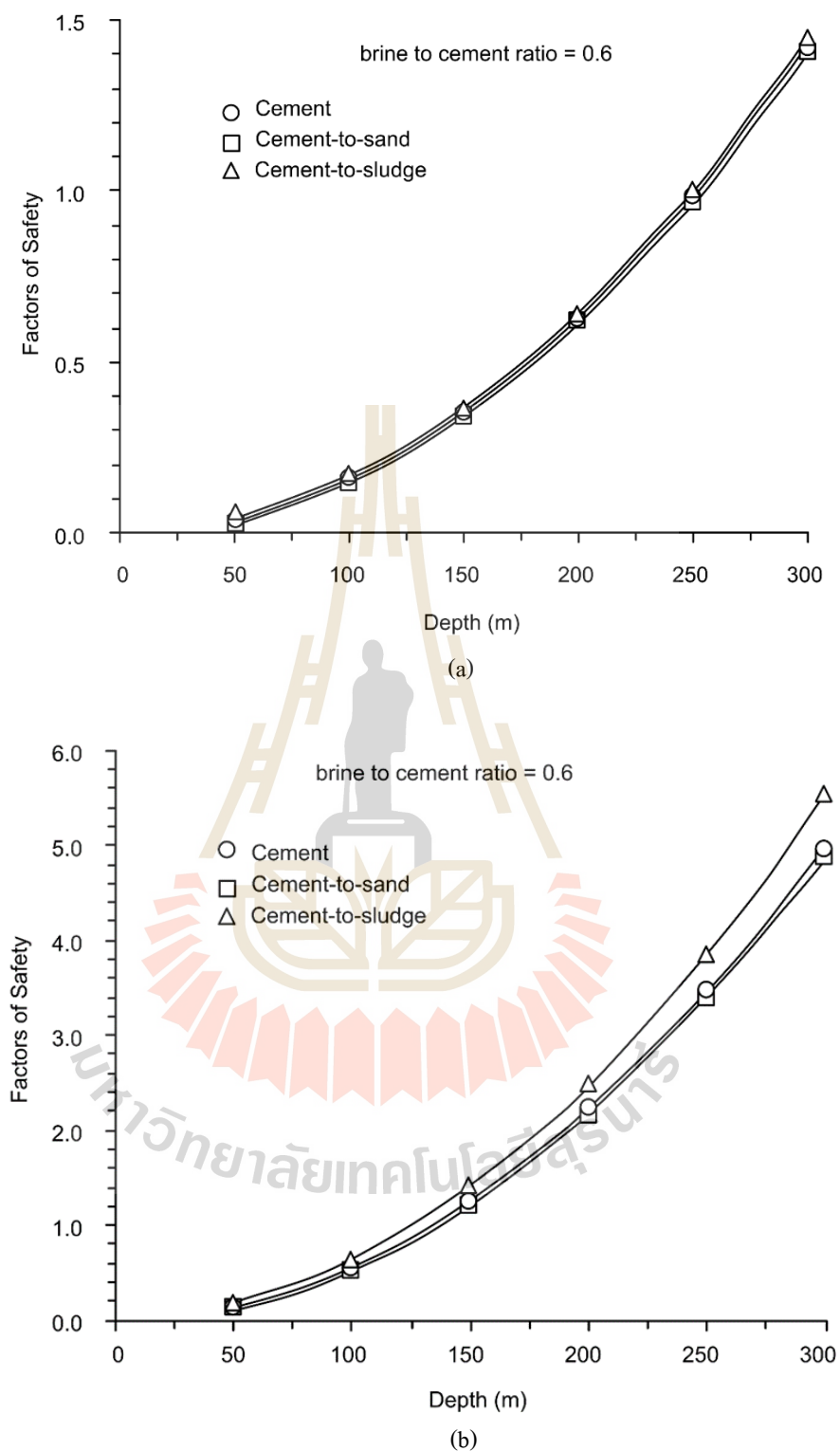
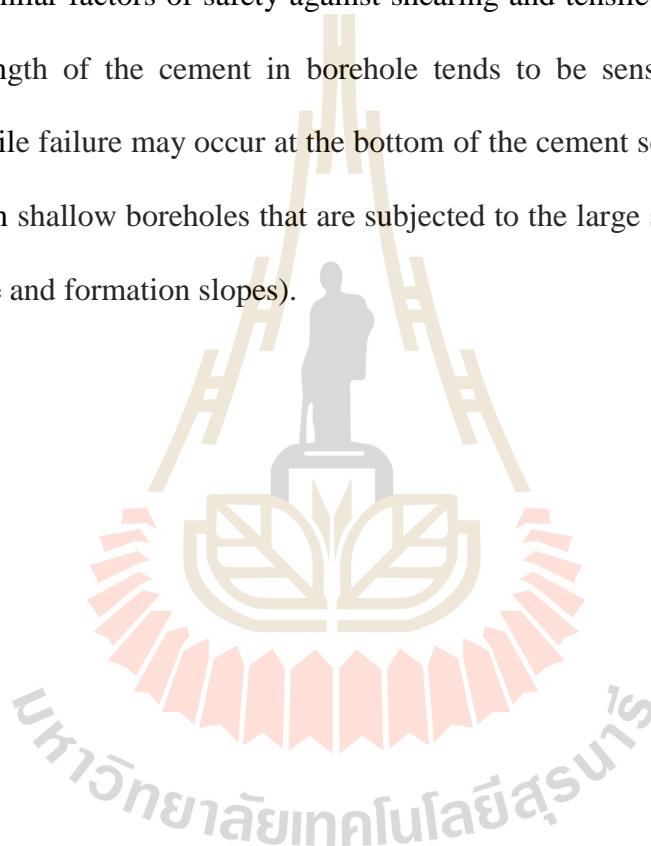


Figure 5.3 Factors of safety as a function of depth calculated by tensile strain energy (a) and the Coulomb's criterion (b).

5.5 Discussions and Conclusions

The compressive and tensile strengths are used to develop criteria in the form of the Coulomb and the tensile strain energy. The two criteria are used to determine the factor of safety of sealing materials in boreholes under various depths. The results show that the factors of safety increase when the depths increase. All mixtures tested here show similar factors of safety against shearing and tensile bending. The tensile bending strength of the cement in borehole tends to be sensitive to the borehole depths. Tensile failure may occur at the bottom of the cement seals in the Lower salt, particularly in shallow boreholes that are subjected to the large subsidence magnitude (large surface and formation slopes).



CHAPTER VI

DISCUSSIONS AND CONCLUSIONS

6.1 Discussions

This section discusses the key issues relevant to the reliability of the test schemes and the adequacies of the test results. Comparisons of the results and findings from this study with those obtained elsewhere under similar test conditions have also been made.

The mechanical properties for the cement seal prepared with different sources of aggregates providing a better understanding of which aggregate characteristics have an impact on the concrete mechanical performance.

Stress and viscosity increase with increasing size of aggregate because the effect of coarse aggregate friction might counteract with the effect of coating thickness on aggregate. An increase of aggregate size used in present study generally results in higher friction angle. As a result, the friction of aggregate in concrete might be stronger because of the increase of aggregate size which agrees with the results obtained by Anwar and Roushdi (2013) and Agrawal and Chandak (2017). Finer aggregate normally provides concrete with lower workability because of the increase of surface area and thus the need for more paste to coat the aggregate particle. On the other hand, graded aggregate can considerably improve the workability of concrete because the optimized packing of aggregate particles results in fewer voids that need to be filled by cement paste to provide the same flow.

The effect of aggregate mixtures on tensile result strength follows the same trend as the compressive strength. The tensile strengths ranges are lower than those obtained for the compressive strengths. The compressive strength is higher than tensile strength because concrete is brittle in tension, but relatively tough in compression as described by Elinwa et al. (2016), Premchand et al. (2016), Caronge et al. (2017) and Sugar et al. (2017).

When increasing brine-to-cement ratio, the uniaxial compressive strength and elastic modulus decrease but Poisson's ratio increases. This is probably due to that the increase of liquid can lower the bonding strength of the cement mixtures when there is decrease in amount of mixing water at the same consistency lead to be higher compressive strength. Adding more water creates the weakness zones and increase susceptibility to crack. When there is a large excess of water, the water bleeds out onto the surface. The void and passages created inside the concrete to allow the water flow become weak zones and micro-cracks. This is because of less number of air voids in the concrete volume. The higher the water/cement ratio, the greater the initial spacing between the cement grains and the greater the volume of residual voids not filled as explained by Mbadike and Elinwab (2011) and Raju et al. (2014).

6.2 Conclusions

All objectives and requirements of this study have been met. The results of the laboratory testing and analyses can be concluded as follows.

The compressive strength increases as brine-to-cement ratio (B/C) decreases. Under the same B/C ratio, the cement-sand mixtures show higher strength than those of the cement pure and cement-sludge mixtures. The higher confining pressures result

in higher stresses and strains at failure. The elastic parameters are determined from the tangent of the stress-strain curves at about 50% of the failure stress. The elastic moduli decrease and Poisson's ratios increase with increasing B/C ratio. The specimens mixed with sand tend to show higher elastic modulus and lower Poisson's ratio than those mixed with sludge. The cohesion and internal friction angle are summarized in Table 4.2. It suggests that increasing the B/C ratio slightly decreases the cohesions and friction angles of the mixtures. The average cohesion and friction angle of the mixtures range from 2.33 to 3.38 MPa and 44 to 55 degrees.

The highest tensile strengths are observed for cement mix with sand which equals to 3.61 MPa, and tensile strains equals to 0.382 mill-strain. Tensile stress and strain and deformation moduli decrease with these ratios. This is probably due to that the increase of liquid can lower the bonding strength of the cement mixtures. The compressive modulus is slightly higher than tensile modulus. The compressive modulus obtained here is comparable to those obtained from the compression tests.

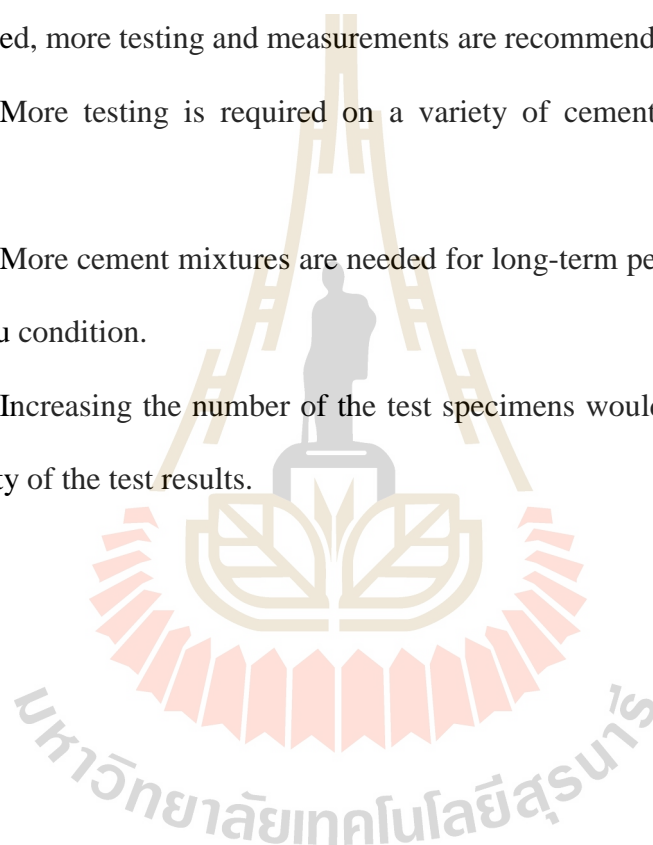
The compression and four point bending tests have been performed to obtain the mechanical properties of cement-aggregate mixtures for use as sealing materials in boreholes drilled in and nearby subsidence area. The results indicate that the cement mixed with sand shows higher strength and elastic modulus and lower Poisson's ratio than other materials do. The compressive and tensile strengths are used to develop criteria in the form of the Coulomb and the tensile strain energy. The two criteria are used to determine the factor of safety of sealing materials in boreholes under various depths. The results show that the factors of safety increase when the depths increase. All mixtures tested here show similar factors of safety against shearing and tensile bending. The tensile bending strength of the cement in borehole tends to be sensitive

to the borehole depths. Tensile failure may occur at the bottom of the cement seals in the Lower salt, particularly in shallow boreholes that are subjected to the large subsidence magnitude (large surface and formation slopes).

6.3 Recommendations for future studies

Recognizing that the numbers of the specimens and the test parameters used here are limited, more testing and measurements are recommended, as follows:

- (1) More testing is required on a variety of cement types with different components.
- (2) More cement mixtures are needed for long-term performance testing and under in-situ condition.
- (3) Increasing the number of the test specimens would statistically enhance the reliability of the test results.



REFERENCES

- Agrawal, A. and Chandak, N.R. (2017). Effect of salt water on mechanical properties of conventional and pervious concrete. **IOSR Journal of Mechanical and Civil Engineering (IOSR-JMCE)**. 14(3): 126-129.
- Akgun, H. and Daemen, J.J.K. (1997). Analytical and experimental assessment of mechanical borehole sealing performance in rock. **Engineering Geology** 47(3): 233-241
- Akgun, H. (1997). An assessment of borehole sealing in a salt environment. **Environmental Geology**. 31: 34-41.
- Akgun, H. and Daemen, J.J.K. (1991c). Bond strength of cementitious borehole plugs in welded tuff. US Nuclear Regulatory Commission Rep. NUREG/CR-4295, Washington, D.C
- Akgun, H. and Daemen, J.J.K. (2002). Influence of degree of saturation on the borehole sealing performance of an expansive cement grout. **Cement and Concrete Research**. 30(2): 281-289.
- Akgun, H. and Daemen, J.J.K. (2004). Stability of expansive cement grout borehole seals emplaced in the vicinity of underground radioactive waste repositories. **Environmental Geology**. 45: 1167-1171.
- American Petroleum Institute (1986). Specifications for materials and testing for well cements. 3rd Edition, American Petroleum Institute, Production Department, Dallas, TX.

- Annon, R.C. (1951). The construction and evaluation of a rating scale for camp personnel. **M.S. thesis**. Boston University, USA.
- Anwar, M., and Roushdi, M. (2013). Improved concrete properties to resist the saline water using environmental by-product. **Water Science**. 27(54): 30-38.
- ASTM C150. Standard specification for Portland cement. **In Annual Book of ASTM Standards**, Vol. 04.01. Philadelphia: American Society for Testing and Materials.
- ASTM D6272-10. Standard test method for flexural properties of unreinforced and reinforced plastics and electrical insulating materials by four-point bending. **In Annual Book of ASTM Standards**, Vol. 04.08. Philadelphia: American Society for Testing and Materials.
- ASTM D7012. Standard test method for compressive strength and elastic moduli of intact rock core specimens under varying states of stress and temperatures. **In Annual Book of ASTM Standards**, Vol. 04.09. Philadelphia: American Society for Testing and Materials.
- ASTM C192/C192M. Standard Practice for Making and Curing Concrete Test Specimens in the Laboratory. **In Annual Book of ASTM Standards**, Vol. 04.02. Philadelphia: American Society for Testing and Materials.
- Bell, F.G., Stacey, T.R. and Genske, D.D. (2000). Mining subsidence and its effect on the environment: some differing examples. **Environmental Geology**. 40(1): 135-152.
- Bozeman, M.T. (2002). Technical report on underground hard-rock mining: subsidence and hydrologic environmental impacts. Center for science in public participation.

- Bumanis, G. and Bajare, D. (2017). Compressive strength of cement mortar affected by sand microfiller obtained with collision milling in disintegrator. **Procedia Engineering**. 172: 149-156.
- Caronge, M.A., Tjaronge, M.W., Hamada, H. and Irmawaty, R. (2017). Effect of water curing duration on strength behaviour of portland composite cement (PCC) mortar. In **IOP Conference Series: Materials Science and Engineering** (Vol. 271, pp. 1-6). United Kingdom: IOP Publishing.
- Chatveera, B., Lertwattanaruk, P. and Makul, N. (2006). Effect of sludge water from ready-mixed concrete plant on properties and durability of concrete. **Cement and concrete composites**. 28(5): 441-450.
- Chrzanowski, A., Monahan, C., Roulston, B. and Szostak-Chrzanowski, A. (1997). Integrated monitoring and modelling of ground subsidence in potash mines. **International Journal of Rock Mechanics and Mining Sciences**. 34(3-4): 55-71.
- Deethouw, P. and Tepnarong, P. (2014). Experimental assessment on borehole sealing performance of sludge-mixed cement grout in rock salt. **Engineering Journal of Research and Development**. 25(3): 17-26.
- Donza, H., Cabrera, O. and Irassar, E.F. (2002). High-strength concrete with different fine aggregate. **Cement and Concrete Research**. 32(11): 1755-1761.
- Economides, M.J., Watters, L.T. and Dunn-Norman, S. (1998). **Petroleum well construction**. Chichester : John Wiley & Sons.

- Elinwa, A.U., Mbadike, E.M. and Elinwa, U.K. (2016). Statistical evaluation of mechanical strengths of salt-water concrete. **International Journal of Engineering Science Invention**. 5(12): 16-21.
- Fehrenbacher, J.B., Rope, R.A., Jansen, I.J., Alexander, J.D. and Ray, B.W. (1978). **Soil productivity in Illinois**. University of Illinois at Urbana–Champaign, Cooperative Extension Service, USA.
- Fuenkajorn, K. (2007). Design process for sealing of boreholes in rock mass. **In Proceedings of the First Thailand Symposium on Rock Mechanics** (pp. 245-252). Nakhon Ratchasima, Thailand: Geomechanics Research Unit.
- Fuenkajorn, K. and Daemen J.J.K. (authors & editors). (1996). **Sealing of Boreholes and Underground Excavations in Rock**, Chapman & Hall, London.
- Gawande, S., Deshmukh, Y., Bhagwat, M., More, S., Nirwal, N. and Phadatare, A. (2017). Comparative Study of Effect of Salt Water and Fresh Water on Concrete. **International Research Journal of Engineering and Technology (IRJET)**. 4(4): 2642-2646.
- Gray, T.A. and Gray, R.E. (1992). Mine closure, sealing, and abandonment. **SME mining handbook**. 1(2): 659-674.
- Güneyisi, E., Gesoğlu, M. and Özturan, T. (2004). Properties of rubberized concretes containing silica fume. **Cement and concrete research**. 34(12): 2309-2317.
- Guo, Q., Chen, L., Zhao, H., Admilson, J. and Zhang, W. (2018). The effect of mixing and curing sea water on concrete strength at different ages. **In MATEC Web of Conferences** (Vol. 142, pp. 1-6). China: EDP Sciences.
- Hadsanan, P., Lertpocasombut, K. and Chatveera, B. (2006). Mechanical properties and durability of cement mortar containing dry sludge ash from Bang Khen

- water supply plant. In **Proceedings of National Convention on Civil Engineering 2006** (pp. 20-22). Thailand: Engineering Institute of Thailand.
- Hartman, H.L. (1992). **SME Mining Engineering Handbook**, 2nd Edition. Denver, CO. Society for Mining, Metallurgy, and Exploration, Inc.
- Hashemi, S.S., Melkounian, N. and Teheri, A. (2015). A borehole stability study by newly designed laboratory tests on thick-walled hollow cylinders. **Journal of Rock Mechanics and Geotechnical Engineering**. 7(5): 519-531.
- Jaeger, J., Cook, N.G. and Zimmerman, R. (2007). **Fundamentals of rock mechanics**. Blackwell Publishing: Malden, New Jersey, USA.
- Japakasetr, T. (1985). Review on rock salt and potash exploration in Northeast Thailand. In **Conference on Geology and Mineral Resources Development of the Northeast of Thailand** (pp. 135-147). Thailand: Khon Kaen University.
- Japakasetr, T. (1992). Thailand's mineral potential and investment opportunity. In **National Conference on Geologic Resources of Thailand: Potential for Future Development** (pp. 641-652). Thailand: Department of Mineral Resources.
- Japakasetr, T. and Suwanich, P. (1982). Potash and Rock Salt in Thailand Appendix A Nonmetallic Minerals Bulletin No. 2. **Economic Geology Division**. Thailand: Department of Mineral Resources.
- Japakasetr, T. and Workman, D.R. (1981). Evaporite deposits of Northeast Thailand. In **Proceedings of the Circum-Pacific Conference**. (pp. 179-187). New York: American Associate of Petroleum Geologist.
- Johnson, K.S. (2005). Subsidence hazards due to evaporite dissolution in the United States. **Environmental geology**. 48(3): 395-409.

- Kanchanamai, P. (2003). The utilization of sludge from Bang Khen water treatment plant in construction industry. **Master's Thesis**. Kasetsart University.
- Karthikeyan, M. and Nagarajan, V. (2016). Feasibility study on utilization of marine sand in concrete for sustainable development. **Indian Journal of Geo Marine Sciences**. 45(2): 313-318.
- Kaushik, S. K. and Islam, S. (1995). Suitability of sea water for mixing structural concrete exposed to a marine environment. **Cement and Concrete Composites**. 17(3): 177-185.
- Kratzsch, H. (1983). Mining Damage above Ground. In **Mining Subsidence Engineering** (pp. 363-418). Springer, Berlin, Heidelberg.
- Kuo, W.Y., Huang, J.S. and Tan, T.E. (2007). Organo-modified reservoir sludge as fine aggregates in cement mortars. **Construction and Building Materials**. 21(3): 609-615.
- Mancini, F., Stecchi, F., Zanni, M. and Gabbianelli, G. (2009). Monitoring ground subsidence induced by salt mining in the city of Tuzla (Bosnia and Herzegovina). **Environ Geol**. 58(2): 381-389.
- Maniyal, S. and Patil, A. (2015). An experimental study on compressive strength of various cement concrete under sea water. **International Journal of Scientific & Engineering Research**. 6(4): 199-203.
- Mbadike, E.M., and Elinwa, A.U. (2011). Effect of salt water in the production of concrete. **Nigerian Journal of Technology**. 30(2): 105-110.
- Moghadam, H.A. and Khoshbin, O.A. (2012). Effect of water-cement ratio (w/c) on mechanical properties of self-compacting concrete (case study). World Academy of Science, Engineering and Technology, **International Journal of Civil,**

Environmental, Structural, Construction and Architectural Engineering. 6
(5): 317-320.

Mun, K.J. (2007). Development and tests of lightweight aggregate using sewage sludge for nonstructural concrete. **Construction and Building Materials.** 21(7): 1583-1588.

Olugbenga, A. (2007). Effects of varying curing age and water/cement ratio on the elastic properties of laterized concrete. **Civil Engineering Dimension.** 9 (2): 85-89.

Olutoge, F. Adeyemi and Amusan, G. Modupeola (2014). The effect of sea water on compressive strength of concrete. **International Journal of Engineering Science Invention.** 3(7):23-31.

Pattani, S. and Tepnarong, P. (2015). Experimental assessment of mechanical and Hydraulic performance of cement sealing in rock salt. **Vietrock2015 an ISRM Specialized Conference.** Vietnam:International Society for Rock Mechanics.

Pierce, F.J., Larson, W.E., Dowdy, R.H. and Graham, W.A.P. (1983). Productivity of soils: assessing long-term changes due to erosion. **Journal of Soil and Water Conservation.** 38(1): 39-44.

Premchand, Mohiuddin, M.Y. and Haleem M.A. (2016). Experimental study on salinity effect on properties of M20 grade concrete in different normality condition. **Journal of Advance in Science and Technology.** 11(22): 1-5.

Pytel, A. and Kiusalaas, J. (2003). **Mechanics of materials.** 2nd ed. USA: Brooks/Cole-Thomson Learning.

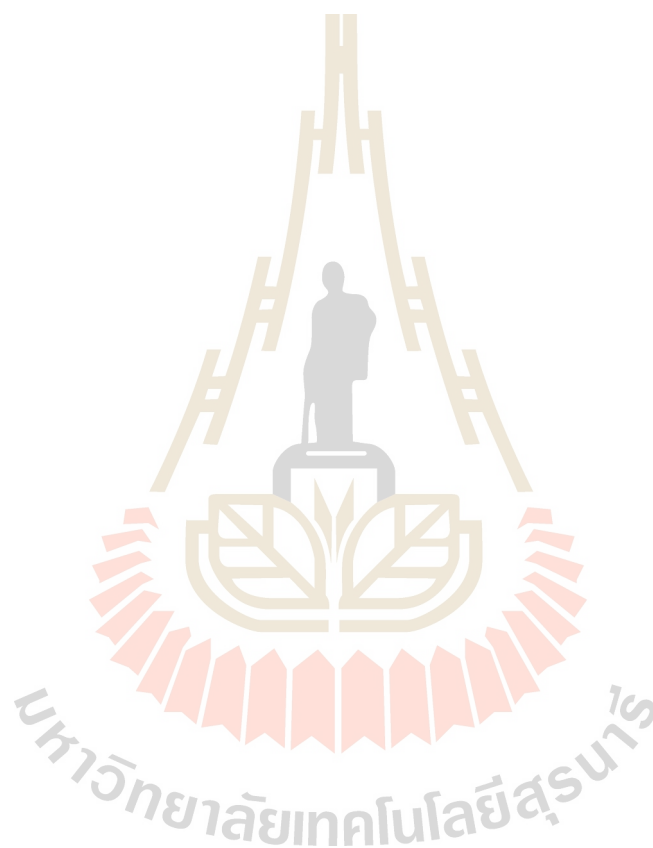
Rahmani, K., Shamsai, A., Saghafian, B. and Peroti, S. (2012). Effect of water and cement ratio on compressive strength and abrasion of microsilica concrete. **Middle-East Journal of Scientific Research.** 12 (8): 1056-1061.

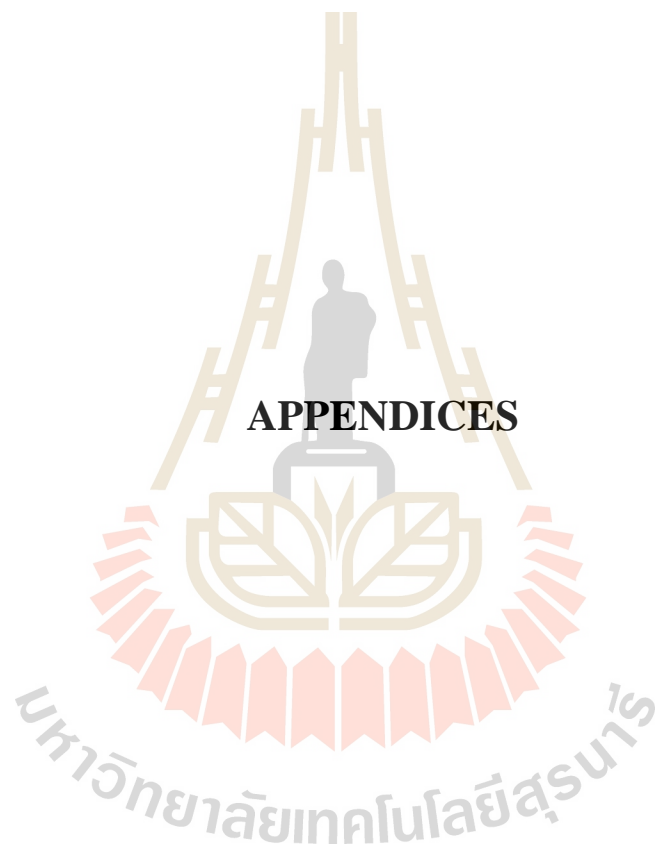
- Raju, P.K., Lakshmi, V. and Pravallika, S.B. (2014). An investigation on fly ash blended cement concrete using sea water. **International Journal of Advanced Scientific & Technical Research**. 2(4): 849-857.
- Rattanajarurak, P. (1990). Formation of the potash deposits, Khorat Plateau, Thailand. **Master's Thesis**. School of Mine, Kensington, Australia.
- Sahu, P. and Lokhande, R.D. (2015). An investigation of sinkhole subsidence and its preventive measures in underground coal mining. **Procedia Earth and Planetary Science**. 11: 63-75.
- Samaiklang, W. and Fuenkajorn, K. (2013). Mechanical and hydraulic performance of cement grouts from 5 suppliers in Thailand. In **The 11th International Conference on Mining, Materials and Petroleum Engineering** (pp.45-51). Thailand: ASEAN Forum on Clean Coal Technology.
- Sattayarak, N. (1983). Review of continental Mesozoic stratigraphy of Thailand. In **Proceedings of the Stratigraphic correlation of Thailand and Malaysia** (Vol. 1, pp. 127-148). Bangkok, Thailand: Geological Society.
- Sattayarak, N. (1985). Review on geology of Khorat Plateau. In **Conference on Geology and Mineral Resources Development of the Northeast, Thailand** (pp. 23-30). Thailand: Khon Kaen University.
- Saxena, A.K. and Singh, J.S. (1980). Analysis of forest-grazingland vegetation in parts of Kumaun Himalaya. **Indian Journal of Range Management**. 1(1): 13-32.
- Singh, M.M. (1992). **SME Mining engineering handbook**. Society for Mining Metallurgy and Exploration: Colorado.
- Smith, D.K. (1993). **Handbook on Plugging and Abandonment**. Oklahoma: Penn Well Publishing Company.

- Smith, S.A. (1994). **Well & Borehole Sealing: Importance, Materials, Methods, and Recommendations for Decommissioning**. Ground Water Publishing Company.
- Sowers, G.F. (1962). Shallow foundations. **Foundation Engineering**. Edited by G. A. Leonards, McGraw-Hill Book Company, Inc., New York.
- Supajanya, T., Vichapan, K. and Sri-issaporn, S. (1992). Surface expression of shallow salt dome in Northeast Thailand. In **National Conference on Geologic Resources of Thailand: Potential for Future Development** (pp. 89-95). Bangkok, Thailand: Department of Mineral Resources.
- Suwanich, P. (1986). Potash and rock salt in Thailand. **Nonmetallic Minerals Bulletin No.2**, Economic Geology Division, Department of Mineral Resources, Bangkok, Thailand.
- Tiwari, P., Chandak, R. and Yadav, R.K. (2014). Effect of salt Water on compressive strength of concrete. **Journal of Engineering Research and Applications**. 4(4): 38-42.
- Utha-aroon, C. (1993). Continental origin of the Maha Sarakham evaporites, Northeastern Thailand. **Journal of Southeast Asian Earth Sciences**. 8(1-4): 193-203.
- Valls, S., Yague, A., Vazque, E. and Mariscal, C. (2004). Physical and mechanical properties of concrete with added dry sludge from a sewage treatment plant. **Cement and Concrete Research**. 34: 2203-2208.
- Warren, J. (1999). Evaporites: Their evolution and economics (pp. 235-239). Philadelphia: Blackwell Science.
- Wetchasat, K. (2013). Performance assessment of sludge-mixed cement grout in rock fractures. **Master's thesis**. Suranaree University of Technology, Thailand.

Yang, C.C., Yang, Y.S. and Huang, R. (1997). The effect of aggregate volume ratio on the elastic modulus and compressive strength of lightweight concrete. **Journal of Marine Science and Technology**. 5(1): 31-38.

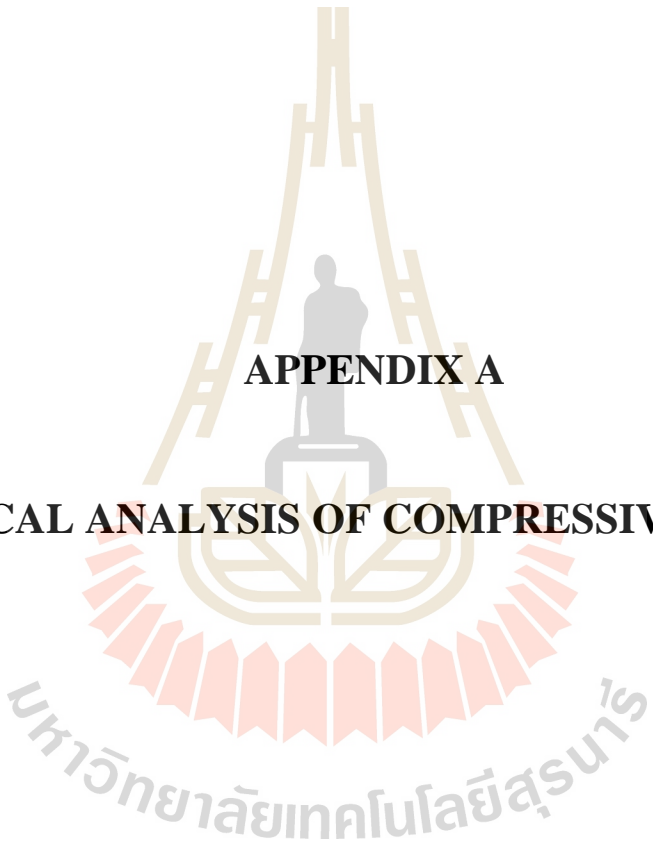
Yumuang, S., Khantapab, C. and Taiyagupt, M. (1986). The evaporate deposits in Bamnet Narong area, Northeastern Thailand. In **Proceedings of the GEOSEA V** (Bulletin 20, Vol. 2, pp. 249-267). Geological Society of Malasia.





APPENDICES

มหาวิทยาลัยเทคโนโลยีสุรนารี



APPENDIX A

NUMERICAL ANALYSIS OF COMPRESSIVE STRENGTH

มหาวิทยาลัยเทคโนโลยีสุรนารี

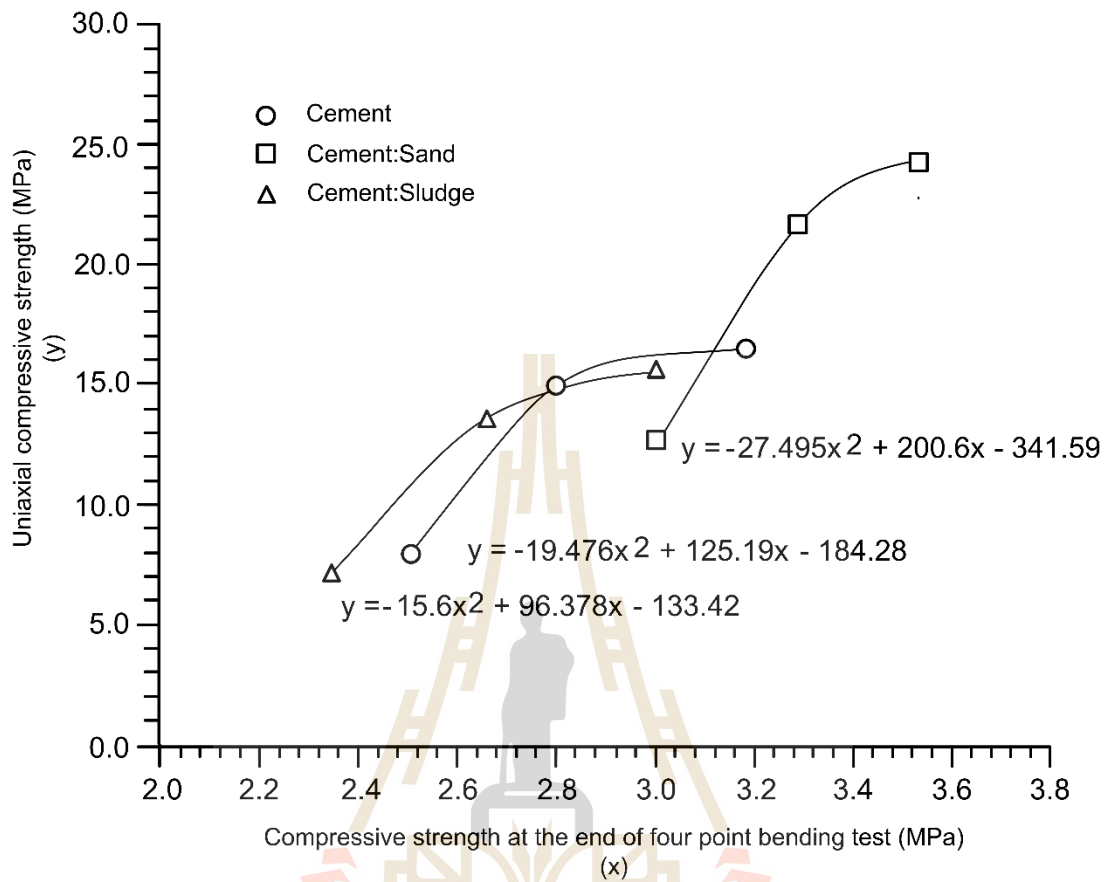


Figure A.1 Uniaxial compressive strength as a function of compressive strength at the end of four point bending test.

APPENDIX B

FACTOR OF SAFETY

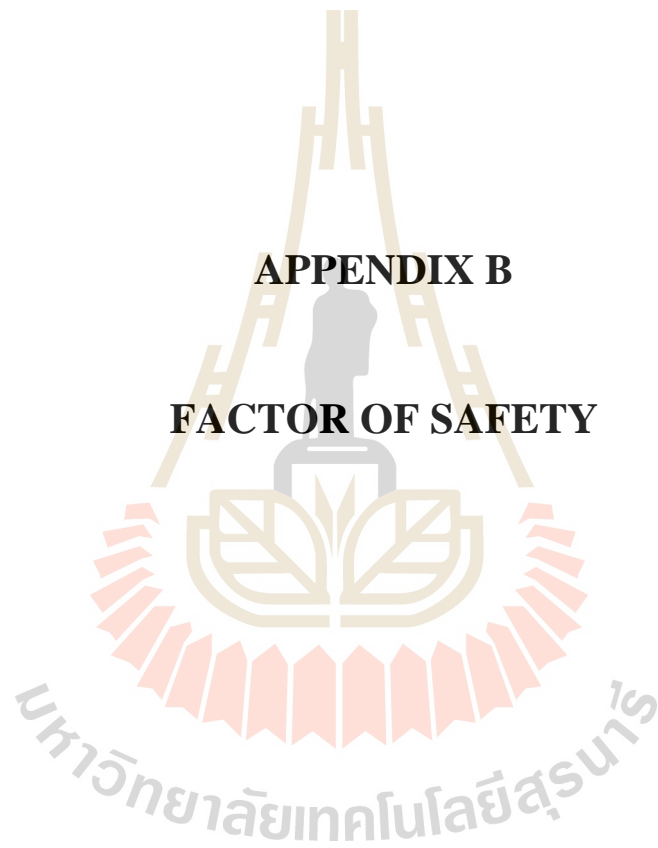


Table B.1 Tensile strain energy ($W_{T,i}$) of the pure cement in borehole as brine to cement ratio = 0.6.

L (m)	ω (N/m)	M (N·m)	σ_T (MPa)	ϵ_T (mm-strain)	$W_{T,i}$ (MPa)	W_T (MPa)	FS
50	18.07	22,582.43	19.26	1.537	14.81	0.58	0.04
10	2.26	11,291.22	9.63	0.769	3.70	0.58	0.16
15	0.67	7,527.48	6.42	0.512	1.65	0.58	0.36
20	0.28	5,645.61	4.82	0.384	0.93	0.58	0.63
25	0.14	4,516.49	3.85	0.307	0.59	0.58	0.99
30	0.08	3,763.74	3.21	0.256	0.41	0.58	1.42

Table B.2 Tensile strain energy ($W_{T,i}$) of the cement mixed with sand in borehole as brine to cement ratio = 0.6.

L (m)	ω (N/m)	M (N·m)	σ_T (MPa)	ϵ_T (mm-strain)	$W_{T,i}$ (MPa)	W_T (MPa)	FS
50	21.03	26,288.55	22.42	1.58	17.73	0.69	0.04
10	2.63	13,144.27	11.21	0.79	4.43	0.69	0.16
15	0.78	8,762.85	7.47	0.53	1.97	0.69	0.35
20	0.33	6,572.14	5.61	0.40	1.11	0.69	0.62
25	0.17	5,257.71	4.48	0.32	0.71	0.69	0.97
30	0.10	4,381.42	3.74	0.26	0.49	0.69	1.40

Table B.3 Tensile strain energy ($W_{T,i}$) of the cement mixed with sludge in borehole
as brine to cement ratio = 0.6.

L (m)	ω (N/m)	M (N·m)	σ_T (MPa)	ϵ_T (mm-strain)	$W_{T,i}$ (MPa)	W_T (MPa)	FS
50	16.57	20,715.54	17.67	1.48	13.06	0.52	0.04
10	2.07	10,357.77	8.84	0.74	3.27	0.52	0.16
15	0.61	6,905.18	5.89	0.49	1.45	0.52	0.36
20	0.26	5,178.89	4.42	0.37	0.82	0.52	0.64
25	0.13	4,143.11	3.53	0.30	0.52	0.52	1.00
30	0.08	3,452.59	2.95	0.25	0.36	0.52	1.44

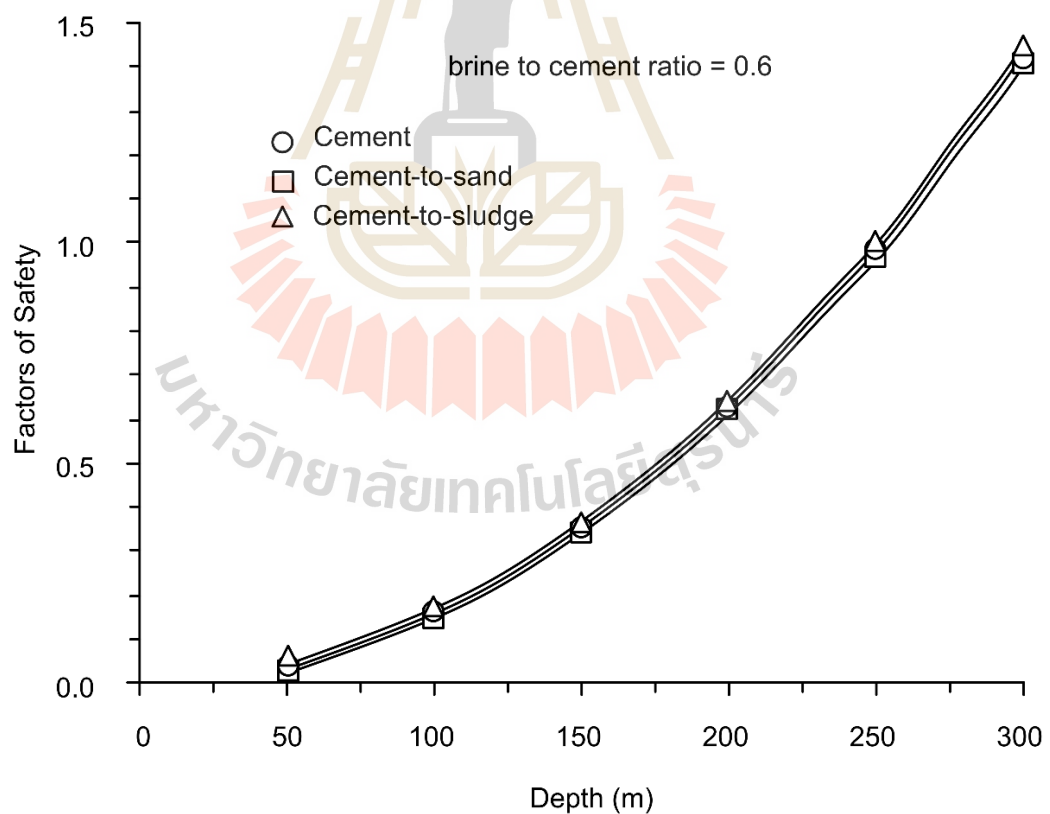


Figure B.1 Factors of safety as a function of depth calculated by tensile strain energy
(B/C = 0.6).

Table B.4 Tensile strain energy ($W_{T,i}$) of the pure cement in borehole as brine to cement ratio = 0.8.

L (m)	ω (N/m)	M (N·m)	σ_T (MPa)	ϵ_T (mm-strain)	$W_{T,i}$ (MPa)	W_T (MPa)	FS
50	15.23	19,042.26	16.24	1.61	13.06	0.39	0.03
100	1.90	9,521.13	8.12	0.80	3.27	0.39	0.12
150	0.56	6,347.42	5.41	0.54	1.45	0.39	0.27
200	0.24	4,760.56	4.06	0.40	0.82	0.39	0.48
250	0.12	3,808.45	3.25	0.32	0.52	0.39	0.75
300	0.07	3,173.71	2.71	0.27	0.36	0.39	1.07

Table B.5 Tensile strain energy ($W_{T,i}$) of the cement mixed with sand in borehole as brine to cement ratio = 0.8.

L (m)	ω (N/m)	M (N·m)	σ_T (MPa)	ϵ_T (mm-strain)	$W_{T,i}$ (MPa)	W_T (MPa)	FS
50	17.15	21,434.64	18.28	1.57	14.31	0.56	0.04
100	2.14	10,717.32	9.14	0.78	3.58	0.56	0.16
150	0.64	7,144.88	6.09	0.52	1.59	0.56	0.35
200	0.27	5,358.66	4.57	0.39	0.89	0.56	0.63
250	0.14	4,286.93	3.66	0.31	0.57	0.56	0.98
300	0.08	3,572.44	3.05	0.26	0.40	0.56	1.41

Table B.6 Tensile strain energy ($W_{T,i}$) of the cement mixed with sludge in borehole
as brine to cement ratio = 0.8.

L (m)	ω (N/m)	M (N·m)	σ_T (MPa)	ϵ_T (mm-strain)	$W_{T,i}$ (MPa)	W_T (MPa)	FS
50	13.49	16,857.31	14.38	1.44	10.36	0.34	0.03
100	1.69	8,428.65	7.19	0.72	2.59	0.34	0.13
150	0.50	5,619.10	4.79	0.48	1.15	0.34	0.30
200	0.21	4,214.33	3.59	0.36	0.65	0.34	0.53
250	0.11	3,371.46	2.88	0.29	0.41	0.34	0.82
300	0.06	2,809.55	2.40	0.24	0.29	0.34	1.18

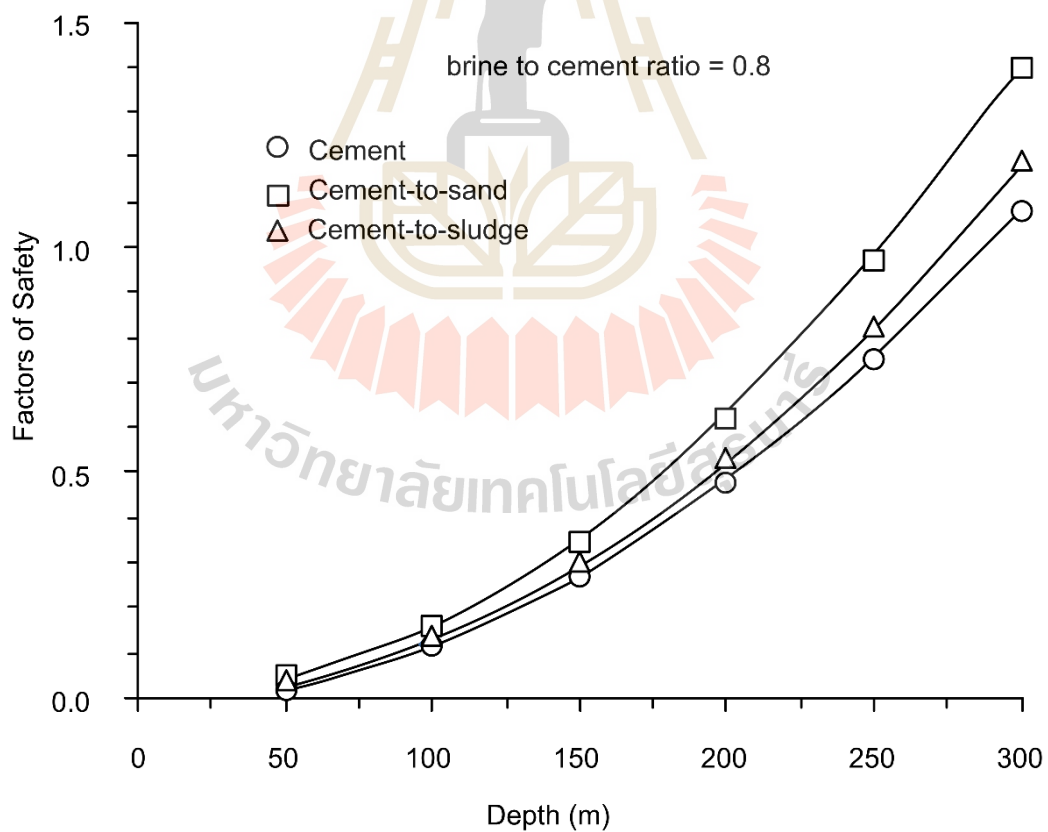


Figure B.2 Factors of safety as a function of depth calculated by tensile strain energy
(B/C = 0.8).

Table B.7 Tensile strain energy ($W_{T,i}$) of the pure cement in borehole as brine to cement ratio = 1.0.

L (m)	ω (N/m)	M (N·m)	σ_T (MPa)	ϵ_T (mm-strain)	$W_{T,i}$ (MPa)	W_T (MPa)	FS
50	13.42	16,774.33	14.31	1.63	11.63	0.30	0.03
100	1.68	8,387.17	7.15	0.81	2.91	0.30	0.10
150	0.50	5,591.44	4.77	0.54	1.29	0.30	0.23
200	0.21	4,193.58	3.58	0.41	0.73	0.30	0.41
250	0.11	3,354.87	2.86	0.33	0.47	0.30	0.64
300	0.06	2,795.72	2.38	0.27	0.32	0.30	0.93

Table B.8 Tensile strain energy ($W_{T,i}$) of the cement mixed with sand in borehole as brine to cement ratio = 1.0.

L (m)	ω (N/m)	M (N·m)	σ_T (MPa)	ϵ_T (mm-strain)	$W_{T,i}$ (MPa)	W_T (MPa)	FS
50	15.68	19,595.41	16.71	1.68	14.02	0.47	0.03
100	1.96	9,797.70	8.36	0.84	3.51	0.47	0.13
150	0.58	6,531.80	5.57	0.56	1.56	0.47	0.30
200	0.24	4,898.85	4.18	0.42	0.88	0.47	0.54
250	0.13	3,919.08	3.34	0.34	0.56	0.47	0.84
300	0.07	3,265.90	2.79	0.28	0.39	0.47	1.21

Table B.9 Tensile strain energy ($W_{T,i}$) of the cement mixed with sludge in borehole
as brine to cement ratio = 1.0.

L (m)	ω (N/m)	M (N·m)	σ_T (MPa)	ϵ_T (mm-strain)	$W_{T,i}$ (MPa)	W_T (MPa)	FS
50	11.41	14257.49	12.16	1.44	8.73	0.25	0.03
100	1.43	7128.75	6.08	0.72	2.18	0.25	0.11
150	0.42	4752.50	4.05	0.48	0.97	0.25	0.26
200	0.18	3564.37	3.04	0.36	0.55	0.25	0.46
250	0.09	2851.50	2.43	0.29	0.35	0.25	0.72
300	0.05	2376.25	2.03	0.24	0.24	0.25	1.03

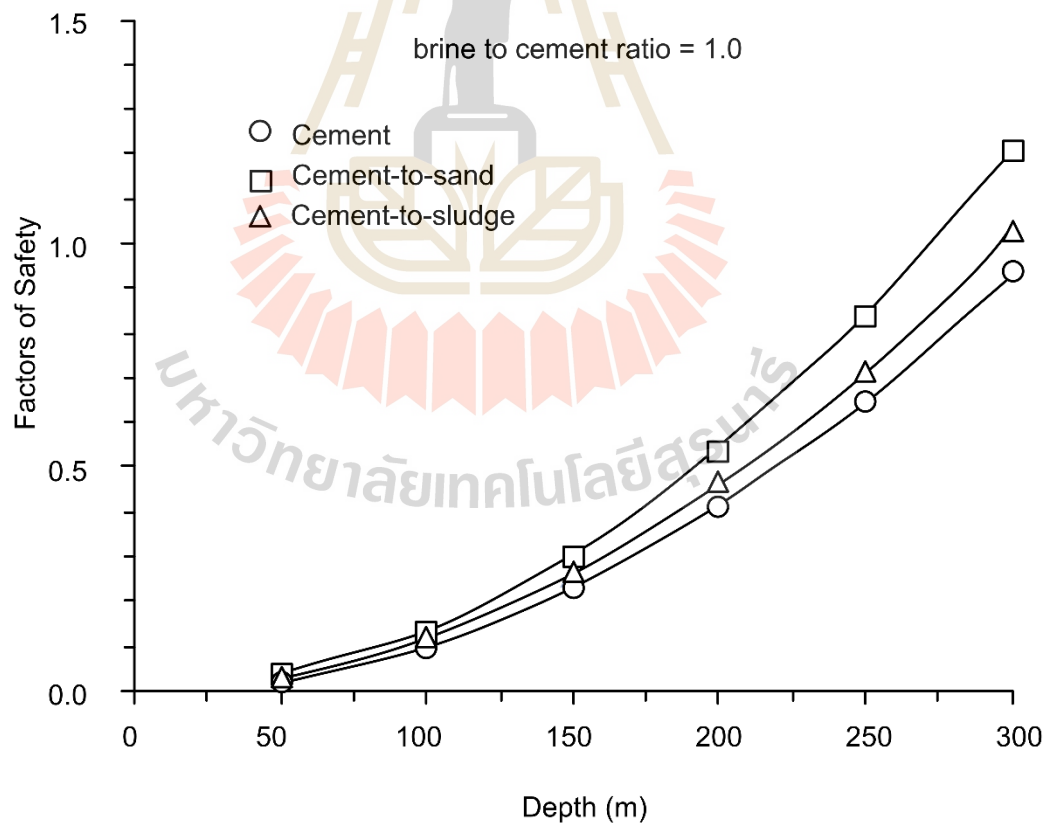


Figure B.3 Factors of safety as a function of depth calculated by tensile strain energy
(B/C = 1.0).

Table B.10 Maximum shear stress (τ_i) of the pure cement in borehole as brine to cement ratio = 0.6.

L (m)	ω (N/m)	V (N)	τ_i (MPa)	τ (MPa)	FS
50	18.07	903,297.22	29.34	3.03	0.10
100	2.26	225,824.30	7.33	3.03	0.41
150	0.67	100,366.36	3.26	3.03	0.93
200	0.28	56,456.08	1.83	3.03	1.65
250	0.14	36,131.89	1.17	3.03	2.58
300	0.08	25,091.59	0.81	3.03	3.72

Table B.11 Maximum shear stress (τ_i) of the cement mixed with sand in borehole as brine to cement ratio = 0.6.

L (m)	ω (N/m)	V (N)	τ_i (MPa)	τ (MPa)	FS
50	21.03	1,051,541.95	34.15	3.47	0.10
100	2.63	262,885.49	8.54	3.47	0.41
150	0.78	116,837.99	3.79	3.47	0.91
200	0.33	65,721.37	2.13	3.47	1.63
250	0.17	42,061.68	1.37	3.47	2.54
300	0.10	29,209.50	0.95	3.47	3.66

Table B.12 Maximum shear stress (τ_i) of the cement mixed with sludge in borehole as
brine to cement ratio = 0.6.

L (m)	ω (N/m)	V (N)	τ_i (MPa)	τ (MPa)	FS
50	16.57	828,621.70	26.91	2.84	0.11
100	2.07	207,155.42	6.73	2.84	0.42
150	0.61	92,069.08	2.99	2.84	0.95
200	0.26	51,788.86	1.68	2.84	1.69
250	0.13	33,144.87	1.08	2.84	2.64
300	0.08	23,017.27	0.75	2.84	3.80

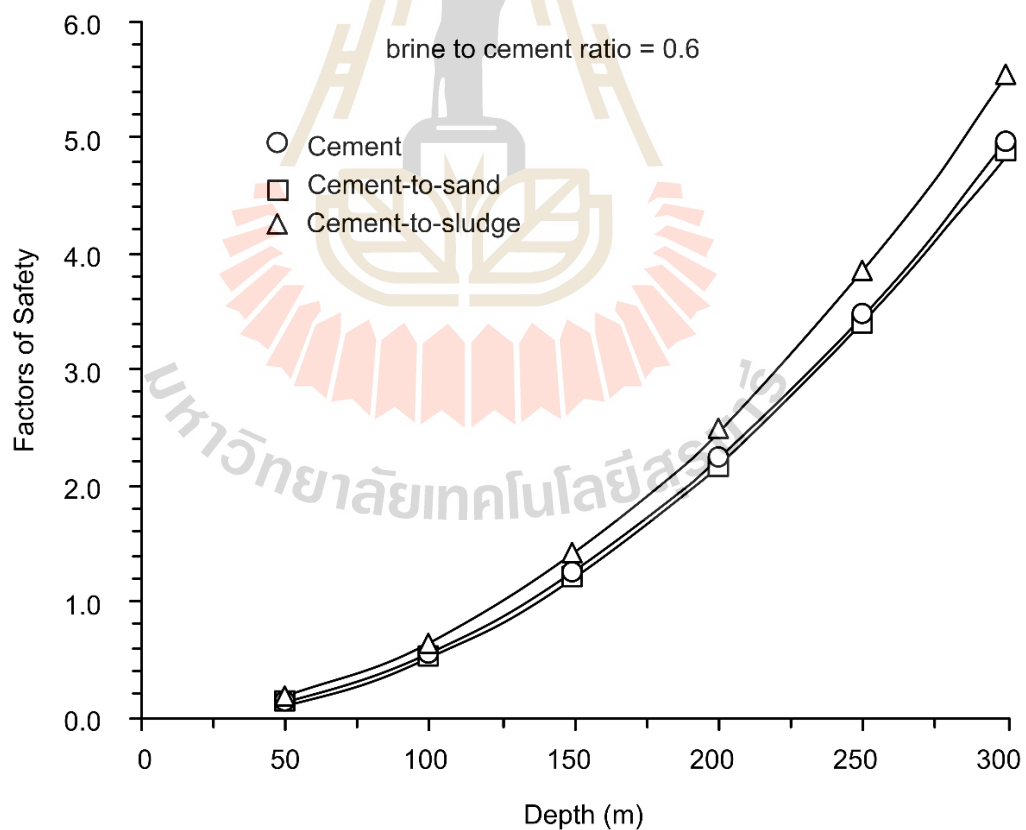


Figure B.4 Factors of safety as a function of depth calculated by the Coulomb's
criterion ($B/C = 0.6$).

Table B.13 Maximum shear stress (τ_i) of the pure cement in borehole as brine to cement ratio = 0.8.

L (m)	ω (N/m)	V (N)	τ_i (MPa)	τ (MPa)	FS
50	15.23	761,690.30	24.74	3.03	0.12
100	1.90	190,422.58	6.18	3.03	0.49
150	0.56	84,632.26	2.75	3.03	1.10
200	0.24	47,605.64	1.55	3.03	1.96
250	0.12	30,467.61	0.99	3.03	3.06
300	0.07	21,158.06	0.69	3.03	4.41

Table B.14 Maximum shear stress (τ_i) of the cement mixed with sand in borehole as brine to cement ratio = 0.8.

L (m)	ω (N/m)	V (N)	τ_i (MPa)	τ (MPa)	FS
50	17.15	857,385.60	27.85	3.47	0.12
100	2.14	214,346.40	6.96	3.47	0.50
150	0.64	95,265.07	3.09	3.47	1.12
200	0.27	53,586.60	1.74	3.47	1.99
250	0.14	34,295.42	1.11	3.47	3.12
300	0.08	23,816.27	0.77	3.47	4.49

Table B.15 Maximum shear stress (τ_i) of the cement mixed with sludge in borehole as
brine to cement ratio = 0.8.

L (m)	ω (N/m)	V (N)	τ_i (MPa)	τ (MPa)	FS
50	13.49	674,292.29	21.90	2.84	0.13
100	1.69	168,573.07	5.47	2.84	0.52
150	0.50	74,921.37	2.43	2.84	1.17
200	0.21	42,143.27	1.37	2.84	2.07
250	0.11	26,971.69	0.88	2.84	3.24
300	0.06	18,730.34	0.61	2.84	4.67

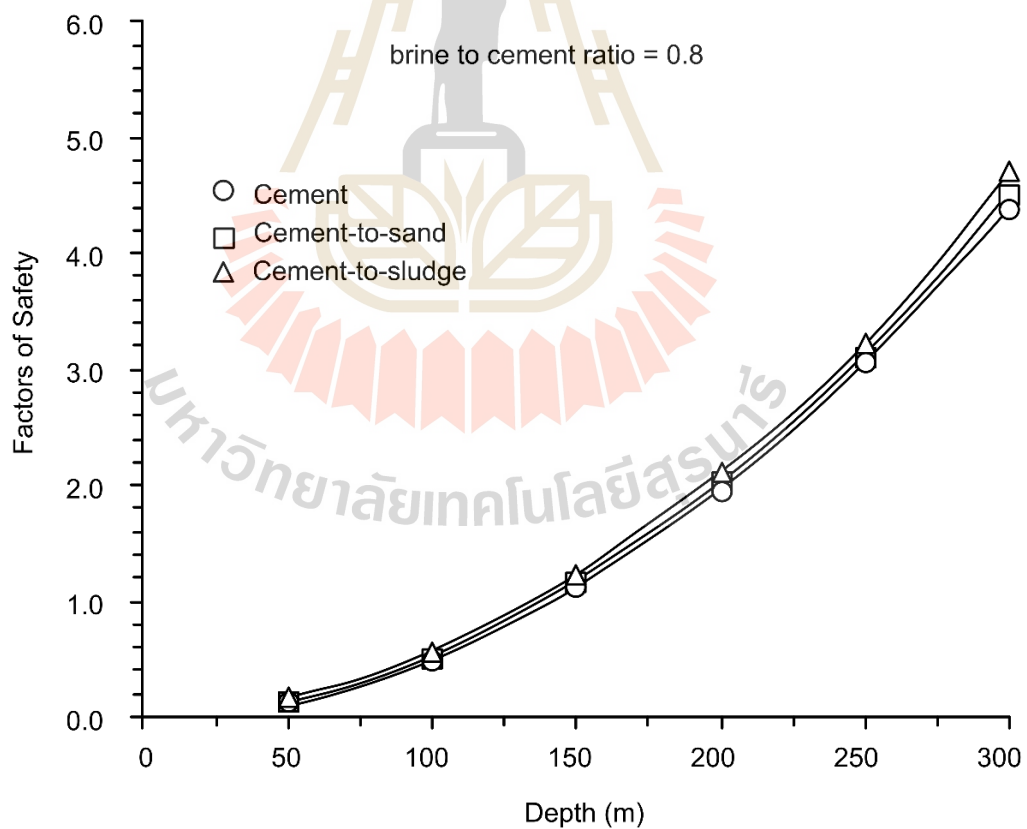


Figure B.5 Factors of safety as a function of depth calculated by the Coulomb's
criterion (B/C = 0.8).

Table B.16 Maximum shear stress (τ_i) of the pure cement in borehole as brine to cement ratio = 1.0.

L (m)	ω (N/m)	V (N)	τ_i (MPa)	τ (MPa)	FS
50	13.42	670,973.38	21.79	3.03	0.14
100	1.68	167,743.34	5.45	3.03	0.56
150	0.50	74,552.60	2.42	3.03	1.25
200	0.21	41,935.84	1.36	3.03	2.22
250	0.11	26,838.94	0.87	3.03	3.48
300	0.06	18,638.15	0.61	3.03	5.01

Table B.17 Maximum shear stress (τ_i) of the cement mixed with sand in borehole as brine to cement ratio = 1.0.

L (m)	ω (N/m)	V (N)	τ_i (MPa)	τ (MPa)	FS
50	15.68	783,816.38	25.46	3.47	0.14
100	1.96	195,954.10	6.36	3.47	0.55
150	0.58	87,090.71	2.83	3.47	1.23
200	0.24	48,988.52	1.59	3.47	2.18
250	0.13	31,352.66	1.02	3.47	3.41
300	0.07	21,772.68	0.71	3.47	4.91

Table B.18 Maximum shear stress (τ_i) of the cement mixed with sludge in borehole as
brine to cement ratio = 1.0.

L (m)	ω (N/m)	V (N)	τ_i (MPa)	τ (MPa)	FS
50	11.41	570,299.71	18.52	2.84	0.15
100	1.43	142,574.93	4.63	2.84	0.61
150	0.42	63,366.63	2.06	2.84	1.38
200	0.18	35,643.73	1.16	2.84	2.45
250	0.09	22,811.99	0.74	2.84	3.83
300	0.05	15,841.66	0.51	2.84	5.52

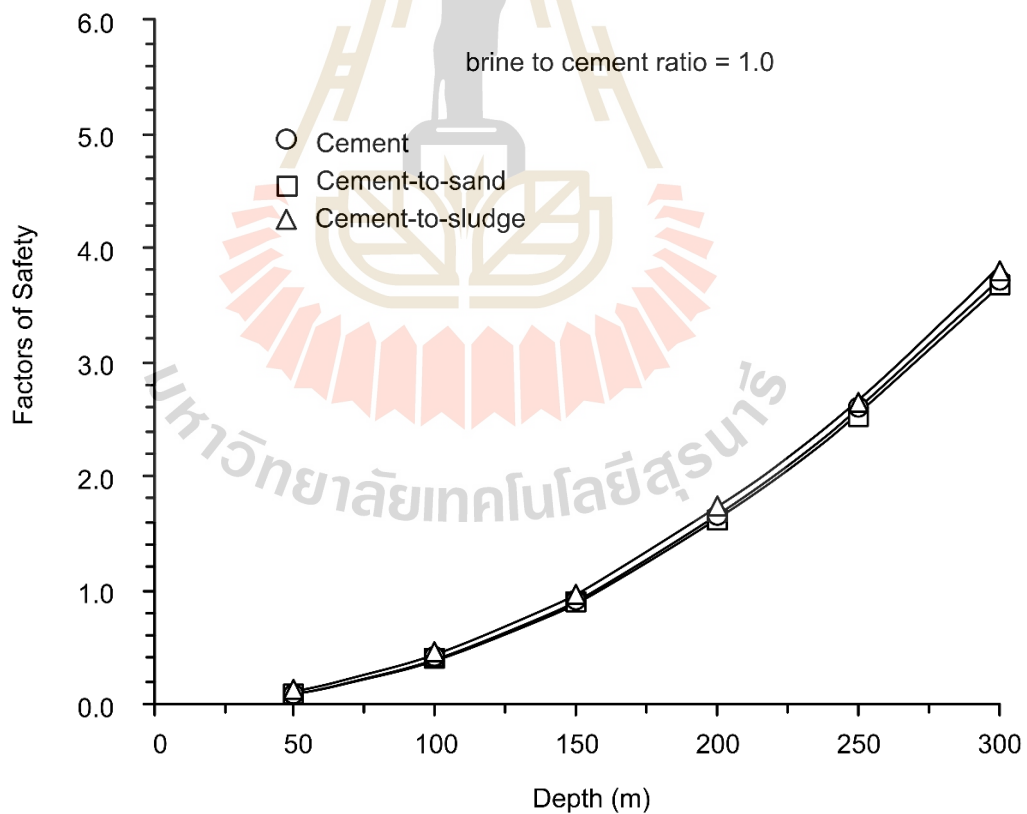


Figure B.6 Factors of safety as a function of depth calculated by the Coulomb's
criterion (B/C = 1.0).

BIOGRAPHY

Miss Sujitra Lahib was born on Feb 12, 1994 in Prachinburi, Thailand. She received her Bachelor's Degree in Engineering (Geotechnology) from Suranaree University of Technology in 2016. For her post-graduate, she continued to study with a Master's degree in the Geological Engineering Program, Institute of Engineering, Suranaree university of Technology. During graduation, 2016-2018, she was a part time worker in position of research assistant at the Geomechanics Research Unit, Institute of Engineering, Suranaree University of Technology.

